

# Singular perturbation theory for interacting fermions in two dimensions

Andrey V. Chubukov

*Department of Physics, University of Maryland, College Park, MD 20742-4111  
and Department of Physics, University of Wisconsin-Madison, 1150 Univ. Ave., Madison, WI 53706-1390*

Dmitrii L. Maslov

*[\*]Department of Physics, University of Florida, P. O. Box 118440, Gainesville, FL 32611-8440  
and Abdus Salam International Centre for Theoretical Physics, 11 Strada Costiera, Trieste 34014, Italy*

Suhas Gangadharaiah

*Department of Physics, University of Florida, P. O. Box 118440, Gainesville, FL 32611-8440*

Leonid I. Glazman

*Theoretical Physics Institute, University of Minnesota, Minneapolis, MN 55455*

We consider a system of interacting fermions in two dimensions beyond the second-order perturbation theory in the interaction. It is shown that the mass-shell singularities in the self-energy, arising already at the second order of the perturbation theory, manifest a non-perturbative effect: an interaction with the zero-sound mode. Resumming the perturbation theory for a weak, short-range interaction and accounting for a finite curvature of the fermion spectrum, we eliminate the singularities and obtain the results for the quasi-particle self-energy and the spectral function to all orders in the interaction with the zero-sound mode. A threshold for emission of zero-sound waves leads a non-monotonic variation of the self-energy with energy (or momentum) near the mass shell. Consequently, the spectral function has a kink-like feature. We also study in detail a non-analytic temperature dependence of the specific heat,  $C(T) \propto T^2$ . It turns out that although the interaction with the collective mode results in an enhancement of the fermion self-energy, this interaction does not affect the non-analytic term in  $C(T)$  due to a subtle cancellation between the contributions from the real and imaginary parts of the self-energy. For a short-range and weak interaction, this implies that the second-order perturbation theory suffices to determine the non-analytic part of  $C(T)$ . We also obtain a general form of the non-analytic term in  $C(T)$ , valid for the case of a generic Fermi liquid, *i.e.*, beyond the perturbation theory.

PACS numbers: 71.10.Ay, 71.10.Pm

## I. INTRODUCTION

The validity of the Landau Fermi liquid (FL) theory continues to be a subject of intense discussions over the last five decades. In essence, the FL theory states that the behavior of interacting fermions at the lowest energies is similar to that of non-interacting fermions [1, 2]. In particular, specific heat,  $C(T)$ , scales linearly with temperature  $T$  at  $T \rightarrow 0$ , whereas the spin susceptibility,  $\chi(T)$ , approaches a finite value at  $T \rightarrow 0$ . This theory has been enormously successful in describing  $\text{He}^3$  and a large number of metals. Yet, it fails to explain the properties of high-temperature superconductors [3] and quite a few heavy-fermion materials [4]. Given that the FL theory is essentially a phenomenological one, built on a number of appealing albeit unproven assumptions, the interest in its relation to microscopic models, which allow for controllable perturbative treatment, has always been intense since the times of the FL's inception. Perturbative calculations of the 1950s within a model of a low-density 3D Fermi gas with a repulsive, short-range interaction (a “non-ideal Fermi gas model” [1, 2]) reproduced the Fermi-liquid results for thermodynamic quantities up to leading terms in parameter  $T/E_F$ , where  $E_F$  is the Fermi energy (we set  $\hbar = k_B = 1$  throughout the paper). These calculations were later extended to arbitrary dimensionality  $D$  with the result that the FL theory is valid for  $D > 1$ , provided that the interaction falls off with the distance rapidly enough, but becomes invalid in one dimension. The energy range for the FL theory, however, may shrink as the system approaches a quantum phase transition of some kind [5].

At the same time, perturbative calculations show that the similarity between a Fermi liquid and ideal Fermi gas does not go beyond the leading order in  $T/E_F$ . In a Fermi gas, sub-leading terms in  $C(T)/T$  and  $\chi(T)$  form regular series in powers of  $T^2$ . For an interacting system, the second-order perturbation theory shows that already next-to-leading terms in  $T/E_F$  are non-analytic in  $D \leq 3$ . In  $D = 3$ , the sub-leading term in  $C(T)/T$  is  $T^2 \ln T$  [6, 7, 8, 9, 10]. In addition, a non-uniform spin susceptibility,  $\chi(Q)$ , scales as  $Q^2 \ln Q$ , where  $Q$  is the boson momentum [11]. The non-analytic behavior becomes more pronounced as the system dimensionality is reduced. In 2D, the sub-leading terms in  $C(T)/T$  and in  $\chi(Q, T)$  scale as  $T$  [12, 13, 14] and  $\max\{Q, T\}$  [11, 13, 15, 16, 17], respectively. Non-analytic

corrections to the FL behavior have been observed in a number of experiments [18]. Quite recently, the interest to these corrections has been revitalized due to their importance for the effective theories of quantum critical phenomena in itinerant ferromagnets [11, 17, 19] of the Hertz-Millis-Moriya type [20].

The non-analytic behavior of the thermodynamic quantities is related to the long-range *effective* interaction between fermions which falls off as a power law of the inter-fermion separation, even if the nominal interaction is short-range. An example of such an interaction is scattering from the Friedel oscillation imposed by a static local perturbation, *e.g.*, an impurity. This interaction falls off as  $r^{-D}$  with the distance from the impurity. Scattering from the  $r^{-D}$  – potential of the Friedel oscillation leads to a non-analytic energy dependence of the scattering amplitude near the Fermi level and, as a result, to non-analytic corrections to the tunneling density of states [21] and conductivity [22]. In a disorder-free-system, fermions interact via *dynamic* charge- and spin-density fluctuations. The non-analyticities in the dynamic density-density correlation function (polarization bubble) also give rise to a long-range *retarded* interaction falling off as  $r^{-(D-1)}$  [12, 13]. These non-analyticities are due to the processes with both small and large ( $2k_F$ ) momentum transfers, where  $k_F$  is the Fermi momentum.

The second order perturbative analysis in 2D not only reveals a non-analytic behavior of  $C(T)$  and  $\chi(Q, T)$ , but also brings about an unexpected result. Namely, the imaginary part of the fermion self-energy diverges logarithmically on the mass shell  $\omega = \epsilon_k$  [23, 24, 25], [13], if one linearizes the single-particle spectrum,  $\epsilon_k$ , near the Fermi level. This log-singularity is the 2D analog of a stronger–power-law–singularity in 1D (“infrared catastrophe”) [26]. Although the mass-shell divergence does not affect the specific heat and the spin susceptibility to second order in the interaction, it does signal a potential breakdown of the perturbation theory in 2D.

The purpose of this paper is to analyze the non-analytic corrections to the FL behavior beyond the second-order perturbation theory. Specifically, we focus on two issues. The first one is what happens to the mass-shell singularity beyond second order. Power counting shows that the mass-shell singularities proliferate with the order of the perturbation theory. At first glance, this confirms Anderson’s conjecture that the FL is destroyed in 2D [27]. However, this issue can be addressed properly only after a re-summation of the perturbation theory, which is what we will do here. The second issue is whether collective modes, which emerge once the perturbation theory is summed up to all orders, give rise to extra non-analytic corrections to thermodynamic quantities. The role of collective modes – zero sound for neutral fermions and plasmon for electrons – is especially intriguing for  $D = 2$ . In this case, power counting combined with the assumption that a collective mode is a free excitation (similar to a phonon) shows that the collective mode contribution to  $C(T)/T$  scales as  $T$ , *i.e.*, it has the same form as the perturbative correction [12]. This argument needs to be treated with caution, however. Indeed, since a collective mode arises at the infinite order in the interaction between fermions, it is unclear whether it can be treated as a free boson mode. We will see that the issues of the collective-mode contribution to  $C(T)$  and mass-shell singularities in the self-energy are related; namely, a contribution to the specific heat from the collective mode can be viewed as coming from the self-energy obtained by summing up mass-shell singularities to all orders in the perturbation theory.

This paper is organized as follows. In Sec. II we introduce relevant scattering processes. In Sec. III, we discuss the self-energy of 2D fermions with both contact and finite-range interactions. In Sec. III A and III B we analyze the mass-shell singularities in the imaginary part of the self-energy arising in the order-by-order perturbation theory. Re-summation of the perturbation series for the vertex part is performed in Sec. III C. The imaginary and real parts of the self-energy upon re-summation are discussed in Secs. III D and III E, respectively. In Sec. III F, we demonstrate that the spectral function exhibits a non-monotonic variation near the mass shell due to the interaction of fermions with the zero-sound mode. In Sec. IV, we discuss the non-analytic contribution to the specific heat in two ways. First, in Sec. IV A, we find  $C(T)$  via the self-energy, utilizing the results of Sec. III. Then, in Sec. IV B, we evaluate the non-analytic part of the thermodynamic potential directly. In Sec. IV C, we consider the specific heat in a generic Fermi liquid. In Sec. IV C 3, we consider the case of a Coulomb potential. Our conclusions are given in Sec. V. Details of some of the calculations are presented in Appendices A-F.

For the convenience of a reader, we present below a summary of the main results of this paper.

## A. Summary of the results

### 1. Self-energy

In Secs. II-III, we consider mostly a 2D system of fermions with a weak, short-range repulsive interaction, specified by its Fourier-transform  $U(Q)$ . The self-energy of such a system consists of two parts: a analytic one and a non-analytic one. The analytic part of the self-energy,

$$\Sigma_{\text{an}} = a\omega + b\epsilon_k + c i\omega^2, \quad (1.1)$$

where  $a, b$ , and  $c$  are real, is determined by scattering events with large momentum transfers, of order  $k_F$ . In this paper, we will be interested only in the non-analytic part of the self-energy, which comes from two types of effectively 1D scattering processes. In the first type (“forward scattering”), all four momenta—two incoming and two outgoing—align almost along the same direction [cf. Fig. 1(a)]. In the second type (“backscattering”), both the initial and final momenta of the fermion pair are close to zero, while the momentum transfer can be near either zero or  $2k_F$  [cf. Figs. 1(b) and (c)]. The angular spreading of the trajectories shrinks in the low-energy limit in proportion to  $|\omega|/E_F$  for both types of scattering. To second order in the interaction and for a linearized single-particle spectrum [ $\epsilon_k = v_F(k - k_F)$ ], the forward (F) and backscattering (B) contributions to the self-energy near the mass shell are [23, 24, 25], [13]

$$\text{Re}\Sigma_{\text{F}}^R(\omega = \epsilon_k) = 0, \quad \text{Im}\Sigma_{\text{F}}^R(\omega, k) = \frac{u^2}{8\pi} \frac{\omega^2}{E_F} \ln \frac{E_F}{|\Delta|}; \quad (1.2a)$$

$$\text{Re}\Sigma_{\text{B}}^R(\omega = \epsilon_k) = -\frac{u_0^2 + u_{2k_F}^2 - u_0 u_{2k_F}}{8} \frac{\omega|\omega|}{E_F}, \quad \text{Im}\Sigma_{\text{B}}^R(\omega, k) = \frac{u_0^2 + u_{2k_F}^2 - u_0 u_{2k_F}}{4\pi} \frac{\omega^2}{E_F} \ln \frac{E_F}{|\omega|}. \quad (1.2b)$$

Here  $E_F = k_F v_F/2$  is the Fermi energy,

$$u_0 \equiv \frac{mU(0)}{2\pi}, \quad u_{2k_F} \equiv \frac{mU(2k_F)}{2\pi} \quad (1.3)$$

are the dimensionless coupling constants which are assumed to be small, and

$$\Delta \equiv \omega - \epsilon_k, \quad (1.4)$$

is the “distance” to the mass shell. On the Fermi surface ( $\epsilon_k = 0$ ),  $\text{Im}\Sigma^R = \text{Im}\Sigma_{\text{F}}^R + \text{Im}\Sigma_{\text{B}}^R$  reduces to a familiar form  $\text{Im}\Sigma^R(\omega, k_F) \propto \omega^2 \ln |\omega|$  [28].

The special role of backscattering processes for the non-analytic corrections to thermodynamic variables of a FL has been considered earlier by two of us [13]. In this paper, we present a complete description of forward-scattering processes. The peculiarities of these processes show up already at the second order: we see from Eq. (1.2a) that on the mass shell, where  $\Delta = 0$ ,  $\text{Im}\Sigma_{\text{F}}^R$  diverges logarithmically. The divergence is regularized [23, 24, 25], [13] by restoring a finite curvature of the single-particle spectrum,  $m_c^{-1} \equiv \partial^2 \epsilon_k / \partial k_{\perp}^2$ , where  $\mathbf{k}_{\perp}$  is the component of  $\mathbf{k}$  transverse to the local Fermi velocity  $\mathbf{v}_F(\mathbf{k})$ . Finite curvature brings in a new scale

$$\Delta_c \equiv \omega^2/W, \quad (1.5)$$

where  $W \equiv m_c v_F^2/2$ , and the logarithmic singularity in Eq. (1.2a) is rounded off at  $\Delta \simeq \Delta_c$ .

At a first glance, this regularization stabilizes the perturbation theory. However, starting from the third order in the interaction, the divergences due to forward scattering become of a power-law form; for a linearized spectrum, we find

$$\text{Im}\Sigma_{\text{F}}^R(\omega, k) \propto (u_0^2 |\omega/\Delta|)^{n/2-1}, \quad (1.6)$$

where  $n$  is the order of the perturbation theory. Finite curvature rounds off the power-law singularity on a scale  $\Delta \simeq \Delta_c$  at every given order, but the resulting series for the self-energy holds in parameter  $\omega_c/|\omega|$ , where  $\omega_c \equiv u_0^2 W/2$ , and does not converge for  $|\omega| < \omega_c$ . *Therefore, the perturbation theory in 2D must be re-summed even for an infinitesimally weak interaction and realistic fermion spectrum.* We show that the most divergent contributions to the forward-scattering part of the self-energy can be re-summed exactly to all orders in  $u_0$ , without exploiting RPA-type approximations.

Upon re-summation, the origin of the mass-shell singularities in the perturbation theory becomes clear: they correspond to the interaction between fermions and the zero-sound (ZS) collective mode. At every finite order of the perturbation theory, the collective mode coincides with the upper edge of the particle-hole continuum, and this degeneracy generates divergences in  $\Sigma_{\text{F}}^R$ . Once the perturbations are summed up to all orders, the ZS mode splits off from the continuum, and the power-law divergences disappear. The remaining logarithmic singularity is eliminated by the finite curvature.

The total self-energy after re-summation is described by a scaling function of two variables  $\Delta/\Delta_c$  and  $\Delta/\Delta^*$ , where  $\Delta_c$  is defined in Eq. (1.5), and

$$\Delta^* \equiv u_0^2 \omega/2. \quad (1.7)$$

is the scale at which perturbation series Eq. (1.6) diverges for a linearized spectrum. A general form of the scaling function is rather complicated, and will be discussed in the main text of the paper. In the limit  $\Delta \rightarrow 0$ , when both

scaling variables are small, and also for low frequencies,  $\Sigma^R$  reduces to

$$\text{Re}\Sigma^R(\omega = \epsilon_k) = \frac{u_{2k_F}(u_0 - u_{2k_F})\omega|\omega|}{8E_F}, \quad (1.8a)$$

$$\text{Im}\Sigma^R(\omega = \epsilon_k) = \frac{u_0^2\omega^2}{4\pi E_F} \ln \frac{W}{|\omega|}, \quad (1.8b)$$

Comparing Eq. (1.8a), (1.8b) with the second-order self-energy, [Eq. (1.2a), (1.2b)], we see that the re-summation (i) eliminates the divergence in  $\text{Im}\Sigma^R(\omega = \epsilon_k)$  and (ii) drastically changes the result for  $\text{Re}\Sigma^R(\omega = \epsilon_k)$ . In particular, for a constant interaction ( $u_0 = u_{2k_F}$ ), re-summation of higher-order terms in the self-energy cancels out the second-order term, so that full  $\text{Re}\Sigma^R(\omega = \epsilon_k)$  vanishes.

Perhaps the most essential result of our analysis is that the interaction with the zero-sound not only leads to a scaling behavior of the self-energy, but also results in a singularity of the self-energy: the derivative  $d\text{Im}\Sigma^R/d\Delta$  diverges as  $1/\sqrt{\Delta - \Delta^*}$  at  $\Delta = \Delta^*$ . This singularity is present in the non-perturbative regime, *i.e.*, for  $|\omega| < \omega_c$ . Physically, it corresponds to a change in kinematics of ZS waves emission. On the mass-shell ( $\Delta = 0$ ), emission of ZS waves by fermions is impossible as the zero-sound velocity is larger than the Fermi one. For  $0 < \Delta < \Delta^*$ , emission is possible but it is subject to a Cherenkov-type restriction: a fermion with frequency  $\omega > 0$  can only emit a ZS wave in the frequency interval  $\Omega < \omega\Delta/\Delta^*$ . For  $\Delta > \Delta^*$ , emission of ZS waves in the whole interval  $0 < \Omega < \omega$  becomes possible. The self-energy is singular right at the onset of the Cherenkov-type restriction for emission of ZS waves.

The singularity in the self-energy translates into a kink in the spectral function,  $A(\omega, k) = -\pi^{-1}\text{Im}G^R(\omega, k)$  at  $\Delta = \Delta^*$  (cf. Fig. 6). This effect is actually present for both short-range and Coulomb interaction. For the latter, the collective mode is a plasmon, and the kink is positioned near the Fermi surface, where  $\epsilon_k = 0$  (or  $\Delta = \omega$ ). The prediction for a kink  $A(\omega, k)$  can be verified in angle-resolved photoemission on layered compounds [29] or in momentum-conserving tunneling between two parallel layers of 2D electron gas [30].

## 2. specific heat

In the second part of the paper (Sec. IV), we analyze the non-analytic behavior of the specific heat,  $C(T)$ , for three types of interaction: i) short-range, weak repulsion; ii) Coulomb interaction; and iii) generic Fermi-liquid interaction. For all three cases, we find that a non-analytic term in  $C(T)$  behaves as  $T^2$ . In the perturbation theory, an origin of this term can be simply related to a non-analytic,  $\omega|\omega|$  form of the real part of the self-energy. To second order in the interaction, a non-analytic part of  $C(T)$

$$\delta C(T) \equiv C(T) - \gamma T, \quad (1.9)$$

where  $\gamma$  is the (interaction-dependent) Sommerfeld factor, was shown earlier [13] to be

$$\delta C(T)/T = - (u_0^2 + u_{2k_F}^2 - u_0 u_{2k_F}) \frac{9\zeta(3)}{\pi^2} C_{\text{FG}}/E_F, \quad (1.10)$$

where

$$C_{\text{FG}} = m\pi T/3 \quad (1.11)$$

is the specific heat of a Fermi gas [Eq. (1.11)] (see also Refs. [12, 14, 31]).

The issue considered in this paper is whether  $\delta C(T)$  is affected by the interactions of fermions with the zero-sound mode. At a first glance, it should be. Indeed,  $C(T)$  is related to an exact retarded Green's function  $G^R(\omega, k) = [\omega - \epsilon_k + \Sigma^R(\omega, k)]^{-1}$  via [1]

$$C(T)/T = -\frac{2}{\pi} \frac{\partial}{\partial T} \left[ \frac{1}{T} \int \frac{d^2k}{(2\pi)^2} \int_{-\infty}^{\infty} d\omega \omega \frac{\partial n_0}{\partial \omega} \arg G^R(\omega, k) \right], \quad (1.12)$$

where  $n_0$  is the Fermi distribution function. As the real part of the self-energy is changed significantly by a non-perturbative contribution from the ZS mode, the corresponding change in  $G^R$  should *a priori* affect  $C(T)$ . However, we see from Eq. (1.12) that—contrary to the common wisdom— not only the real but also the imaginary part of  $\Sigma^R$  affect  $C(T)$ . Indeed, at low frequencies, which we only need at small  $T$ , both perturbative and non-perturbative parts of the self-energy are asymptotically smaller than  $|\omega|$ ; thus  $G^R$  in Eq. (1.12) can be expanded to first order in  $\Sigma^R$  with the result

$$\delta C(T)/T = \frac{2}{\pi} \frac{\partial}{\partial T} \left[ \frac{1}{T} \int \frac{d^2k}{(2\pi)^2} \int_{-\infty}^{\infty} d\omega \omega \frac{\partial n_0}{\partial \omega} \{ \text{Re}\Sigma^R(\omega, k)\text{Im}G_0^R(\omega, k) + \text{Im}\Sigma^R(\omega, k)\text{Re}G_0^R(\omega, k) \} \right]. \quad (1.13)$$

Substituting the second-order result for  $\text{Re}\Sigma^R$ , Eq. (1.2b), into Eq. (1.13), we indeed reproduce the  $T$ -dependence of  $\delta C(T)/T$ , as given by Eq. (1.10) (more care is required to reproduce a numerical prefactor as it turns out that one should use an expression for  $\text{Re}\Sigma^R(\omega, k)$  at finite temperatures—cf. Sec. IV A). The perturbative part of  $\text{Im}\Sigma^R(\omega, k)$  does not contribute to the specific heat as it depends on  $\omega$  but not on  $k$ ; as a result, the second term in Eq. (1.13) vanishes by parity upon switching from integration over  $d^2k$  to that over  $d\epsilon_k$ . However, the non-perturbative contribution to  $\text{Im}\Sigma^R(\omega, k)$  due to the interaction with the zero-sound mode depends strongly on  $k$ . As a result, both  $\text{Re}\Sigma^R(\omega, k)$  and  $\text{Im}\Sigma^R(\omega, k)$  contribute to  $C(T)$ . We show that non-perturbative terms in these two contributions *cancel* each other, *i.e.*, there is no non-perturbative contribution to the specific heat. A non-analytic,  $T^2$ -term in  $\delta C(T)$  then comes entirely from the perturbative part of  $\Sigma^R$ , and Eq. (1.10) is the complete result for  $\delta C(T)$  to second order in the interaction.

Another way to understand an absence of the non-perturbative contribution to the specific heat is to evaluate the thermodynamic potential,  $\Xi$ , directly in Matsubara frequencies, and then use the relation between  $\Xi$  and  $C(T)$ . This is done in Sec. IV B. In contrast to the real-frequency description of the self-energy, there are no singularities at any order of the perturbation theory for  $\Xi$  in Matsubara frequencies. This means that, as long as the interaction is weak, one can truncate the perturbative series at an arbitrary order and be sure that the higher-order terms would give only sub-leading contributions. In this approach, *there simply cannot be non-perturbative contributions to the thermodynamic potential*, and hence to  $C(T)$ . To second order, this procedure gives the same result as in Eq. (1.10). For completeness, we also evaluate thermodynamic potential in real frequencies and demonstrate explicitly how the collective-mode contribution to the specific heat cancels out.

Finally, we extend our analysis to a Fermi liquid with not necessarily weak interaction. We find that the  $T^2$  term in the specific heat for a generic Fermi liquid is expressed via the charge (c) and spin (s) components,  $f_{c,s}(\theta)$ , of the quasi-particle scattering amplitude between particles at the Fermi surface, at angle  $\theta = \pi$  between two incoming momenta as

$$\delta C(T)/T = -\frac{3\zeta(3)}{2\pi (v_F^*)^2} [f_c^2(\pi) + 3f_s^2(\pi)] T, \quad (1.14)$$

where  $v_F^* = k_F/m^*$  and  $m^*$  is the renormalized effective mass. We remind the reader that the scattering amplitude (as a tensor in the spin space) is related to a particular limiting form of the interaction vertex,  $\Gamma_a^k(\theta)$ , as [1, 2]

$$\hat{f}(\theta) = Z^2 \hat{\Gamma}^k(\theta), \quad (1.15)$$

where

$$\hat{\Gamma}^k(\theta) = \lim_{|\Omega|/Q \rightarrow 0} \hat{\Gamma}(k_F \hat{n}_1, 0; k_F \hat{n}_2, 0 | \mathbf{Q}, \Omega), \quad (1.16)$$

where  $\hat{\Gamma}(\mathbf{k}_1, \omega_1; \mathbf{k}_2, \omega_2 | \mathbf{Q}, \Omega)$  is the vertex for a process  $(\mathbf{k}_1, \omega_1; \mathbf{k}_2, \omega_2 \rightarrow \mathbf{k}_1 - \mathbf{Q}, \omega - \Omega; \mathbf{k}_2 + \mathbf{Q}, \omega + \Omega)$ , and  $\theta$  is the angle between  $\mathbf{k}_1$  and  $\mathbf{k}_2$ . In the FL theory, the renormalizations of the thermodynamic quantities are expressed via the angular moments of the Landau interaction function, which is related to another limiting form of the vertex,

$$\hat{\Gamma}^\omega(\theta) = \lim_{Q/|\Omega| \rightarrow 0} \hat{\Gamma}(k_F \hat{n}_1, 0; k_F \hat{n}_2, 0 | \mathbf{Q}, \Omega). \quad (1.17)$$

Simple algebraic relations between the *partial components* of  $\hat{\Gamma}^k(\theta)$  and  $\hat{\Gamma}^\omega(\theta)$  enable one to express the analytic parts of thermodynamic quantities either via the moments of the Landau interaction function or that of the scattering amplitude. However, the non-analytic,  $T^2$ - part of the specific heat is related to  $\hat{\Gamma}^k(\theta)$  at a particular angle ( $\theta = \pi$ ), rather than to its angular average. As there is no simple relation between  $\hat{\Gamma}^k(\theta)$  and  $\hat{\Gamma}^\omega(\theta)$  for any given angle, including  $\theta = \pi$ , the non-analytic in the specific heat in general *cannot* be expressed in a compact form in terms of the Landau interaction function without making additional model approximations [9]. In this respect, our result for  $\delta C(T)$  differs from that of Ref. [31], where  $\delta C(T)$  was expressed via the charge and spin components of a single Landau parameter  $\hat{F}^0 \propto \int d\theta \hat{\Gamma}^\omega(\theta)$ . We did, however, obtain  $\delta C(T)$  in terms of  $\hat{\Gamma}^\omega(\pi)$  in the limit when its charge component is much larger than the spin one. The limit when the charge component tends to infinity whereas the spin one tends to zero describes the Coulomb interaction in the high-density limit. In this case, we find that the  $T^2$  term in  $C(T)$  is universal and independent of the electron charge [cf. Eq. (4.57)], in agreement with Ref. [31].

In the rest of the paper we present the details of our analysis.

## II. SCATTERING PROCESSES

In a typical event of interaction between low-energy quasi-particles with momenta  $k_1 \approx k_2 \approx k_F$ , the change in the momentum of a given quasi-particle,  $\delta k \equiv |\mathbf{k}_1 - \mathbf{k}'_1|$ , is of order  $k_F$ , but not necessarily close either to zero or to

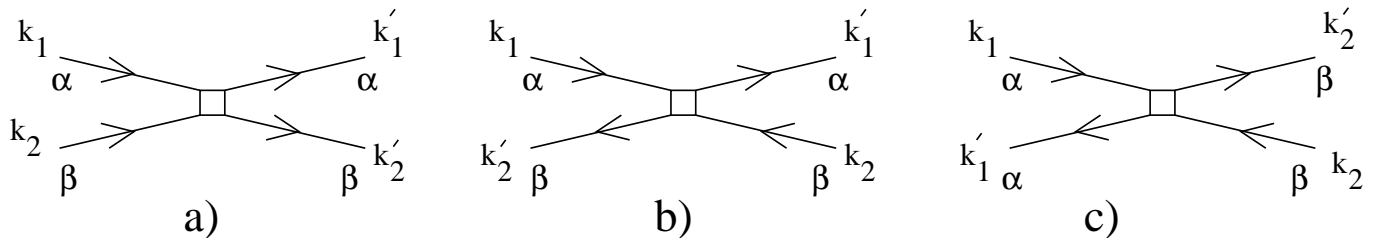


FIG. 1: Scattering processes responsible for divergent and/or non-analytic corrections to the self-energy in 2D. a) “Forward scattering”—an analog of the “ $g_4$ ”-process in 1D. All four fermion momenta are close to each other. b) Backscattering—an analog of the “ $g_2$ ”-process in 1D. The net momentum before and after collision is small. Initial momenta are close to the final ones. Although the momentum transfer in such a process is small, we still refer to this process as “backscattering” (see the discussion in the main text). c) Another component of the backscattering process:  $2k_F$ -scattering.

$2k_F$ . These large-angle scattering events are responsible for the analytic part of the self-energy, Eq. (1.1). In addition, there are special scattering events in which either  $\delta k \simeq |\Omega|/v_F \ll k_F$  or  $|\delta k - 2k_F| \simeq |\Omega|/v_F \ll k_F$ , where  $\Omega$  is the energy transfer. Although the phase space associated with these events is small for  $D > 1$ , these processes give rise to non-analyticities in the dynamic density-density correlation function and eventually determine non-analyticities in  $\Sigma(\omega)$  [13]. The role of these special processes increases as the dimensionality is reduced. For  $D = 3$ , the non-analytic part of the self-energy  $\Sigma_{\text{na}} \propto \omega^3 \ln(-i\omega)$ , resulting from the special processes, is sub-leading to the analytic one, resulting from the generic processes. However, already for  $D = 2$ , the non-analytic part ( $\Sigma_a \propto i\omega^2 \ln(-i\omega)$ ) dominates over the analytic one.

In 2D, kinematics of processes with small momentum is essentially *one-dimensional*, *i.e.*, the initial and final momenta of two interacting fermions are either almost parallel or antiparallel to each other. (In 3D, both 1D and non-1D processes contribute to the non-analytic behavior.) Accordingly, these processes can be divided into two types. In the first type, the two colliding particles move initially almost in the same direction ( $\mathbf{k}_1 \approx \mathbf{k}_2$ ) and retain their respective momenta after the collision, so that all four momenta (two initial and two final) are close to each other

$$\mathbf{k}'_1 \approx \mathbf{k}_1 \approx \mathbf{k}_2 \approx \mathbf{k}'_2. \quad (2.1)$$

This type of process is shown in Fig. 1(a). In  $g$ -ology [32], such an event is called “ $g_4$ -scattering”. The deviation from the purely 1D kinematics is due to finite energy transfers: a typical angle between momenta in Fig. 1(a) is of order  $|\omega|/v_F k_F \ll 1$ . In what follows, we will refer to the process in Fig. 1(a) as simply “forward scattering”. In the second type, the colliding particles move initially in almost opposite directions ( $\mathbf{k}_1 \approx -\mathbf{k}_2$ ) but, as for the forward scattering case, they also retain their respective momenta after the collision. The difference between such an event and the forward-scattering one is that not only the transferred but also the *total* initial and final momenta are small. This type of process is depicted in Fig. 1(b). In  $g$ -ology notations, this is a “ $g_2$ -process”.

Another process which contributes to the non-analytic part of  $\Sigma^R(\omega)$  is a “ $2k_F$ - process” (or  $g_1$ -scattering, in  $g$ -ology notations), in which two fermions moving initially in almost opposite directions, reverse their respective momenta [see Fig. 1(c)]. Since both processes in Figs. 1(b) and (c) contribute to the same scattering amplitude  $f(\mathbf{k}_1, \mathbf{k}_2)$  with the angle between *initial* momenta  $\mathbf{k}_1$  and  $\mathbf{k}_2$  being close to  $\pi$ , we will refer to both of them as “backscattering”. To distinguish between the two, we will refer to Fig. 1(b) as “ $g_2$ -backscattering” and to Fig. 1(c) as “ $2k_F$ - backscattering”.

Scattering by  $2k_F$  is one-dimensional in all dimensions. As we just said, forward- and backscattering become one-dimensional in  $D = 2$ . We thus conclude that for  $D = 2$  the non-analytic part of the self-energy comes from essentially 1D scattering processes, embedded into the 2D phase space.

We pause here for an important remark. Although there is a strong similarity between special scattering processes, resulting in non-analytic behavior in 2D, and their 1D analogs, there is also an important difference. Namely, neither  $g_2$  nor  $g_4$  processes lead to a non-analytic behavior of thermodynamic quantities in 1D. This is already obvious from the fact that a 1D Hamiltonian with a linearized spectrum and in the absence of  $g_1$ -scattering (Tomonaga-Luttinger model) allows for an exact diagonalization in terms of new excitations—free bosons. As a result, the specific heat is strictly linear in  $T$  and the spin susceptibility is simply a constant within the Tomonaga-Luttinger model. However, if  $g_1$ -scattering is present even as a marginally relevant perturbation, exact diagonalization in terms of free bosons is no longer possible, as the spin sector is now described by the sine-Gordon rather than Gaussian theory. This results in strong non-analyticities in both the specific heat  $\delta C(T) (\propto T \ln T)$  and spin susceptibility  $\delta \chi_s (\propto |\ln H|)$ , where  $H$

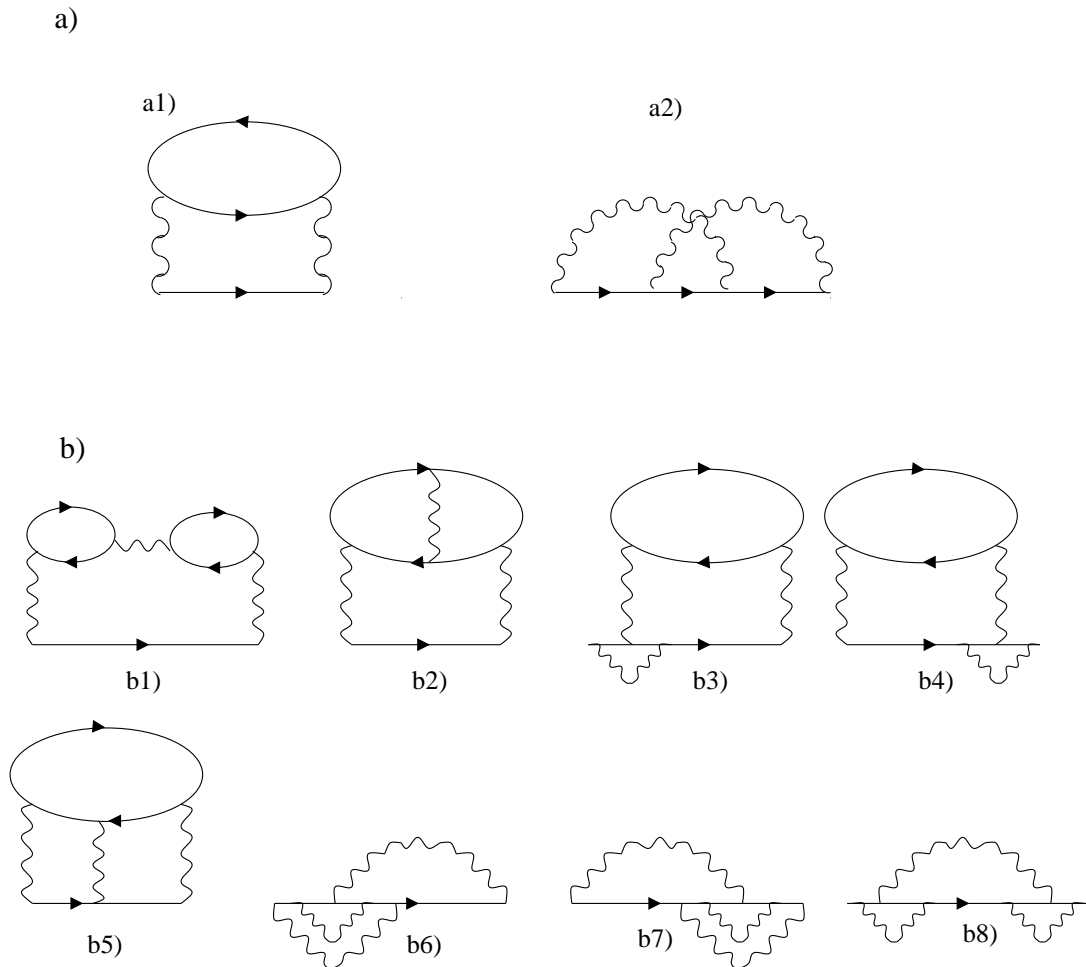


FIG. 2: Non-trivial second (a) and third (b) order diagrams for the self-energy.

is the magnetic field [33, 34]. It is possible to obtain these 1D non-analyticities within the same framework as their 2D analogs are analyzed in this paper, but we defer this discussion to a separate publication [35].

### III. SELF-ENERGY

In this Section, we derive an expression for the self-energy to all orders in the interaction. We analyze and resum the mass-shell singularities in the forward-scattering part of the self-energy, and also review the behavior of the backscattering part. For the sake of completeness, however, we start with the brief discussion of the second-order results for the self-energy. The fermion self-energy is defined via the Dyson equation

$$G^{-1} = G_0^{-1} + \Sigma, \quad (3.1)$$

where  $G_0$  and  $G$  are the bare and exact Green's functions, respectively. (Notice that we define  $\Sigma$  with an opposite sign compared to Refs. [1, 2].)

#### A. second order

To second order in the interaction, there are only two non-trivial diagrams for  $\Sigma$ , which are shown in Fig. 2(a). For a contact interaction,  $V(r) = U\delta(r)$ , the contribution from diagram (a2) is  $(-1/2)$  of that from diagram (a1). The

net contribution to the imaginary part of the retarded self-energy at  $T = 0$  is given by

$$\text{Im}\Sigma_2^R(\omega, k) = -U^2 \int_{-\omega}^0 \frac{d\Omega}{\pi} \int \frac{d^2Q}{(2\pi)^2} \text{Im}G_0^R(\omega + \Omega, \mathbf{k} + \mathbf{Q}) \text{Im}\Pi^R(\Omega, Q), \quad (3.2)$$

where  $G_0^R(\omega, k) = (\omega - \epsilon_k + i0^+)^{-1}$  is the free retarded Green's function,  $\Pi^R(\Omega, Q)$  is the polarization bubble of free fermions, and subindex 2 of the self-energy denotes the order of the perturbation theory. A general expression for  $\Pi^R(\Omega, Q)$  is rather complicated [36], but in what follows we will need only its two asymptotic forms. The first of these forms is valid for small  $Q$

$$\Pi^R(\Omega, Q) = -\frac{m}{2\pi} \left( 1 + \frac{i\Omega}{\sqrt{(v_F Q)^2 - (\Omega + i0^+)^2}} \right), \quad (3.3)$$

and the other one is valid near  $Q = 2k_F$

$$\Pi^R(\Omega, Q) = -\frac{m}{2\pi} \left( 1 - \left( \frac{Q - 2k_F}{2k_F} + \sqrt{\left( \frac{Q - 2k_F}{2k_F} \right)^2 - \left( \frac{\Omega + i0^+}{2k_F v_F} \right)^2} \right)^{1/2} \right). \quad (3.4)$$

Here  $m$  is the fermion's mass and  $v_F$  is the Fermi velocity. Non-analyticities in the two limiting forms of the bubble describe Landau damping and Kohn anomaly, respectively. Landau damping of an excitation with energy  $\Omega$  and momentum  $Q$  is possible only within the particle-hole (PH) continuum, *i.e.*, for  $\Omega < v_F Q$ . For  $\Omega \ll v_F Q$ , the non-analytic term in Eq. (3.3) scales as  $\Pi_{\text{sing}}^R(\Omega, Q) \propto i\Omega/|Q|$ . The Kohn anomaly near  $2k_F$  is static for  $Q > 2k_F$  [in this range, the non-analytic part of  $\Pi^R$  behaves as  $\Pi_{\text{sing}}^R(0, Q) \propto (Q - 2k_F)^{1/2}$ ] but is dynamic for  $Q < 2k_F$  [in this range,  $\Pi_{\text{sing}}^R(\Omega, Q) \propto i\Omega/(2k_F - Q)^{1/2}$ ].

### 1. backscattering

To logarithmic accuracy, both  $g_2$ - and  $2k_F$ -processes [Fig. 1(b) and (c), respectively] contribute equally to the non-analytic part of the fermion self-energy. For a contact interaction, the sum of the two contributions is [13]

$$\text{Im}\Sigma_{2,B}^R(\omega, k) = \frac{u^2}{4\pi} \frac{\omega^2}{E_F} \ln \frac{E_F}{|\omega|}, \quad (3.5)$$

where  $B$  stands for backscattering and  $u$  is defined in Eq. (1.3). It is important in what follows that, to logarithmic accuracy,  $\text{Im}\Sigma_{2,B}^R$  depends only on  $\omega$  but not on  $\epsilon_k$ . For the sake of completeness, we present the derivation of Eq. (3.5) in Appendix A. We find that for  $2k_F$ -processes, a non-analytic part of the self-energy originates from the *dynamic* Kohn anomaly, whereas the static Kohn anomaly contributes only to the regular part.

Higher-order contributions to the backscattering part of the self-energy form regular series in  $u$  which result in the renormalization of the prefactor. As we keep  $u$  small, it suffices to stop the perturbation theory at order  $u^2$ . Consequently, we set

$$\Sigma_B^R = \Sigma_{2,B}^R \quad (3.6)$$

in the rest of the paper.

### 2. forward scattering

The second-order forward-scattering contribution to the self-energy is given by [13]

$$\text{Im}\Sigma_{2,F}^R(\omega, k) = \frac{u^2}{8\pi} \frac{\omega^2}{E_F} \ln \frac{E_F}{|\Delta|}, \quad (3.7)$$

where  $F$  stands for forward scattering, and we remind that  $\Delta \equiv \omega - \epsilon_k$  is the “distance” to the mass shell. Away from the mass shell, this contribution behaves as  $\omega^2 \ln |\omega|$ , *i.e.*, it has the same functional form as  $\text{Im}\Sigma_B^R$ . In contrast to



the backscattering part, however, the forward-scattering contribution diverges at the mass shell, *i.e.*, for  $\Delta \rightarrow 0$ . The origin of this divergence can be traced back to the form of the polarization bubble at small momenta. From Eq. (3.3), we find that

$$\text{Im}\Pi^R(\Omega, Q) = -\left(\frac{m}{2\pi}\right) \frac{\Omega}{\sqrt{(v_F Q)^2 - \Omega^2}} \theta(v_F Q - |\Omega|), \quad (3.8)$$

where  $\theta(x)$  is the step function.  $\text{Im}\Pi^R(\Omega, Q)$  has square-root singularities at  $|\Omega| = v_F Q$ . On the other hand, expanding  $\epsilon_{\mathbf{k}+\mathbf{Q}}$  in  $G_0^R(\omega + \Omega, \mathbf{k} + \mathbf{Q})$  in Eq. (3.2) as  $\epsilon_{\mathbf{k}+\mathbf{Q}} = \epsilon_k + v_F Q \cos \theta$  and integrating over  $\theta$ , we obtain another square-root singularity

$$\int d\theta \text{Im}G_0^R = -\frac{2\pi}{\sqrt{(v_F Q)^2 - (\omega + \Omega - \epsilon_k)^2}}. \quad (3.9)$$

On the mass shell ( $\omega = \epsilon_k$ ), the arguments of the square roots in Eq. (3.8) and Eq. (3.9) coincide, hence the integral over  $d^2Q$  diverges logarithmically. **DM** (3.7) is valid only for a linearized fermion dispersion. Two of us demonstrated in Ref. [13] that finite curvature of the dispersion eliminates the logarithmic singularity in  $\text{Im}\Sigma_{2,F}^R$ . To keep our presentation uninterrupted, we continue to proceed with the analysis of the singularities due to forward scattering, assuming that the curvature is equal to zero, *i.e.*, the dispersion is linear. We then discuss separately the modifications imposed by a finite curvature of the dispersion (cf. Sec. III D 4). We emphasize again that the logarithmic singularity in the self-energy arises from essentially 1D scattering processes, embedded in a 2D phase space. Therefore, this singularity can be viewed as a pre-cursor of a stronger (power-law) singularity in 1D (“infrared catastrophe”) [26], [13]a.

### B. higher-order forward-scattering contributions

Higher orders of the perturbation theory contain more bubbles with small momenta (“soft bubbles”). As a result, the mass-shell singularities proliferate. The third-order diagrams, shown in Fig. 2, contain the square of the soft bubbles. These bubbles appear either explicitly (as in diagram b1) or are generated upon integrating over fermion energies/momenta in the rest of the diagrams. The singular part of the self-energy at this order is given by

$$\text{Im}\Sigma_{3,F}^R(\omega, k) = U^3 \int_{-\omega}^0 \frac{d\Omega}{2\pi} \int \frac{d^2Q}{(2\pi)^2} \text{Im}G_0^R(\omega + \Omega, \mathbf{k} + \mathbf{Q}) \Pi_2^R(\Omega, Q),$$

where

$$\Pi_2^R(\Omega, Q) \equiv \text{Im}\Pi^2(\Omega + i0^+, Q). \quad (3.10)$$

The most singular term in  $\Pi_2^R(\Omega, Q)$  is given by

$$[\Pi_2^R(\Omega, Q)]_{\text{sing}} = -(m/2\pi)^2 \pi \Omega |\Omega| \delta(\Omega^2 - v_F^2 Q^2). \quad (3.11)$$

The product of the square-root and delta-function singularities (from  $\int G_0^R d\theta$  and  $\Pi_2^R(\Omega, Q)$ , respectively) gives rise to a one-sided, square-root singularity on the mass shell:

$$\text{Im}\Sigma_{3,F}^R(\omega, k) = -\frac{\sqrt{2}u^3}{20} \frac{\omega^2}{E_F} \sqrt{\frac{\omega}{\Delta}} \theta\left(\frac{\omega}{\Delta}\right). \quad (3.12)$$

It can be readily verified that at  $n$ -th order

$$\text{Im}\Sigma_{n,F}^R \propto U^n \omega^{\frac{n}{2}+1} / \Delta^{\frac{n}{2}-1}, \quad (3.13)$$

for  $n > 2$ . Collecting forward-scattering contributions to all orders in  $u$ , we obtain

$$\text{Im}\Sigma_F^R(\omega) = \frac{u^2}{8\pi} \frac{\omega^2}{E_F} \left[ \ln \frac{E_F}{|\Delta|} + \sum_{n=1}^{\infty} C_n \left(u^2 \frac{\omega}{\Delta}\right)^{n/2} \right], \quad (3.14)$$

where  $C_n$  are the numerical coefficients. We see that perturbative expansion in  $u$  works only for  $u^2\omega/\Delta \ll 1$ . Outside this range, series in  $u$  does not converge, and one needs to re-sum the perturbation theory.

### C. Re-summation of forward-scattering contributions

To perform the re-summation of the perturbation theory, we need to select diagrams with the maximum number of particle-hole bubbles at small frequency/momentum. It is convenient to select first analogous diagrams for the four-fermion vertex,  $\Gamma_{\alpha\beta,\gamma\varepsilon}(p_1,p;p_3,p_4)$ , and then relate  $\Sigma$  to  $\Gamma$  via the Dyson equation. In this subsection, we will be using notations  $p \equiv (\omega_n, \mathbf{k})$  and  $q \equiv (\Omega_m, Q)$ , where  $\omega_m = \pi(2m+1)T$  and  $\Omega_m = 2\pi mT$ .

#### 1. four-fermion vertex, zero-sound mode

The diagrams for  $\Gamma$  with the maximum number of particle-hole bubbles form familiar ladder series (see Fig. 3), when  $\Gamma$  is anti-symmetrized with respect to a permutation of either initial or final states. However, the procedure of finding an overall prefactor at order  $\nu$  is somewhat involved [1], as it requires counting the number of diagrams at the same order in a conventional diagrammatic technique operating with a non-symmetrized vertex,  $\bar{\Gamma}$ . We choose to sum the diagrams for a non-symmetrized vertex to all orders first, and then anti-symmetrize the result. The second- and third-order diagrams for  $\bar{\Gamma}$  are shown in Fig. 3. A general procedure of summing such diagrams to all orders is described in Appendix B. It leads to the following result for  $\bar{\Gamma}$

$$\bar{\Gamma}_{\alpha\beta,\gamma\varepsilon}(p_1, p_2; p_1 - q, p_2 + q) = \bar{\Gamma}(q) = -U \left[ \delta_{\alpha\gamma} \delta_{\beta\varepsilon} \left( \frac{1}{2} + \mathcal{G}_\rho \right) + \sigma_{\alpha\gamma}^a \sigma_{\beta\varepsilon}^a \left( \frac{1}{2} + \mathcal{G}_\sigma \right) \right], \quad (3.15)$$

where  $\sigma_{\alpha\beta}^a$  are Pauli matrices ( $a = x, y, z$ ), and

$$\mathcal{G}_\rho \equiv \frac{1}{2} \frac{1}{1 - U\Pi(q)}; \quad \mathcal{G}_\sigma = -\frac{1}{2} \frac{1}{1 + U\Pi(q)} \quad (3.16)$$

are the (dimensionless) charge- and spin vertices, respectively. An anti-symmetrized vertex is obtained from  $\bar{\Gamma}$  by the following procedure

$$\Gamma_{\alpha\beta;\gamma\varepsilon}(q) = \bar{\Gamma}_{\alpha\beta;\gamma\varepsilon}(q) - \bar{\Gamma}_{\alpha\beta;\gamma\varepsilon\gamma}(q). \quad (3.17)$$

For the case of  $U > 0$ , which we are interested in, the retarded charge vertex,  $\mathcal{G}_\rho^R$ , has a pole determined from the equation  $1 - U\Pi^R(\mathbf{q}, \Omega) = 0$ . A two-particle excitation corresponding to the pole in  $\mathcal{G}_\rho$  is a zero-sound collective mode. Since  $\Pi^R$  is real for  $\Omega^2 > v_F^2 Q^2$ , and can be arbitrarily large (and positive) when  $|\Omega|$  approaches  $v_F Q$ , the zero-sound pole exists already for an arbitrarily small  $U$ . Near the pole,  $\mathcal{G}_\rho^R$  is of the form

$$\mathcal{G}_\rho^R = \frac{u^2 v_F^2 Q^2}{(\Omega + i0^+)^2 - c^2 Q^2}, \quad (3.18)$$

where  $c$  is the zero-sound velocity

$$c = v_F \sqrt{1 + u^2 / (1 + 2u)} \approx v_F (1 + u^2 / 2) > v_F. \quad (3.19)$$

We see that zero-sound velocity  $c$  differs from  $v_F$  only by a  $u^2$ -term. This means that the zero-sound mode  $|\Omega| = cQ$  is just above the upper boundary of the particle-hole continuum, which, for small  $Q$ , is given by  $v_F Q$ . We also see from Eq. (3.18) that the quanta of zero sound are *not* free bosons as the residue of the zero-sound pole in Eq. (3.18) is proportional to  $Q^2$ . The spin vertex ( $\mathcal{G}_\sigma^R$ ) also has a pole, but it is located on the imaginary axis. Consequently, the corresponding collective mode is over-damped. As an independent check, we verified that the diagrams in Fig. 3 sum up to zero for the case of spinless fermions. This result is a manifestation of the Pauli principle: spinless fermions do not interact via contact forces as the Pauli principle forbids them to be at the same point in space.

#### 2. Dyson equation

The self-energy due to forward scattering is related to the vertex function via the Dyson equation [2]

$$\Sigma_{\mathbf{F},\alpha\beta}(p) = \delta_{\alpha\beta} \int_q U G(p-q) - \int_{p',p''} U \Gamma_{\alpha;\gamma\beta}(p, p' + p'' - p; p', p'') G(p') G(p'') G(p' + p'' - p), \quad (3.20)$$

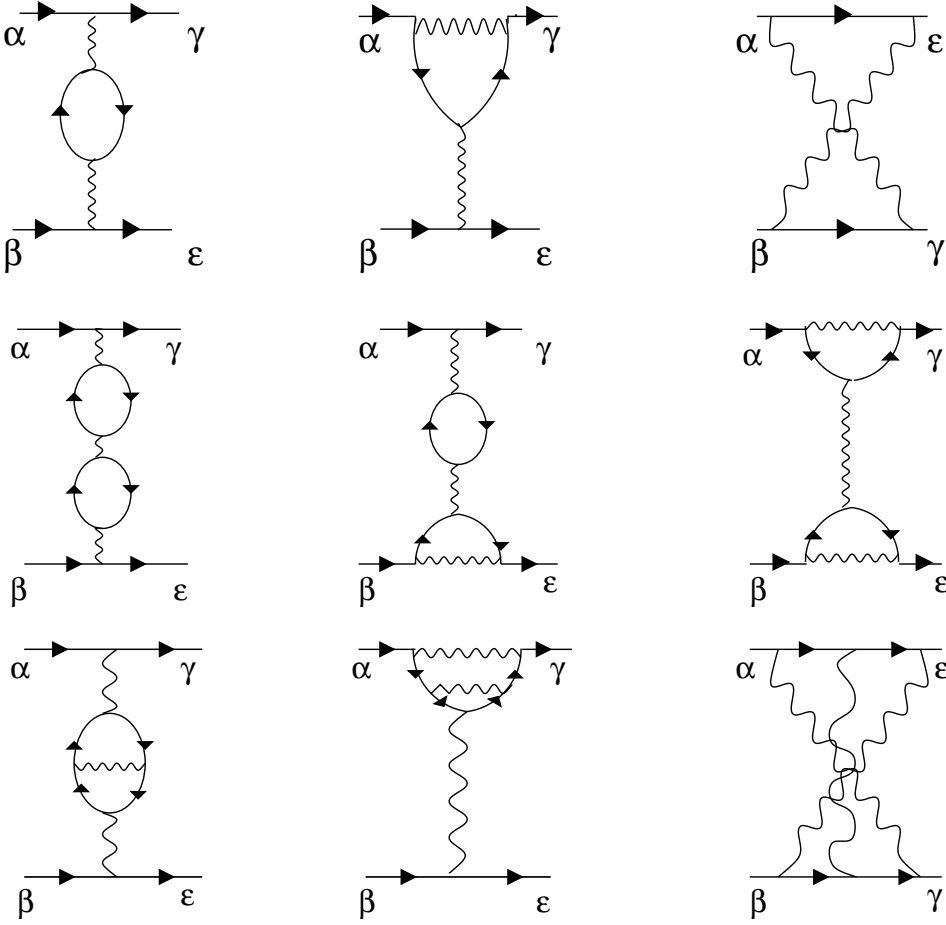


FIG. 3: Vertex diagrams with maximum number of particle-hole bubbles to third in the interaction. Additional diagrams, obtained from those in the second column by a permutation  $\alpha \rightarrow \beta, \gamma \rightarrow \epsilon$ , are not shown.

where

$$\int_k \dots \equiv T \sum_{\omega_m} \int d^2k / (2\pi)^2 \dots \quad (3.21)$$

In principle, the Green's functions in the Dyson equation are the exact ones. However, it can be verified that self-energy insertions into the diagrams diverging near the mass shell do not give rise to additional mass-shell singularities. As we keep  $u$  small, regular corrections are thus irrelevant, and we can safely use bare  $G$ 's instead of the exact ones in Eq. (3.20). Substituting Eq. (3.15) into Eq. (3.20), we obtain  $\Sigma_{\text{F},\alpha\beta} = \delta_{\alpha\beta} \Sigma_{\text{F}}$  where

$$\Sigma_{\text{F}}(p) = \int_q \left[ U + U^2 \Pi(q) + \frac{1}{2} \frac{U^3 \Pi^2(q)}{(1 - U \Pi(q))} - \frac{3}{2} \frac{U^3 \Pi^2(q)}{(1 + U \Pi(q))} \right] G(p - q). \quad (3.22)$$

Technical details of the derivation leading to Eq. (3.22) are presented in Appendix B. Expanding Eq. (3.22) to third order in  $U$ , we reproduce the results of the conventional perturbation theory, Eqs. (3.7) and (3.12). We remind that in the perturbation theory  $\text{Im} \Sigma^R$  diverges upon approaching the mass shell—logarithmically to second order in  $U$ , and as  $1/\sqrt{\omega - \epsilon_k}$  to third order. It is convenient to rearrange the terms in (3.22) and decompose  $\Sigma_{\text{F}}$  into three parts

making use of the charge- and spin vertices, introduced in Eq. (3.16), as

$$\Sigma_{\text{F}}(p) = \Sigma_{\rho}(p) + \Sigma_{\sigma}(p) + \Sigma_{\text{ex}}; \quad (3.23\text{a})$$

$$\Sigma_{\rho}(p) = U \int_q \mathcal{G}_{\rho}(q) G(p-q); \quad (3.23\text{b})$$

$$\Sigma_{\sigma}(p) = 3U \int_q \mathcal{G}_{\sigma}(q) G(p-q); \quad (3.23\text{c})$$

$$\Sigma_{\text{ex}} = \int_q [2U - U^2 \Pi(q)] G(p-q). \quad (3.23\text{d})$$

Terms  $\Sigma_{\rho}$  and  $\Sigma_{\sigma}$  correspond to the interaction in the charge- and spin channels, respectively, and are summed to all orders in  $U$ . The remainder,  $\Sigma_{\text{ex}}$ , contains extra contributions of the first and second orders in  $U$ , not included in the first two terms, reproduces the second-order result Eq. (3.7).

Before we proceed further, a comment is in order. Our results for the vertex and self-energy formally coincide with those found in the paramagnon (spin-fluctuation) model [8] (except for the remainder term,  $\Sigma_{\text{ex}}$ , in Eq. (3.23a) which was neglected in Ref. [8]). However, our results have been obtained in a more general approach. In the paramagnon model, the self-energy is given only by diagrams of the type (b1) and (b5) in Fig. 2, *i.e.*, it involves only RPA diagram in the charge-channel and ladder diagrams in the spin channel. We included *all* diagrams with the maximum number of bubbles and found that the overall combinatorial coefficients at each order are such that the summation to all orders results in two independent geometric series—one for the charge channel, and the other for the spin channel. It does not mean, however, that we have obtained exact results for  $\Gamma$  and  $\Sigma$ . Indeed, we considered only forward scattering, kept  $u$  small, and neglected all diagrams that constitute regular series in  $u$  and does not give rise to proliferating mass-shell singularities in  $\Sigma$ . From this perspective, the controlling parameter for our approximation is not the coupling constant  $u$  itself but a combined parameter  $u^2|\omega|/|\Delta|$  which measures the proximity to the mass shell. We sum up the series in  $u^2|\omega|/|\Delta|$ , and neglect regular corrections in  $u$  at every order.

#### D. Imaginary part of the self-energy to all orders in the interaction

We now evaluate the forward-scattering part of  $\text{Im}\Sigma^R$  near the mass shell. The imaginary part of the retarded self-energy comes from two sources: from the particle-hole continuum ( $|\Omega| < v_F Q$ ), where  $\text{Im}\Pi^R \neq 0$ , and from the collective mode at  $|\Omega| = cQ$ , where  $\mathcal{G}_{\rho}^R$  has a pole. The spin-channel part of the self-energy,  $\text{Im}\Sigma_{\sigma}^R$ , comes only from the continuum, whereas the charge-channel part contains contributions from both the continuum and collective mode. Accordingly, the imaginary part of the total self-energy can be represented as

$$\text{Im}\Sigma_{\text{F}}^R = \text{Im}\Sigma_{\text{PH}}^R + \text{Im}\Sigma_{\text{ZS}}^R + \text{Im}\Sigma_{\text{ex}}^R, \quad (3.24)$$

where  $(\dots)_{\text{PH}}$  and  $(\dots)_{\text{ZS}}$  stand for the particle-hole and zero-sound contributions, respectively:

$$\text{Im}\Sigma_{\text{PH}}^R = (\text{Im}\Sigma_{\rho}^R + \text{Im}\Sigma_{\sigma}^R)_{\text{PH}}, \quad \text{Im}\Sigma_{\text{ZS}}^R = (\text{Im}\Sigma_{\rho}^R)_{\text{ZS}}. \quad (3.25)$$

##### 1. remainder term $\Sigma_{\text{ex}}$

Comparing Eq. (3.23d) and Eq. (3.2), we see that the remainder term in decomposition Eq. (3.23a),  $\text{Im}\Sigma_{\text{ex}}^R$ , is opposite in sign and equal in magnitude to the second-order forward-scattering contribution to the self-energy, Eq. (3.7):

$$\text{Im}\Sigma_{\text{ex}}^R = -\frac{u^2}{8\pi} \frac{\omega^2}{E_F} \ln \frac{E_F}{|\Delta|}. \quad (3.26)$$

##### 2. particle-hole contribution

Term  $\text{Im}\Sigma_{\text{PH}}^R$  contains the imaginary parts of the retarded vertices in the charge- and spin channels:

$$\text{Im}\mathcal{G}_{\rho,\sigma}^R = \frac{1}{2} \frac{U \text{Im}\Pi^R}{(1 \mp U \text{Re}\Pi^R)^2 + (U \text{Im}\Pi^R)^2}. \quad (3.27)$$

The first term in the denominator of Eq. (3.27) can be replaced by unity because for  $q \leq 2k_F$ ,  $\text{Re}\Pi^R = -m/2\pi$ , *i.e.*,  $-U\text{Re}\Pi^R = u \ll 1$ . Substituting then Eq. (3.27) into Eq. (3.23b) and Eq. (3.23c), we obtain

$$\text{Im}\Sigma_{\text{PH}}^R = -2U^2 \int_{-\omega}^0 \frac{d\Omega}{\pi} \int \frac{d^2Q}{(2\pi)^2} \text{Im}G^R(\omega + \Omega, \mathbf{k} + \mathbf{Q}) \frac{\text{Im}\Pi^R}{1 + (U\text{Im}\Pi^R)^2}. \quad (3.28)$$

Substituting  $\text{Im}\Pi^R$  from Eq. (3.8) and  $\text{Im}G^R$  from Eq. (3.9) into Eq. (3.28) and keeping only the forward scattering contribution, we obtain after some algebra

$$\text{Im}\Sigma_{\text{PH}}^R = \frac{u^2}{4\pi} \frac{\omega^2}{E_F} \left[ \ln \frac{E_F}{u^2|\omega|} + G_I \left( \frac{2\Delta}{u^2|\omega|} \right) \right], \quad (3.29)$$

where

$$G_I(x) = 2 \ln 2 - 1/2 + \ln |x|^{-1} - 2 \text{Re} \int_0^1 z dz \frac{1}{\sqrt{1-x/z}} \ln \frac{1 + \sqrt{1-x/z}}{1 - \sqrt{1-x/z}}. \quad (3.30)$$

Subscript  $I$  in  $G_I$  implies that this is a scaling function for the imaginary part of the self-energy. We subtracted off a constant term in  $G_I$  so that  $G_I(0) = 0$ . This is equivalent to neglecting a regular,  $\omega^2$ -contribution to  $\text{Im}\Sigma_{\text{PH}}^R$ . A plot of  $G_I(x)$  is presented in Fig. 4. At large and positive  $x$ , the integral term in scaling function  $G_I(x)$  falls off as  $x^{-1/2}$ , whereas for large and negative  $x$ , it falls off as  $(-x)^{-1}$ . In either of these limits,  $G_I \approx \ln |x|^{-1}$  and, consequently,

$$\text{Im}\Sigma_{\text{PH}}^R = \frac{u^2}{4\pi} \frac{\omega^2}{E_F} \ln \frac{E_F}{|\Delta|}. \quad (3.31)$$

Further expansion in powers of  $1/x$  yields

$$\text{Im}\Sigma_{3,\text{PH}}^R = -2 \frac{\sqrt{2}u^3}{20} \frac{\omega^2}{E_F} \sqrt{\left| \frac{\omega}{\Delta} \right|}. \quad (3.32)$$

In the opposite limit of small  $x$ , function  $G_I(x)$  vanishes as  $x \ln |x|$ . As a result, net  $\text{Im}\Sigma_{\text{PH}}^R$  remains finite at  $\Delta = 0$ , and for  $x \ll 1$  (*i.e.*, for  $\Delta \ll u^2\omega$ ) it behaves as

$$\text{Im}\Sigma_{\text{PH}}^R = \frac{u^2}{4\pi} \frac{\omega^2}{E_F} \left[ \ln \frac{E_F}{u^2|\omega|} + \frac{2\Delta}{u^2\omega} \ln \frac{|\Delta|}{u^2|\omega|} \right]. \quad (3.33)$$

Comparing the limiting forms of Eq. (3.31) and Eq. (3.33), we see that higher order terms in  $u$  simply cut the logarithmic divergence in  $\text{Im}\Sigma_{\text{PH}}^R$  for  $|\Delta| < u^2|\omega|$ . To logarithmic accuracy, one can then approximate  $\text{Im}\Sigma_{\text{PH}}^R$  by

$$\text{Im}\Sigma_{\text{PH}}^R = \frac{u^2}{4\pi} \frac{\omega^2}{E_F} \ln \frac{E_F}{|w|}, \quad (3.34)$$

where  $w \equiv \max\{\Delta, u^2|\omega|\}$ . The appearance of  $u$  under the logarithm in Eq. (3.34) is a reminder that Eq. (3.34) includes all orders of the perturbation theory. Indeed, a crossover between Eqs. (3.31) and (3.33) occurs at a scale  $|\Delta| \simeq u^2|\omega|$ , which is not accessible within the perturbation theory.

### 3. zero-sound contribution

For the collective-mode contribution to the self-energy in the vicinity of the mass shell, *i.e.*, for  $|\Delta| \ll |\omega|$ , we obtain from Eq. (3.23b) and Eq. (3.27)

$$\text{Im}\Sigma_{\text{ZS}}^R = \frac{u^2U}{4\pi} \text{Re} \left[ \int_0^{|\omega|/v_F} \frac{QdQ}{\sqrt{(2\Delta/v_F Q) \text{sgn}\omega - u^2}} \right] = \frac{u^2}{4\pi} \frac{\omega^2}{E_F} F_I \left( \frac{2\Delta}{u^2\omega} \right). \quad (3.35)$$

For  $x > 0$ , scaling function  $F_I(x)$  is given by

$$F_I(x) \equiv 2\pi \int_0^{\min\{1, \sqrt{x}\}} dy \frac{y^4}{\sqrt{x-y^2}} = \begin{cases} 3\pi^2 x^2/8, & \text{for } x < 1; \\ \frac{\pi}{2} \left[ \frac{3x^2}{2} \sin^{-1} \frac{1}{\sqrt{x}} - \sqrt{x-1} \left( \frac{3}{2}x + 1 \right) \right], & \text{for } x > 1. \end{cases} \quad (3.36)$$

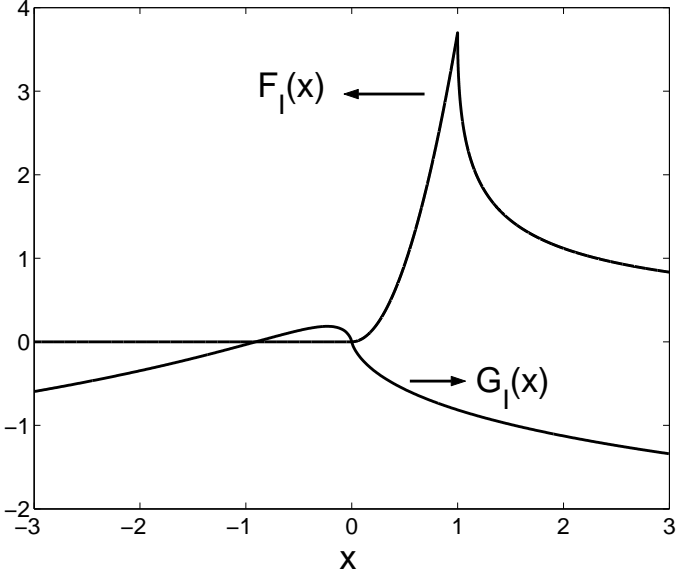


FIG. 4: Scaling functions  $G_I(x)$  [ Eq. (3.30)] and  $F_I(x)$  [ Eq. (3.36)].

For negative  $x$ ,  $F_I(x) = 0$ . At  $x = 1$ ,  $F_I(x)$  is continuous but its derivative is singular:  $dF_I(x)/dx \propto 1/\sqrt{x-1}$  for  $x > 1$ . A plot of  $F_I(x)$  is shown in Fig. 4. For  $x \gg 1$ , *i.e.*, for  $u \rightarrow 0$ ,

$$F_I(x) \approx 2\pi/5\sqrt{x}. \quad (3.37)$$

In this limit,  $F_I(x) \propto u$  and thus  $\text{Im}\Sigma_{ZS}^R \propto u^3$ , as is to be expected, as the zero-sound propagator,  $UG_\rho$ , is of third order in  $U$  near the pole. Substituting this limiting form into Eq. (3.35), we obtain for  $\omega/\Delta > 0$

$$\text{Im}\Sigma_{ZS}^R = \frac{\sqrt{2}u^3}{20} \frac{\omega^2}{E_F} \sqrt{\frac{\omega}{\Delta}}. \quad (3.38)$$

Combining Eq. (3.38) and the third-order particle-hole contribution as given in Eq. (3.32), we reproduce the result of the third-order perturbation theory, Eq. (3.12). Expanding  $(\text{Im}\Sigma_\rho)^R$  in powers of  $u$  further, we indeed reproduce the structure of higher order terms in the perturbation theory, Eq. (3.13). All these terms diverge when  $\Delta \rightarrow 0$ . However, the full result shows that the perturbative expansion in  $u$  for the zero-sound contribution is valid only for  $|\Delta| \gg u^2|\omega|$ . At  $|\Delta| = u^2|\omega|/2$ , *i.e.*, at  $x = 1$ ,  $\text{Im}\Sigma_{ZS}^R$  has a maximum. Upon further approach to the mass-shell,  $\text{Im}\Sigma_{ZS}^R$  decreases as  $\Delta^2$  and eventually vanishes on the mass shell ( $\Delta = 0$ ). Vanishing of  $\text{Im}\Sigma_{ZS}^R$  on the mass shell is due to a Cherenkov-type restriction: because the zero-sound velocity  $c > v_F$ , an on-shell fermion cannot emit a zero-sound boson, hence the fermion's lifetime becomes infinite.

Observe that  $\text{Im}\Sigma_{ZS}^R$  is asymmetric with respect to a change in sign of  $\Delta$ :  $\text{Im}\Sigma_{ZS}^R \neq 0$  only if  $\Delta$  and  $\omega$  are of the same sign. This asymmetry follows simply from the energy and momentum conservation. For example, a fermion of energy  $\omega > 0$  above the Fermi level can emit a soft zero-sound boson of frequency  $0 \leq \Omega \leq \omega$  provided that

$$\omega - \epsilon_k = \Omega - v_F Q \cos \theta = \Omega [1 - (v_F/c) \cos \theta], \quad (3.39)$$

which, for  $c \approx v_F (1 + u^2/2)$ , is equivalent to

$$0 \leq u^2\Omega/2 \leq \Delta \leq 2\Omega \leq 2\omega. \quad (3.40)$$

Thus, emission is possible only if both  $\omega$  and  $\Delta$  are positive. A similar consideration for the case when a fermion of energy  $\omega < 0$  below the Fermi level absorbs a zero-sound boson of frequency  $\Omega$  in the interval  $(-|\omega|, 0)$  shows that absorption is possible only for  $\Delta < 0$ . Eq. (3.40) also clarifies the meaning of a characteristic scale  $\Delta^* = \omega u^2/2$ . For  $\Delta > \Delta^*$  emission of bosons with any frequency in the interval  $0 \leq \Omega \leq \omega$  is possible. In particular, a fermion can emit only one boson of frequency  $\Omega = \omega$  and “land” on the Fermi level. For  $\Delta < \Delta^*$ , *i.e.*, when a fermion is close

to the Fermi level, emission of bosons with frequency  $\Omega > 2\Delta/u^2$  is impossible, and the fermion relaxes to the Fermi level via emitting a large number of low-frequency bosons. As a result, the relaxation slows down which corresponds to a decrease in  $\text{Im}\Sigma_{\text{ZS}}^R$  for  $\Delta < \Delta^*$ .

Combining the results for  $\Sigma_{\text{ex}}^R$ ,  $\Sigma_{\text{PH}}^R$  and  $\Sigma_{\text{ZS}}^R$ , we see that the summation of the power-law divergent diagrams for the self-energy leads to a non-trivial result: the total self-energy due to forward scattering undergoes a non-monotonic variation near the mass-shell. All power-law divergences of the form  $u^n \Delta^{1-n/2}$  are now eliminated. However, we still have a logarithmically divergent term  $\text{Im}\Sigma_{\text{ex}}^R$ , given by Eq. (3.26). As this term does not contain higher than the second order in  $u$ , its divergence can be cut only by a finite curvature of the fermion dispersion (see Sec. III D 4).

Notice also that the collective-mode contribution to  $\text{Im}\Sigma_{\text{F}}^R$  is smaller than the rest of the contributions by a large logarithm. Indeed, the maximum value of  $F_I(x)$  in Eq. (3.35) is of order one, so that  $\text{Im}\Sigma_{\text{ZS}}^R \lesssim u^2 \omega^2 / E_F$ , whereas

$$\text{Im}\Sigma_{\text{B}}^R \simeq \text{Im}\Sigma_{\text{PH}}^R \simeq \text{Im}\Sigma_{\text{ex}}^R \simeq (u^2 \omega^2 / E_F) \ln E_F / |\omega| \gg u^2 \omega^2 / E_F. \quad (3.41)$$

Still,  $\text{Im}\Sigma_{\text{ZS}}^R$  exhibits a non-monotonic and rapid variation near the mass shell at  $\Delta \simeq u^2 \omega \ll \omega$ , whereas other contributions are either constant or vary only smoothly on this scale. This feature will have consequences for the spectral function, discussed in Sec. III F.

#### 4. modifications due to a finite curvature of the fermion dispersion

As we have already mentioned in Sec. III A, the logarithmic mass-shell singularity in  $\text{Im}\Sigma_{\text{F}}^R$  at the second order can be eliminated by accounting for the finite curvature of the dispersion. Technically, this amounts to retaining the quadratic-in- $q$  term in the expansion of  $\epsilon_{\mathbf{k}+\mathbf{Q}}$  in  $\mathbf{Q}$ . A straightforward analysis shows [13] that the logarithmic singularity in the second-order diagram is cut at a certain distance to the mass shell  $|\Delta| \simeq \Delta_c$ , where, we remind,  $\Delta_c \equiv \omega^2 / W$ ,  $W = k_F^2 / (2m_c)$ , and  $1/m_c$  is the curvature. For the quadratic dispersion  $\epsilon_k = k^2 / (2m)$ ,  $m_c = m$ , hence  $W = E_F$ . For a non-quadratic dispersion,  $W$  and  $E_F$  are not equivalent, but, at least for any power-law spectrum, they are of the same order. Therefore we will not distinguish between  $W$  and  $E_F$  in the rest of the paper. Cutting the log-singularity in  $\text{Im}\Sigma_{2,\text{F}}^R$  at  $\Delta_c$ , we obtain

$$\text{Im}\Sigma_{2,\text{F}}^R(\Delta = 0, \omega) = \frac{u^2 \omega^2}{4\pi E_F} \ln \frac{E_F}{|\omega|}. \quad (3.42)$$

The net second-order self-energy, *i.e.*, the sum of backscattering and forward-scattering contributions, is then given by

$$\text{Im}\Sigma_2^R(\omega) = \text{Im}\Sigma_{\text{B}}^R(\omega) + \text{Im}\Sigma_{2,\text{F}}^R(\omega, \Delta = 0) = 2\text{Im}\Sigma_{\text{B}}^R(\omega) = \frac{u^2 \omega^2}{2\pi E_F} \ln \frac{E_F}{|\omega|}. \quad (3.43)$$

The elimination of  $\ln|\Delta|$  singularity at the second order does not eliminate the need for re-summation of the perturbation theory, since higher-order terms diverge as powers of  $|\Delta|^{-1}$ . Indeed, cutting the singularities at  $|\Delta| = \Delta_c$  in the general expression Eq. (3.14) for  $\text{Im}\Sigma_{\text{F}}^R(\omega)$ , we obtain

$$\text{Im}\Sigma_{\text{F}}^R(\omega) = \frac{u^2 \omega^2}{4\pi E_F} \left[ \ln \frac{E_F}{|\omega|} + \sum_{n=1}^{\infty} C_n \left( \frac{\omega_c}{\omega} \right)^{n/2} \right], \quad (3.44)$$

where

$$\omega_c \equiv u^2 E_F \simeq \frac{\omega^2}{u^2} \Delta_c. \quad (3.45)$$

Obviously, the series for  $\text{Im}\Sigma_{\text{F}}^R$  does not converge for  $|\omega| \lesssim \omega_c$ , *i.e.*, one still needs to re-sum the perturbation theory. We already know, however, that all power-law divergences are eliminated after such re-summation even for infinite  $\omega_c$ . Finite curvature is not going to modify the results for  $\Delta \gg \Delta_c$ . For arbitrary  $\Delta$ , inclusion of the curvature will modify scaling functions  $F_I$  and  $G_I$ , which will now depend on two variables:  $F_I(2\Delta/(u^2\omega), \Delta/\Delta_c)$  and  $G_I(2\Delta/(u^2\omega), \Delta/\Delta_c)$ . We have not attempted to determine the most general form of these functions. However, we can make certain conclusions about their behavior near the mass shell. Indeed, as power-law singularities are cut at  $\Delta_c$ , a particular contribution to the self-energy for  $\Delta \ll \Delta_c$  is obtained by taking an explicit result for this contribution for  $\Delta \gg \Delta_c$  and replacing  $\Delta$  by  $\Delta_c$ . For example, the particle-hole contribution, given by Eq. (3.29) for  $\Delta \gg \Delta_c$ , takes the following form for  $\Delta \ll \Delta_c$ :

$$\text{Im}\Sigma_{\text{PH}}^R = \frac{u^2 \omega^2}{4\pi E_F} \left[ \ln \frac{E_F}{u^2 |\omega|} + G_I \left( \frac{2|\omega|}{\omega_c} \right) \right]. \quad (3.46)$$

Function  $G_I(x)$  in this form is still given by Eq. (3.30). We recall that  $G_I(x)$  behaves as  $\ln|x|^{-1}$  and  $x \ln|x|$  for  $|x| \gg 1$  and  $|x| \ll 1$ , correspondingly. Using the small- $x$  asymptotic form of  $G_I(x)$ , we find that the second term in Eq. (3.46) is much smaller than the first one for  $|\omega| \ll \omega_c$ . Therefore,  $\text{Im}\Sigma_{\text{PH}}^R$  in this limit is given by

$$\text{Im}\Sigma_{\text{PH}}^R(\omega) = \frac{u^2}{4\pi} \frac{\omega^2}{E_F} \ln \frac{E_F}{u^2|\omega|}, \quad \text{for } \omega \ll \omega_c. \quad (3.47)$$

The opposite limit of  $|\omega| \gg \omega_c$  (large  $x$ ) exists only for a finite curvature. In this limit,  $\text{Im}\Sigma_{\text{PH}}^R$  reduces to

$$\text{Im}\Sigma_{\text{PH}}^R(\omega) = \frac{u^2}{2\pi} \frac{\omega^2}{E_F} \ln \frac{E_F}{|\omega|}, \quad \text{for } \omega \gg \omega_c. \quad (3.48)$$

A similar procedure is applied to the contribution from  $\text{Im}\Sigma_{\text{ex}}^R$ . Away from the mass-shell,  $\text{Im}\Sigma_{\text{ex}}^R$  is given by Eq. (3.26). A finite curvature cuts the infrared logarithmic divergence in the same way as in the second-order diagram. As a result, we obtain on the mass shell

$$\text{Im}\Sigma_{\text{ex}}^R(\omega) = -\frac{u^2}{4\pi} \frac{\omega^2}{E_F} \ln \frac{E_F}{|\omega|}. \quad (3.49)$$

To logarithmic accuracy, a general form of  $\text{Im}\Sigma_{\text{ex}}^R$  can be written as

$$\text{Im}\Sigma_{\text{ex}}^R(\omega, \Delta) = -\frac{u^2}{8\pi} \frac{\omega^2}{E_F} \ln \frac{E_F}{\max\{|\Delta|, \Delta_c\}}. \quad (3.50)$$

Finally, the scaling function for the zero-sound contribution [ $F_I(x)$  from Eq. (3.36)] is small as a power-law of either  $x$  (for small  $x$ ) or  $x^{-1}$  (for large  $x$ ). Therefore, for both  $|\omega| \ll \omega_c$  and  $|\omega| \gg \omega_c$  regimes, the zero-sound contribution  $\text{Im}\Sigma_{\text{ZS}}^R$  can be neglected compared to  $\text{Im}\Sigma_{\text{PH}}^R + \text{Im}\Sigma_{\text{ex}}^R$ .

Combining the formulas for the mass-shell forms of  $\text{Im}\Sigma_{\text{PH}}^R$  [Eqs. (3.47) and (3.48)] and  $\text{Im}\Sigma_{\text{ex}}^R$  [Eq. (3.49)], we arrive at

$$\text{Im}\Sigma_{\text{F}}^R = \frac{u^2}{4\pi} \frac{\omega^2}{E_F} \times \begin{cases} |\ln u^2|, & \text{for } |\omega| \ll \omega_c; \\ \ln E_F/|\omega|, & \text{for } |\omega| \gg \omega_c. \end{cases} \quad (3.51)$$

Notice that for  $|\omega| \ll \omega_c$ , there is no  $\omega$ -dependence in the logarithm, *i.e.*, the frequency dependence of  $\text{Im}\Sigma_{\text{F}}^R$  is perfectly regular in this range of  $\omega$ . Notice also that  $\text{Im}\Sigma_{\text{F}}^R(\omega)$  remains positive for all frequencies, as it should in order for the quasi-particles to be stable.

## 5. final result for imaginary part of the self-energy on the mass shell

**a. contact potential** The net self-energy is a sum of forward scattering and backscattering contributions. On the mass shell ( $\Delta = 0$ ), forward- and backscattering contributions to  $\text{Im}\Sigma^R$  are equal to each other for  $|\omega| \gg \omega_c$  [see Eqs. (3.5) and (3.51)], whereas in the opposite limit of  $|\omega| \ll \omega_c$ , the forward-scattering part [Eq. (3.51)] is smaller by a large logarithmic factor than the backscattering one. The leading-order result for the on-shell  $\text{Im}\Sigma^R$  can then be written as

$$\text{Im}\Sigma^R(\omega) = \text{Im}\Sigma_{\text{F}}^R(\omega) + \text{Im}\Sigma_{\text{B}}^R(\omega) = \frac{u^2}{2\pi} \frac{\omega^2}{E_F} \ln \frac{E_F}{|\omega|} \Phi_0\left(\frac{|\omega|}{u^2 E_F}\right), \quad (3.52)$$

where

$$\Phi_0(x) = \begin{cases} 1, & \text{for } x \gg 1; \\ 1/2, & \text{for } x \ll 1. \end{cases} \quad (3.53)$$

As we see, the non-perturbative effect in  $\text{Im}\Sigma^R$  on the mass shell is rather benign: all we have is a smooth crossover function interpolating between two different values of the numerical prefactor in a familiar  $\omega^2 \ln|\omega|$ -dependence [28]. Away from the mass shell (at  $\Delta \neq 0$ ), the non-perturbative effect in  $\text{Im}\Sigma^R$  is much more pronounced, and a non-monotonic behavior of the zero-sound term (3.35, 3.36) gives rise to a non-monotonic variation of  $\text{Im}\Sigma^R$  near  $\Delta = 0$ . We will return to this issue in Sec. III F, where we discuss the spectral function.



*b. finite range potential* For a finite-range potential, a factor of  $u^2$  in the backscattering contribution is [13] replaced by  $u_0^2 + u_{2k_F}^2 - u_0 u_{2k_F}$ , where

$$u_0 \equiv mU(0)/2\pi, \quad u_{2k_F} \equiv mU(2k_F)/2\pi. \quad (3.54)$$

In the forward-scattering contribution,  $u$  is just replaced by  $u_0$ . As a result, the net imaginary part of the self-energy on the mass shell becomes

$$\text{Im}\Sigma^R(\omega) = \text{Im}\Sigma_F^R(\omega) + \text{Im}\Sigma_B^R(\omega) = \frac{u_0^2}{2\pi} \frac{\omega^2}{E_F} \ln \frac{E_F}{|\omega|} \Phi\left(\frac{|\omega|}{u_{\max}^2 E_F}\right), \quad (3.55)$$

where  $u_{\max} \equiv \max\{u_0, u_{2k_F}\}$ , and

$$\Phi(x) = \begin{cases} 1 + (2u_0)^{-1} u_{2k_F} (u_{2k_F} - u_0), & \text{for } x \gg 1; \\ 1/2 + (2u_0)^{-1} u_{2k_F} (u_{2k_F} - u_0), & \text{for } x \ll 1. \end{cases} \quad (3.56)$$

### E. Real part of the self-energy

Next, we consider what happens to  $\text{Re}\Sigma^R(\omega)$  near the mass shell. For definiteness, we consider  $\omega > 0$  but  $\Delta = \omega - \epsilon_k$  can be of any sign. The real part of the self-energy can be obtained either by a Kramers-Krönig transformation of  $\text{Im}\Sigma^R$  or directly, by evaluating the self-energy in Matsubara frequencies and analytically continuing it to real frequencies.

#### 1. backscattering

First, we present the result for the total backscattering contribution to the self-energy. (By “total”, we mean the sum of  $g_{2-}$  and  $2k_F-$  contributions). A Kramers-Krönig transformation of Eq. (3.5) yields, on the mass shell,

$$\text{Re}\Sigma_B^R(\omega) = \frac{2}{\pi} \mathcal{P} \int \frac{\text{Im}\Sigma_B^R(E, \epsilon_k = \omega)}{E - \omega} = -\frac{u^2}{8} \frac{\omega |\omega|}{E_F}. \quad (3.57)$$

A non-analytic,  $\omega|\omega|$ -behavior of  $\text{Re}\Sigma_B^R(\omega)$  is obviously related to a non-analytic,  $\omega^2 \ln|\omega|$ -behavior of  $\text{Im}\Sigma_B^R(\omega, k)$ .

#### 2. forward scattering

The real part of the self-energy consists of three contributions: from the remainder term ( $\Sigma_{\text{ex}}^R$ ), from the particle-hole continuum ( $\Sigma_{\text{PH}}^R$ ), and the from the collective mode ( $\Sigma_{\text{ZS}}^R$ ).

*a. remainder* Performing Kramers-Krönig transformation of  $\text{Im}\Sigma_{\text{ex}}^R$  (given by (3.26)), we find

$$\begin{aligned} \text{Re}\Sigma_{\text{ex}}^R(\omega, k) &= -\frac{u^2}{8\pi^2 E_F} \mathcal{P} \int_{-\infty}^{\infty} dz \frac{z^2}{z - \omega} \ln \frac{E_F}{|z - \epsilon_k|} \\ &= -\frac{u^2}{8\pi^2 E_F} \mathcal{P} \lim_{E_F \rightarrow \infty} \int_{-E_F}^{E_F} dx \frac{(x + \omega - \Delta)^2}{x - \Delta} \ln \frac{E_F}{|x|} \\ &= -\frac{u^2}{2\pi^2} \left( \omega - \frac{1}{2} \Delta \right) + \frac{u^2}{16} \frac{\omega |\omega|}{E_F} \text{sgn} \Delta + \mathcal{O}(E_F^{-2}) + \dots \end{aligned} \quad (3.58)$$

The first term in Eq. (3.58) is responsible for the renormalization of the effective mass and  $Z-$  factor, and we neglect it. The second term has the right  $-\omega|\omega|$ - frequency dependence, but its value on the mass shell depends on how we take the limit  $\Delta \rightarrow 0$ . This ambiguity is due to the logarithmic singularity in  $\text{Im}\Sigma_{\text{ex}}^R$  [cf. Eq. (3.26)]. To eliminate this ambiguity, one has to re-evaluate the integral using the full form of  $\text{Im}\Sigma_{\text{ex}}^R$ , obtained by keeping the curvature finite. This form is given by Eq. (3.49) and is independent of  $\Delta$  for  $\Delta \rightarrow 0$ . Performing a Kramers-Krönig transformation of Eq. (3.49), we obtain

$$\text{Re}\Sigma_{\text{ex}}^R = \frac{u^2}{8} \frac{\omega |\omega|}{E_F} + \mathcal{O}(\Delta^2 \log \Delta). \quad (3.59)$$

Alternatively, one could just notice that

$$\ln |\omega| = \text{Im} \left( \frac{i}{2} \ln [-(\omega + i0^+)^2] \right). \quad (3.60)$$

Substituting Eq. (3.60) into Eq. (3.49), one obtains the full (complex)  $\Sigma_{\text{ex}}^R$ :

$$\Sigma_{\text{ex}}^R = -\frac{u^2}{8\pi} \frac{\omega^2}{E_F} i \ln \left[ -\frac{E_F^2}{(\omega + i0^+)^2} \right]. \quad (3.61)$$

Taking the real part of Eq. (3.61), we indeed reproduce Eq. (3.59).

*b. particle-hole contribution* The same reasoning can be applied to the particle-hole contribution,  $\Sigma_{\text{PH}}^R$ . The imaginary part of  $\Sigma_{\text{PH}}^R$  near the mass shell is given by Eq. (3.33). Using relation (3.60) again, we restore the full  $\Sigma_{\text{PH}}^R$  as

$$\Sigma_{\text{PH}}^R = i \frac{u^2}{8\pi} \frac{\omega^2}{E_F} \ln \left[ -\frac{E_F^2}{u^2(\omega + i0^+)^2} \right] + i \frac{|\omega|\Delta}{4\pi E_F} \ln \left[ -\frac{\Delta^2}{u^4(\omega + i0^+)^2} \right], \quad (3.62)$$

where we have also kept a first sub-leading term in  $\Delta$ . The real part of Eq. (3.62) is given by

$$\text{Re}\Sigma_{\text{PH}}^R = -\frac{u^2}{8} \frac{\omega|\omega|}{E_F} - \frac{|\omega|\Delta}{4E_F}. \quad (3.63)$$

Adding up Eqs. (3.59) and (3.63), we see that the leading  $\omega|\omega|$ -terms cancel each other, whereas the rest vanishes linearly on the mass shell:

$$\text{Re}\Sigma_{\text{PH}}^R + \text{Re}\Sigma_{\text{ex}}^R = -\frac{|\omega|\Delta}{4E_F}. \quad (3.64)$$

Absence of a non-analytic,  $\omega|\omega|$ -term in  $\text{Re}\Sigma_{\text{PH}}^R + \text{Re}\Sigma_{\text{ex}}^R$  is consistent with our earlier observation that on the mass shell  $\text{Im}\Sigma_{\text{PH}}^R + \text{Im}\Sigma_{\text{ex}}^R$  is an analytic function of frequency [it scales as  $\omega^2 u^2 \ln u$ , see (3.51)]. Notice also that Eq. (3.64) is independent of  $u$ . On its own, such a term in the self-energy will give rise to the linear-in- $\omega$  and  $u$ -independent correction to the density of states. We will see, however, that this term will be cancelled out by the contribution from the zero-sound collective mode, so that the full density of states remains analytic in  $\omega$ .

*c. zero-sound contribution* Next, we consider the contribution from the zero-sound collective mode. The real part of  $\Sigma_{\text{ZS}}^R$  can be obtained either by a Kramers-Krönig transformation of Eq. (3.35), or directly from Eq. (3.23b), by expanding  $1 - U\Pi(q)$  near the pole and performing the frequency and angular integrations. Either way, we obtain for  $\Delta \ll \omega$

$$\text{Re}\Sigma_{\text{ZS}}^R = \frac{u^2 U}{4\pi} \text{Re} \left[ \int_0^{\omega/v_F} \frac{QdQ}{\sqrt{u^2 - 2\Delta/(v_F Q)}} \right]. \quad (3.65)$$

Evaluating the integral, we obtain

$$\text{Re}\Sigma_{\text{ZS}}^R = \frac{u^2}{8} \frac{\omega^2}{E_F} F_R \left( \frac{2\Delta}{u^2 \omega} \right), \quad (3.66)$$

where

$$F_R(x) = \text{Re} \left[ \left(1 + \frac{3}{2}x\right)\sqrt{1-x} + \frac{3}{2}x^2 \ln \frac{1 + \sqrt{1-x}}{\sqrt{-x}} \right]. \quad (3.67)$$

Subindex  $R$  implies that this is the scaling function for  $\text{Re}\Sigma_{\text{ZS}}^R$ . A plot of  $F_R(x)$  is presented in Fig. 5. Contrary to  $F_I(x)$  [Eq. (3.36)], scaling function  $F_R(x)$  is not one-sided, *i.e.*, it is nonzero for both positive and negative  $x$ . However, it is clear from the plot that this function is asymmetric with respect to  $x$ . In fact,  $F_R(x) = 0$  for  $x > 1$ . For large and negative  $x$ ,

$$F_R(x) \approx 4\text{Re}[1/(5\sqrt{-x})], \quad (3.68)$$

which means that

$$\text{Re}\Sigma_{\text{ZS}}^R \propto u^3 \omega^2 (\omega/ - \Delta)^{1/2} \quad (3.69)$$

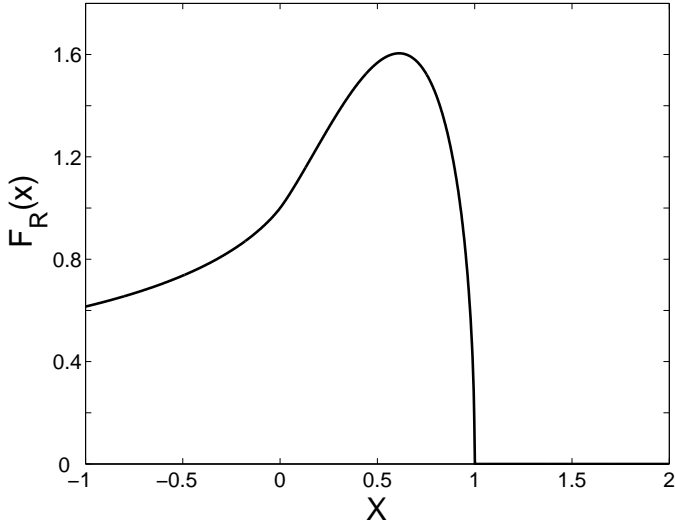


FIG. 5: Scaling function  $F_R(x)$  [ Eq. (3.67)].

for  $\Delta < 0$ . This is consistent with the large  $x$  behavior of  $F_I(x) \approx \text{Im}[2\pi/(5\sqrt{-x})]$ . Obviously, for large  $x$ , full  $\Sigma_{\text{ZS}}^R$  can be written as

$$\Sigma_{\text{ZS}}^R = \frac{u^3\sqrt{2}}{20} \frac{\omega|\omega|}{E_F} \left(-\frac{\omega}{\Delta}\right)^{1/2}. \quad (3.70)$$

We see that away from the mass shell, *i.e.*, at  $|\Delta| \gg \omega$ , the collective-mode component of  $\text{Re}\Sigma^R(k, \omega)$  scales as  $u^3\omega^2$ , which is smaller by a factor of  $u$  compared to the  $u^2\omega^2$ -contribution to the self-energy from backscattering ( Eq. (3.57)). This smallness is another consequence of the fact that quanta of zero sound are not free bosons: the residue of the corresponding propagator scales as  $u^2\omega^2$  and is thus small. For  $x \rightarrow 0$ ,

$$F_R(x) = 1 + x + \frac{3}{4}x^2 \ln x^{-1} + \dots \quad (3.71)$$

On the mass shell, *i.e.*, for  $x = 0$ , the function  $F_R$  approaches a finite value  $F_R = 1$ , so that

$$\text{Re}\Sigma_{\text{ZS}}^R|_{\Delta=0} = \frac{u^2}{8} \frac{\omega|\omega|}{E_F}. \quad (3.72)$$

We see that the real part of the self-energy due to the interaction with the collective mode is strongly enhanced near the mass shell, such that at  $\Delta = 0$  one power of the small parameter  $u$  is eliminated, and  $\text{Re}\Sigma_{\text{ZS}}^R$  becomes of the same order as the self-energy due to backscattering. This is one of the central results of this paper. Keeping the linear-in- $x$  term in Eq. (3.71) results in a linear-in- $\Delta$  correction to the self-energy

$$\text{Re}\Sigma_{\text{ZS}}^R = \frac{u^2}{8} \frac{\omega|\omega|}{E_F} + \frac{|\omega|\Delta}{4E_F}. \quad (3.73)$$

Adding up this result with Eq. (3.64), we find for the total contribution to the on-shell  $\text{Re}\Sigma^R$  from forward scattering

$$\text{Re}\Sigma_{\text{F}}^R = \text{Re}\Sigma_{\text{PH}}^R + \text{Re}\Sigma_{\text{ex}}^R + \text{Re}\Sigma_{\text{ZS}}^R = \frac{u^2}{8} \frac{\omega|\omega|}{E_F}. \quad (3.74)$$

### 3. final result for the real part of the self-energy

*a. contact-potential* Combining the backscattering and forward scattering contributions to the self-energy for the contact potential [Eqs. (3.57) and (3.74), respectively], we find that non-analytic ( $\omega|\omega|$  and  $\omega\Delta$ ) terms cancel out,

and the net self-energy vanishes on the mass shell:

$$\text{Re}\Sigma^R = \text{Re}\Sigma_{\text{B}}^R + \text{Re}\Sigma_{\text{F}}^R = O(u^2\Delta^2 \ln \Delta). \quad (3.75)$$

This is another central result of the paper. It means that a non-perturbative contribution of the zero-sound mode totally changes the result of the second order perturbation theory, where to order  $u^2$  we had  $\text{Re}\Sigma^R \propto u^2\omega|\omega|$ .

*b. finite-range potential* For a finite-range potential, the backscattering part of the self-energy changes to [13]

$$\text{Re}\Sigma_{\text{B}}^R = -\frac{\omega|\omega|}{8E_F} (u_0^2 + u_{2k_F}^2 - u_0u_{2k_F}), \quad (3.76)$$

where  $u_0$  and  $u_{2k_F}$  are given by Eq. (3.54). The forward-scattering contribution comes only with  $u_0^2$  and is obtained from Eq. (3.74) by replacing  $u \rightarrow u_0$ . A cancellation between backward and forward-scattering parts of  $\text{Re}\Sigma^R$  is no longer in place, and the net  $\text{Re}\Sigma^R$  is given by

$$\text{Re}\Sigma^R = \frac{\omega|\omega|}{8E_F} u_{2k_F} (u_0 - u_{2k_F}). \quad (3.77)$$

For  $u_0 \neq u_{2k_F}$ , it is a non-analytic function of  $\omega$  on the mass shell.

Finally, in the ZS contributions to the self-energy, Eq.(3.35),  $u$  is replaced by  $u_0$  as this contribution comes only from forward scattering.

## F. Spectral function

### 1. short-range potential

A non-monotonic variation in the zero-sound part of the self-energy is manifested in a specific feature in the spectral function

$$\begin{aligned} A(\omega, k) &= -\frac{1}{\pi} \text{Im}G^R(\omega, k) \\ &= \frac{1}{\pi} \frac{\text{Im}\Sigma^R(\omega, k)}{[\Delta + \text{Re}\Sigma^R(\omega, k)]^2 + [\text{Im}\Sigma^R(\omega, k)]^2}. \end{aligned} \quad (3.78)$$

Having in mind a potential comparison with the experiment, we present a detailed discussion of  $A(\omega, k)$  in this Section.

A variation of  $\text{Re}\Sigma^R(\omega, k)$  has only a little effect on the shape of the spectral function, and we verified that it can be safely ignored. The effect of  $\text{Im}\Sigma^R(\omega, k)$  is much stronger. As we have shown in Sec. III D,  $\text{Im}\Sigma^R(\omega, k)$  is a sum of four contributions

$$\text{Im}\Sigma^R(\omega, k) = \text{Im}\Sigma_{\text{B}}^R + \text{Im}\Sigma_{\text{ex}}^R + \text{Im}\Sigma_{\text{PH}}^R + \text{Im}\Sigma_{\text{ZS}}^R. \quad (3.79)$$

The particle-hole and zero-sound contributions contain scaling functions  $G_I$  and  $F_I$  which evolve as a function of  $\Delta = \omega - \epsilon_k$  on a scale  $\Delta \simeq \Delta^* \equiv u^2\omega/2 \ll \omega$ . The backscattering part, on the other hand, evolves only on much larger scale:  $\Delta \simeq \omega$  (cf. Appendix A). Therefore, one can safely put  $\Delta = 0$  in  $\text{Im}\Sigma_{\text{B}}^R$ , *i.e.*, use its mass-shell value given by Eq. (3.5). Finally,  $\text{Im}\Sigma_{\text{ex}}^R$  crosses over between the forms given by Eqs. (3.26) and (3.49) at  $\Delta \simeq \Delta_c = \omega^2/E_F$ . Two situations are then possible, depending on the relation between  $\Delta_c$  and  $\Delta^*$ . If  $\Delta_c \gg \Delta^*$  or, equivalently,  $\omega \gg \omega_c = u^2E_F$ , the variation of  $\text{Im}\Sigma_{\text{ZS}}^R$  and  $\text{Im}\Sigma_{\text{PH}}^R$  occurs in the range where  $\text{Im}\Sigma_{\text{ex}}^R$  can be approximated by its small- $\Delta$  form [ Eq. (3.49)], which is independent of  $\Delta$ . The sum of  $\text{Im}\Sigma_{\text{ex}}^R$  and  $\text{Im}\Sigma_{\text{B}}^R$  then vanishes, so that  $\text{Im}\Sigma^R(\omega, k) = \text{Im}\Sigma_{\text{PH}}^R + \text{Im}\Sigma_{\text{ZS}}^R$ . This sum can be further decomposed as

$$\text{Im}\Sigma^R(\omega, k) = \Gamma_0 + \Gamma_1(x). \quad (3.80)$$

where  $x = 2\Delta/u^2\omega = \Delta/\Delta^*$ ,  $\Gamma_0$  is a  $\Delta$ - independent part of the self-energy [the first term in the particle-hole contribution, Eq. (3.29)]:

$$\Gamma_0 = \frac{u^2}{4\pi} \frac{\omega^2}{E_F} \ln \frac{E_F}{u^2|\omega|}, \quad (3.81)$$

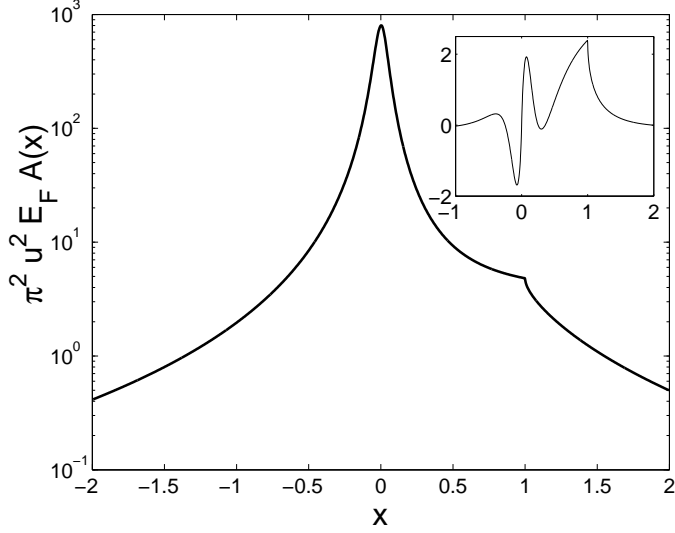


FIG. 6: Main panel: a log-plot of the spectral function  $A(\omega, k)$  [ Eq. (3.83)] in units of  $1/\pi^2 u^2 E_F$  as a function of  $x = 2(\omega - \epsilon_k)/u^2 \omega$  for  $L_\omega = 2$  and  $\gamma = 0.05$ . A kink at  $x = 1$  is due to the interaction of fermions with the zero-sound mode. Inset: part of the spectral function  $A_1(\omega, k)$  [ Eq. (3.85c)] in the same units function of  $x$  for  $\gamma = 0.25$ . A maximum in  $A_1$  at  $x = 1$  gives rise to a kink in total  $A$  (main panel).

and  $\Gamma_1(x)$  is a sum of the scaling terms in  $\text{Im}\Sigma_{\text{PH}}^R$  and  $\text{Im}\Sigma_{\text{ZS}}^R$  [Eqs. (3.29) and (3.35), respectively]

$$\Gamma_1(x) = \frac{u^2 \omega^2}{4\pi E_F} [G_I(x) + F_I(x)]. \quad (3.82)$$

Notice that  $F_I(0) = 0$  and  $G_I(0) = 0$ . Substituting Eq. (3.80)-(3.82) into Eq. (3.78) and neglecting  $\text{Re}\Sigma^R$ , we obtain a scaling form of the spectral function

$$A(\omega, k) = \frac{1}{\pi^2 u^2 E_F} \frac{L_\omega + G_I(x) + F_I(x)}{x^2 + \gamma^2 [L_\omega + G_I(x) + F_I(x)]^2}, \quad (3.83)$$

where

$$\gamma \equiv \frac{|\omega|}{2\pi E_F} \ll 1, \quad (3.84)$$

and  $L_\omega \equiv \ln(E_F/u^2|\omega|)$  is a large factor. We consider a setup when  $\omega$  is fixed and the spectral function is measured as a function of the momentum. This is equivalent to varying  $x$  at fixed  $\omega$  in Eq. (3.83). In photoemission measurements, this setup produces what is known as a ‘‘momentum distribution curve’’ (MDC). A plot of  $A$  [ Eq. (3.83)] as a function of  $x$  is shown in the main panel of Fig. 6. For solely illustrative purposes, we have chosen  $L_\omega = 2$  and  $\gamma = 0.05$ . We see that the spectral function contains not only a narrow quasi-particle peak at  $x = 0$  (i.e,  $\omega = \epsilon_k$ ) but also a well-pronounced kink at  $x = 1$ . To understand the reasons for the kink in  $A(\omega, k)$ , we notice that at typical  $\Delta \simeq \Delta^*$ ,  $\Gamma_1$  is of order  $\omega^2/E_F$ , which is smaller than  $\Gamma_0$  by a large  $L_\omega$ . Therefore, we can expand the spectral function in  $\Gamma_1$  and represent  $A(\omega, k)$  as a sum of two contributions

$$A(\omega, k) = A_0(\omega, k) + A_1(\omega, k) \quad (3.85a)$$

$$A_0(\omega, k) = \frac{1}{\pi^2 u^2 E_F} \frac{L_\omega}{x^2 + \gamma_1^2} \quad (3.85b)$$

$$A_1(\omega, k) = \frac{1}{\pi^2 u^2 E_F} [G_I(x) + F_I(x)] \frac{x^2 - \gamma_1^2}{(x^2 + \gamma_1^2)^2}. \quad (3.85c)$$

where  $\gamma_1 = \gamma L_\omega$ . The first term Eq. (3.85b) describes a regular quasi-particle peak at  $\Delta = 0$  of width  $\gamma_1$ . The scaling behavior of the self-energy shows up in the second term, Eq. (3.85c). Since  $\gamma_1 \ll 1$ , damping affects the behavior

of  $A_1(\omega, k)$  only at very small  $x$ :  $x \simeq \gamma_1 \ll 1$ . For these  $x$ ,  $A_1$  exhibits a rapid non-monotonic variation, but it is overshadowed by the rapid variation of  $A_0$ . For  $|x| \gg \gamma_1$ ,  $A_0$  is smooth, whereas  $A_1$  is determined by the sum of the scaling functions, which is non-monotonic in  $x$

$$A_1(\omega, k) \approx \frac{1}{u^2 E_F} \frac{G_I(x) + F_I(x)}{x^2}. \quad (3.86)$$

Comparing now the behavior of two scaling functions,  $G_I$  and  $F_I$ , we see from Fig. 4 that  $G_I(x)$  varies smoothly at  $x \simeq 1$ , whereas  $F_I(x)$  has a sharp peak at  $x = 1$ . We remind (cf. discussion in Sec. III D) that this sharp peak is associated with the fact that, for  $|\Delta| > \Delta^*$ , a fermion with energy  $\omega > 0$  above the Fermi level can emit ZS bosons with any frequency in the interval  $0 < \Omega < \omega$  (or absorb bosons in the interval  $0 < \Omega < -\omega$  for  $\omega < 0$ ), whereas for  $|\Delta| < \Delta^*$ , a Cherenkov-type restriction makes it impossible to emit and absorb bosons with frequencies above  $|\Delta|/(1 - v_F/c) \approx 2|\Delta|/u^2$ . The sharp peak in  $F_I(x)$  gives rise to a peak in  $A_1(\omega, k)$  at  $x = 1$ , see inset in Fig. 6. The peak in  $A_1$  gives rise to a kink in the full  $A(\omega, k)$  at  $x = 1$ . We emphasize that the kink originates from the zero-sound contribution to the self-energy, *i.e.*, it reflects an essentially non-perturbative effect.

The second situation occurs when  $\Delta_c \gg \Delta^*$ , *i.e.*,  $\omega \ll \omega_c = u^2 E_F$ . In this case, for  $x \simeq 1$ ,  $\text{Im}\Sigma_{\text{ex}}^R$  can be replaced by its large- $\Delta$  form [ Eq. (3.26)]. Re-expressing  $\text{Im}\Sigma_{\text{ex}}^R$  in terms of the dimensionless variable  $x$  we obtain

$$\text{Im}\Sigma_{\text{ex}}^R = -\frac{u^2 \omega^2}{8\pi E_F} \left( \ln \frac{E_F}{u^2 |\omega|} - \ln |x| \right). \quad (3.87)$$

Decomposing again  $\text{Im}\Sigma^R$  into  $x$ - independent and  $x$ - dependent parts, we obtain instead of Eqs. (3.85a-3.85c)

$$A(\omega, k) = A_0(\omega, k) + A_1(\omega, k) \quad (3.88a)$$

$$A_0(\omega, k) = \frac{1}{2\pi^2 u^2 E_F} \frac{\ln E_F^3 / u^2 |\omega|^3}{x^2 + \gamma_2^2} \quad (3.88b)$$

$$A_1(\omega, k) = \frac{1}{2\pi^2 u^2 E_F} \left[ G_I(x) + F_I(x) + \frac{1}{2} \ln |x| \right] \frac{x^2 - \gamma_2^2}{(x^2 + \gamma_2^2)^2}, \quad (3.88c)$$

where

$$\gamma_2 \equiv \frac{|\omega|}{4\pi E_F} \ln \frac{E_F^3}{u^2 |\omega|^3}. \quad (3.89)$$

The behavior of  $A(\omega, k)$  in this case is a bit more involved than for  $\Delta_c < \Delta^*$ ; nevertheless, the a general structure is the same as before: the spectral function has both a quasi-particle peak at  $x = 0$  and a kink at  $x = 1$ , due to the contribution from the zero-sound mode.

## 2. Coulomb potential

A kink in the spectral function due to the interaction of fermions with the collective mode is not a special feature of the model with a short-range repulsion but a general phenomenon. To illustrate this point, we consider a 2D system with the Coulomb interaction, when the collective mode is a plasmon with dispersion  $\Omega_0(Q) = (e^2 m v_F^2 Q)^{1/2}$ . An on-shell electron can emit plasmons only if its energy exceeds a certain critical value:  $|\omega| = |\epsilon_k| \geq \omega_{\text{pl}} = \sqrt{2} r_s E_F$  [37], where  $r_s$  is the usual ideal-gas parameter for a charged system, which is assumed to be small. Although formally there is an interval of energies in between  $\omega_{\text{pl}}$  and  $E_F$ , in practice it cannot be very large. In what follows, we will consider only the low-energy limit:  $|\omega|, |\epsilon_k| \ll \omega_{\text{pl}}$ . In this case, emission of plasmons by electrons is possible only away from the mass shell ( $\omega \neq \epsilon_k$ ), and the effect we are interested in is a kink in the spectral function rather than the lifetime of an electron.

Near the plasmon pole, the Coulomb potential reduces to

$$V(\Omega, Q) = \frac{2\pi e^4 m v_F^2}{(\Omega + i\delta)^2 - \Omega_0^2(Q)} \quad (3.90)$$

and, correspondingly, the imaginary part of the self-energy is given by ( $\omega > 0$ )

$$\text{Im}\Sigma^R(\omega, \epsilon_k) = 2\pi e^4 m v_F^2 \int_0^\omega d\Omega \int d^2 Q \delta(\omega - \epsilon_k - \Omega - v_F Q \cos \theta) \delta(\Omega^2 - \Omega_0^2(Q)). \quad (3.91)$$

The second  $\delta$ -function forces the boson momentum  $Q$  to be small:  $Q = |\Omega|^2 / me^2 v_F^2 \simeq (|\Omega|/v_F) (|\Omega|/\omega_{\text{pl}}) \ll |\Omega|/v_F$ . Therefore, one can neglect the  $Q$ -dependent term in the argument of the first  $\delta$ -function. Performing an elementary integration and considering the case of  $\omega < 0$  in the same way, we obtain for  $\text{Im}\Sigma^R(\omega, \epsilon_k)$ :

$$\text{Im}\Sigma^R(\omega, \epsilon_k) = \begin{cases} \pi (\epsilon_k - \omega)^2 / E_F, & \min\{0, \omega\} \leq \epsilon_k \leq \max\{0, \omega\}; \\ 0, & \text{otherwise.} \end{cases}$$

For fixed  $\omega$ ,  $\text{Im}\Sigma^R$  has a kink at  $\epsilon_k = 0$ , *i.e.*, at the Fermi surface, where  $\text{Im}\Sigma^R$  vanishes discontinuously (see comment [38]). (Keeping the  $Q$ -dependence in the first  $\delta$ -function in Eq. (3.91), one sees that in fact the kink and zero of  $\text{Im}\Sigma^R$  are separated by a small energy scale  $\omega^2/\omega_{\text{pl}}$ .) Notice that the electron charge dropped out of the result. It can be shown that the spectral function of a bi-layer system with two plasmon modes—with  $\sqrt{Q}$  and acoustic dispersions—behaves in a similar way but we defer a detailed discussion of this case to later occasion.

A kink in the spectral function could, in principle, be detected in photoemission experiments on layered materials [29] or in a momentum-conserving tunneling between two parallel layers of 2D gases [30].

### 3. absence of a non-analytic correction to the tunneling density of states

Both the particle-hole and zero-sound contributions to the real part of the self-energy contain a specific term, which is proportional to the product  $|\omega| \Delta$  and is independent of the interaction [cf. Eqs. (3.63) and (3.73)]. Each of these terms on its own would give rise to a linear-in- $|\omega|$  and  $u$ -independent correction to the density of states. Indeed, a term in the self-energy of the form

$$s |\omega| \Delta / E_F, \quad (3.92)$$

where  $s$  is a numerical coefficient, gives rise to a non-analytic frequency dependence of the renormalization factor:

$$Z(\omega) = \left(1 + s \frac{|\omega|}{E_F}\right)^{-1} \approx 1 - s \frac{|\omega|}{E_F}. \quad (3.93)$$

[We defined  $Z(\omega)$  in such a way that  $G^R(k, \omega) = Z(\omega)/(\omega - \epsilon_k + i0^+)$ .] The linear -in- $|\omega|$ -term in  $Z(\omega)$  results in a linear frequency dependence of the tunneling density of states

$$N(\omega) = -\frac{2}{\pi} \int \frac{d^2k}{(2\pi)^2} \text{Im}G^R(\omega, k) = \frac{m}{\pi} Z(\omega) \approx (m/\pi) \left(1 - s \frac{|\omega|}{E_F}\right). \quad (3.94)$$

However, we see that the  $\Delta|\omega|$ -terms in Eqs. (3.64) and (3.73) cancel out in full  $\text{Re}\Sigma^R$  [Eq. (3.74)], so that  $s = 0$ . Therefore, to order  $u^2$ ,  $N(\omega)$  is *analytic* in  $\omega$ . This result is valid for any finite-range potential as the cancellation of  $|\omega| \Delta$ -terms occurs between the forward-scattering contributions to the self-energy, all of which contain the same coupling  $u_0$ . Our result that there is no linear-in- $|\omega|$  correction to the DOS is in agreement with Ref. [39], where the tunneling density of states was obtained for the case of a multi-layer system with the Coulomb interaction. Inter-layer screening gives rise to an acoustic branch of the plasmon spectrum which is an analog of the ZS mode of our model. Notice that an  $|\omega|$ -correction to the density of states does exist for a single layer with the Coulomb potential [39, 40].

## IV. SPECIFIC HEAT

As we pointed out in the Introduction, the  $\omega|\omega|$ -non-analyticity in the second-order self-energy gives rise to a non-analytic,  $u^2 T$ -correction to the ratio  $C(T)/T$  [13]. However, it was shown in Sec. III E that, upon re-summation, higher-order forward-scattering contributions to  $\text{Re}\Sigma^R$  also becomes of the order  $U^2$  near the mass shell and modify the second order result. For a contact interaction, the non-perturbative contribution even cancels the second-order  $u^2 \omega|\omega|$ -term in  $\text{Re}\Sigma^R$ . The question addressed in this Section is whether the forward-scattering component of the self-energy modifies the non-analytic term in the specific heat. We show in several ways that this does not happen, *i.e.*, the enhancement of the forward scattering self-energy near the mass shell does not affect the specific heat.

We also go beyond the weak-coupling limit in this Section, and consider the non-analytic behavior of the specific heat in a generic Fermi liquid.

### A. Specific heat via self-energy

A relation between the entropy (and thus the specific heat) and an exact fermion Green's function can be found in Ref. [1]. However, this relation is justified only for the Fermi-liquid, linear-in- $T$  part of  $C(T)$ . In order to find a sub-leading, non-analytic contribution to  $C(T)$ , one needs to re-examine the assumptions, made in Ref. [1], and to establish a correct relation between  $C(T)$  and the self-energy beyond the leading order in  $T$ .

The relation between the thermodynamic potential and the Green's function reads [1]

$$\Xi = 2T \sum_{\omega_m} \int \frac{d^2k}{(2\pi)^2} \ln G(\omega_m, k, T = 0), \quad (4.1)$$

where  $G(\omega_m, k, T = 0)$  is the Green's function evaluated at discrete Matsubara frequencies but with no additional  $T$ -dependence. Converting the Matsubara sum into the contour integral and using a familiar thermodynamic relation

$$C(T) = -T \frac{\partial^2 \Xi}{\partial T^2}, \quad (4.2)$$

one obtains

$$C(T)/T = -\frac{2T}{\pi} \frac{\partial}{\partial T} \left[ \frac{1}{T} \int \frac{d^2k}{(2\pi)^2} \int_{-\infty}^{\infty} d\omega \omega \frac{\partial n_0}{\partial \omega} \arg G^R(\omega, k) \right]. \quad (4.3)$$

(Notice that there is no need to distinguish between  $C_P$  and  $C_V$  here, as we are interested in the  $T^2$ - term in  $C(T)$ , whereas the difference between  $C_P$  and  $C_V$  is of the order  $T^3$  [2].) Both the retarded and advanced Green's functions in Eq. (4.3) are evaluated at  $T = 0$ , thus the derivative in the r.h.s. of Eq. (4.3) affects only the Fermi function [the temperature derivative of  $n_0$  was converted into the frequency dependence by using a familiar identity:  $\partial n_0 / \partial T = -(\omega/T) \partial n_0 / \partial \omega$ ].

Eq. (4.3) correctly describes the regular, linear-in- $T$  part of the specific heat. Indeed, substituting the analytic, FL form of the self-energy, Eq.(1.1), into Eq. (4.3), one finds that  $C(T)$  is given by the Fermi-gas result [ Eq. (1.11)] but with a renormalized mass, which is composed from coefficients  $a$  and  $b$  in Eq. (1.1).

It was conjectured in Ref. [1] that Eq. (4.3) describes not only the leading but also the sub-leading terms in  $C(T)$ . However, this conjecture is questionable, as the accuracy of the low-temperature expansion used in the derivation of Eq. (4.3) is not specified. In other words, it is not obvious that if one retains contain higher powers of  $\omega$  in  $\Sigma$ , one should not at the same time take into account an explicit temperature dependence of  $\Sigma$ . Of particular concern are the situations when the self-energy depends on  $T$  via a scaling function of variable  $\omega/T$  (this happens in our case; see below). As typical  $\omega$  are of order  $T$ , the argument of the scaling function is of order unity, thus neglecting the  $T$ -dependence is not justified. Moreover, it was shown in Ref.[9] that the zero-temperature and temperature-dependent parts of the self-energy give comparable contributions to the non-analytic,  $T^3 \ln T$  part of  $C(T)$  in 3D.

We will still be considering the case of a weak interaction, when  $|\Sigma^R| \ll |\omega|$ . In this case, Eq. (4.3) can be simplified further by expanding the logs of Green's function in the self-energy, which results in

$$C(T) = C_{\text{FG}}(T) + \delta C(T), \quad (4.4)$$

where  $C_{\text{FG}}(T)$  is the specific heat for free fermions in 2D [ Eq. (1.11)] and  $\delta C(T)$  is given by

$$\delta C(T)/T = \frac{2}{\pi} \frac{\partial}{\partial T} \left[ \frac{1}{T} \int \frac{d^2k}{(2\pi)^2} \int_{-\infty}^{\infty} d\omega \omega \frac{\partial n_0}{\partial \omega} \text{Im} [\Sigma^R(\omega, k, T = 0) G_0^R(\omega, k)] \right]. \quad (4.5)$$

There are two contributions to  $\delta C(T)$ —one from  $\text{Re}\Sigma^R$  and another from  $\text{Im}\Sigma^R$ —which we label as  $C_1(T)$  and  $C_2(T)$ , correspondingly:

$$\delta C(T) = C_1(T) + C_2(T); \quad (4.6a)$$

$$C_1(T)/T = -2 \frac{\partial}{\partial T} \left[ \frac{1}{T} \int \frac{d^2k}{(2\pi)^2} \int_{-\infty}^{\infty} d\omega \omega \frac{\partial n_0}{\partial \omega} \delta(\omega - \epsilon_k) \text{Re}\Sigma^R(\omega, k, T = 0) \right]; \quad (4.6b)$$

$$C_2(T)/T = \frac{2}{\pi} \frac{\partial}{\partial T} \left[ \frac{1}{T} \int \frac{d^2k}{(2\pi)^2} \int_{-\infty}^{\infty} d\omega \omega \frac{\partial n_0}{\partial \omega} \mathcal{P} \frac{1}{\omega - \epsilon_k} \text{Im}\Sigma^R(\omega, k, T = 0) \right]. \quad (4.6c)$$

In the expression for  $C_1(T)$ , we have used the fact that  $\text{Im}G_0^R(\omega - k) = -\pi\delta(\omega - \epsilon_k)$ . The delta-function in (4.6b) implies that  $C_1(T)$  is determined by  $\text{Re}\Sigma^R$  only on the mass shell, where  $\omega = \epsilon_k$ . The second term  $C_2(T)$  contains



the integral of  $\text{Im}\Sigma^R(\omega, k)$ . If  $\text{Im}\Sigma^R(\omega, k)$  depends on  $\omega$  but not  $k$ , which is the case, *e.g.*, for the electron-phonon interaction [41], the momentum integral in Eq. (4.6c) vanishes once one approximates the density of states by a constant, so that  $C_2(T)$  drops out. Indeed,

$$C_2(T) \propto \int d\omega \omega \frac{\partial n_0}{\partial \omega} \text{Im}\Sigma^R(\omega) \mathcal{P} \int_{-\infty}^{\infty} d\epsilon_k \frac{1}{\omega - \epsilon_k} = 0. \quad (4.7)$$

However, for a general case, when  $\Sigma$  depends on both  $\omega$  and  $k$ , there are no *a priori* reasons for  $C_2(T)$  to vanish, and thus the imaginary part of the self-energy contributes to the specific heat as well. In what follows, we will omit the analytic terms in  $\Sigma^R$  which just renormalizes the coefficient of the linear  $T$ -dependence in Eq. (1.11), and consider only the non-analytic contributions to  $C_1$  and  $C_2$ .

Next, we compare the result for the correction to the specific heat given by Eqs. (4.6a-4.6c) to the one obtained in a different way, namely, employing the Luttinger-Ward formula for the thermodynamic potential  $\Xi$ :

$$\Xi - \Xi_0 = -2T \sum_{\omega_m} \int \frac{d^2k}{4\pi^2} \left[ \ln(G_0 G^{-1}) - \Sigma G + \sum_{\nu} \frac{1}{2\nu} \Sigma_{\nu} G \right]. \quad (4.8)$$

Here,  $\Xi_0$  is the thermodynamic potential of the free Fermi gas per unit area,  $G_0 = (i\omega_m - \epsilon_k)^{-1}$ ,  $G = (i\omega_m - \epsilon_k + \Sigma)^{-1}$ ,  $\Sigma$  is the exact (to all orders in the interaction) self-energy, and  $\Sigma_{\nu}$  is the skeleton self-energy of order  $\nu$ . Both the skeleton and full self-energy, related via

$$\Sigma = \sum_{\nu} \Sigma_{\nu}, \quad (4.9)$$

are evaluated at *finite*  $T$ . The diagrams for  $\Sigma_{\nu}$  are obtained from those in Fig. 2 by replacing the bare Green's function and interaction lines by the exact ones. Expanding both  $G$  and  $\Sigma_{\nu}$  in Eq. (4.8) back in  $\Sigma$ , one generates a perturbative expansion for  $\Xi$ . To second order, diagrams generated by the first two terms in Eq. (4.8) correspond to self-energy insertions into a free thermodynamic potential (circle). Such diagrams just renormalize the prefactor of the leading, linear-in- $T$  part of  $C(T)$ . The non-analytic contributions come from the third (skeleton) term. To second order in the interaction, this contribution is

$$\delta\Xi = -\frac{1}{2} T \sum_{\omega_m} \int \frac{d^2k}{4\pi^2} \Sigma(\omega_m, k, T) G_0(k, \omega_m), \quad (4.10)$$

where  $\Sigma(\omega_m, k, T)$  is (a non-analytic part of) the second-order self-energy. Converting the Matsubara sum to an integral over real frequencies and using relation Eq. (4.2) between  $\Xi$  and  $C(T)$ , one obtains

$$\delta C(T)/T = -\frac{1}{2\pi} \frac{\partial^2}{\partial T^2} \left[ \int \frac{d^2k}{(2\pi)^2} \int_{-\infty}^{\infty} d\omega \text{Im} \{ G_0^R(\omega, k) \Sigma^R(\omega, k, T) \} \left( n_0(\omega) - \frac{1}{2} \right) \right]. \quad (4.11)$$

We emphasize that in this approach  $\Sigma^R(k, \omega_m, T)$  is evaluated at finite temperature.

Generally speaking, Eq. (4.11) and Eqs. (4.6a-4.6c) give different results for  $\delta C$ . Indeed, let us assume for a moment that  $\Sigma^R$  depends only on frequency but not on  $k$  and  $T$ . Then  $\delta C(T)$  from Eq. (4.6b) and from Eq. (4.11) differ by a factor of four. The derivation based on the Luttinger-Ward formula is free from assumptions on what constitutes the main source of the  $T$ -dependence in  $\delta C(T)$ . In fact, Eq. (4.11) is valid for *any* temperature albeit for weak interactions. The safe way to proceed therefore is to use Eq. (4.11) but not Eq. (4.5). It appears, though that for our case, there exists a deeper relation between the two formulas. Namely, the two expressions yield identical results for  $\delta C(T)$ , provided that one replaces  $\Sigma(\omega, k, T = 0)$  by the temperature-dependent self-energy in Eq. (4.5), *i.e.*

$$(4.5) \rightarrow \delta C(T)/T = \frac{2}{\pi} \frac{\partial}{\partial T} \left[ \frac{1}{T} \int \frac{d^2k}{(2\pi)^2} \int_{-\infty}^{\infty} d\omega \omega \frac{\partial n_0}{\partial \omega} \text{Im} [\Sigma^R(\omega, k, T) G_0^R(\omega, k)] \right]. \quad (4.12)$$

This is how  $\delta C(T)$  was calculated in Ref. [13]. The overall factor of four difference between Eq. (4.11) and Eq. (4.5) is eliminated by two reasons. First, the imaginary part of the self-energy to order  $u^2$  does depend on  $\epsilon_k$  albeit only logarithmically:  $\text{Im}\Sigma^R(\omega, k) \propto \omega^2 \ln|\omega + \epsilon_k|$ . Then Eq. (4.6c) gives the same contribution as Eq. (4.6b). The details of this calculation are presented in Appendix C. An additional factor of two appears because the derivative over  $T$  in Eq. (4.12) now acts not only on  $n_0$  but also on  $\Sigma^R$ . In Appendix C, we show that these two terms contribute equally to  $\delta C(T)$ ; hence, an additional factor of two.

To summarize, Eq. (4.11) gives a correct result for a non-analytic term in  $C(T)$  to second order in the interaction without any assumptions or constraints. At the same time, Eq. (4.5) gives the correct result provided that the self-energy in Eq. (4.5) is evaluated at finite  $T$  rather than at  $T = 0$ , as specified by Eq. (4.12). This is a consequence of the  $\omega/T$  scaling in the non-analytic part of  $\Sigma(\omega, T)$ . We did not study, however, whether or not this statement is specific to our weak-coupling case or has a wider range of applicability. Having this precaution in mind, we will be using Eq. (4.12) in the following analysis.

It is convenient now to separate the self-energy into the zero-sound part and the rest, which includes the backscattering- and PH-contributions from spin- and charge channels, as well as the remainder term,  $\Sigma_{\text{ex}}$ . Such a separation is convenient because the imaginary part of  $\text{Im}\Sigma^R$  has a substantial  $k$ -dependence and thus, according to the discussion in the previous Section, gives a contribution to the specific heat. On the other hand, the imaginary part of the rest of the self-energy depends on  $k$  only logarithmically, and will be shown not to contribute to  $C(T)$ .

### 1. non-zero-sound contribution to $C(T)$

We begin with the part of the self-energy that contains all contributions but the zero-sound one:

$$\tilde{\Sigma} \equiv \Sigma - \Sigma_{\text{ZS}} = \Sigma_B + \Sigma_{\text{PH}} + \Sigma_{\text{ex}}.$$

Consider first the contribution to the specific heat from the real part of the self-energy,  $C_1(T)$ , Eq. (4.6b). A sum of the two contributions,  $\text{Re}\Sigma_{\text{PH}} + \text{Re}\Sigma_{\text{ex}}$ , vanishes on the mass shell and therefore does not contribute to  $C_1(T)$ . A non-analytic part of  $\text{Re}\Sigma_B^R$  on the mass shell and at  $T = 0$  is given by Eq. (3.57). At finite temperatures,  $\text{Re}\Sigma_B^R$  has been calculated in [13]; the result of this calculation is that  $\text{Re}\Sigma_B^R(k, \omega, T)$  differs from  $\text{Re}\Sigma_B^R(k, \omega, T = 0)$  by a multiplicative factor which is a scaling function of  $\omega/T$ :

$$\begin{aligned} \text{Re}\Sigma_B^R(k, \omega, T) &= \text{Re}\Sigma_B^R(k, \omega, T = 0)g(\omega/T); \\ g(x) &= 1 + \frac{4}{x^2} \left[ \frac{\pi^2}{12} + \text{Li}_2\left(-e^{-|x|}\right) \right], \end{aligned} \quad (4.13)$$

where  $\text{Li}_2(x)$  is a polylogarithmic function.

Substituting Eq. (4.13) into Eq. (4.6b) we obtain [13]

$$C_1(T)/T = -\frac{9\zeta(3)}{\pi^2} u^2 C_{\text{FG}}/E_F, \quad (4.14)$$

where  $C_{\text{FG}}$  is given by Eq. (1.11). As is expected, the non-analytic  $\omega/|\omega|$ -dependence of  $\text{Re}\Sigma_B^R$  gives rise to a non-analytic contribution to the specific heat  $C_1(T)/T \propto u^2 T$ .

To logarithmic accuracy,  $\text{Im}\tilde{\Sigma}(\omega, k) \propto \omega^2 \ln|\omega|$  does not depend on  $k$ , hence, according to Eq. (4.7),  $C_2(T)$  vanishes. To demonstrate unambiguously that  $C_2(T)$  vanishes, one has to go a bit deeper and analyze  $\text{Im}\Sigma^R(k, \omega)$  beyond the logarithmic accuracy, focusing specifically on the momentum dependence under the logarithm. In Appendix C, we show that the contributions to  $C_2(T)$  from  $\text{Im}\Sigma_B^R$  and  $\text{Im}\Sigma_{\text{PH}} + \text{Im}\Sigma_{\text{ex}}$  cancel each other, *i.e.*, there is indeed no contribution to the specific heat from  $\text{Im}\tilde{\Sigma}^R$ .

### 2. zero-sound mode contribution to $C(T)$

We now use the results for  $\text{Re}\Sigma_{\text{ZS}}^R$  and  $\text{Im}\Sigma_{\text{ZS}}^R$  from Sec. III and calculate the contribution to the specific heat from the zero-sound mode. We show that the contributions from  $\text{Re}\Sigma_{\text{ZS}}^R$  and  $\text{Im}\Sigma_{\text{ZS}}^R$  cancel each other, *i.e.*, that the zero-sound mode does not contribute to  $C(T)$  despite the fact that  $\text{Re}\Sigma_{\text{ZS}}^R$  is enhanced near the mass shell. As we only need to prove the cancellation, we just use zero-temperature forms of  $\Sigma_{\text{ZS}}^R$ ; as we explained in the previous Section, the difference between the results for the specific heat found using the zero- or finite-temperature forms of the self-energy, is just an overall numerical factor.

Substituting  $\text{Re}\Sigma_{\text{ZS}}^R$  from Eq. (3.72) into Eq. (4.6b), we obtain

$$C_1(T)/T = \frac{4}{\pi} N u^2 \frac{T}{v_F^2}, \quad (4.15)$$

where

$$N \equiv \int_0^\infty \frac{dx x^3}{\cosh^2 x} = \frac{9}{8} \zeta(3). \quad (4.16)$$

Substituting next Eq. (3.35) for  $\text{Im}\Sigma_{\text{ZS}}^R(k, \omega)$  into Eq. (4.6c), we obtain

$$C_2(T)/T = -\frac{1}{\pi} \frac{\partial}{\partial T} \left( \frac{Z}{T^2} \right), \quad (4.17)$$

where

$$Z(T) = \frac{1}{2m} u^3 \mathcal{P} \int_0^\infty \frac{d\omega}{\cosh^2 \frac{\omega}{2T}} \int \frac{d^2k}{\omega - \epsilon_k} \text{Im} \left[ \int_0^{\epsilon_k/v_F} \frac{Q dQ}{\sqrt{u^2 - 2(\omega - \epsilon_k)/(v_F Q)}} \right]. \quad (4.18)$$

Re-scaling the variables and replacing  $\int d^2k$  by  $(m2\pi) \int d\epsilon_k$ , we obtain from Eq. (4.18)

$$Z(T) = \frac{u^3}{4\pi} \int_0^\infty \frac{d\omega \omega}{\cosh^2 \omega/(2T)} J(\omega), \quad (4.19)$$

where

$$J(\omega) = \mathcal{P} \int_{-\infty}^\infty \frac{dP}{P} \text{Im} \left[ \int_0^{\frac{\omega}{v_F} - \frac{P}{2}} \frac{Q^{3/2} dQ}{\sqrt{u^2 Q - P}} \right]. \quad (4.20)$$

The integration region over momenta  $P$  and  $Q$  are defined by the following conditions:  $P > u^2 Q$  and  $\omega > v_F P/2$ . Evaluating the integrals in (4.20) over this region, we find

$$J(\omega) = \frac{\pi}{2u} \left( \frac{\omega}{v_F} \right)^2. \quad (4.21)$$

Substituting this result into Eq. (4.19), and then into (4.17), we obtain

$$C_2(T)/T = -\frac{u^2}{8\pi v_F^2} \frac{\partial}{\partial T} \left[ \frac{1}{T^2} \int_0^\infty \frac{\omega^3 d\omega}{\cosh^2 \omega/(2T)} \right] = -\frac{4}{\pi} u^2 N \frac{T}{v_F^2}. \quad (4.22)$$

Comparing Eqs. (4.15) and (4.22), we find that these two contributions to the specific heat cancel each other, *i.e.*, there is no non-analytic contribution to the specific heat from the zero-sound collective mode to second-order in the interaction, despite the non-perturbative enhancement of  $\Sigma_{\text{ZS}}^R$  near the mass shell. An absence of the zero-sound contribution to the specific heat is another central result of the paper.

The final result for a weak, contact interaction is then given just by the perturbative contribution, Eq. (4.14):

$$C_1(T)/T = -\frac{9\zeta(3)}{\pi^2} u^2 C_{\text{FG}}/E_F. \quad (4.23)$$

### 3. finite-range potential

For a finite-range potential, the forward-scattering part of the self-energy involves only  $u_0$ . Hence, all cancellations discussed in the preceding Sections are still in place. In particular, the sum of  $\text{Re}\Sigma_{\text{ex}}^R$  and  $\text{Re}\Sigma_{\text{PH}}^R$  still vanishes on the mass shell and the contributions from real and imaginary parts of  $\Sigma_{\text{ZS}}^R$  to  $C(T)$  still cancel each other. In addition, the momentum integral in Eq. (4.6c) of each of the three terms  $\text{Im}\Sigma_{\text{B}}^R$ ,  $\text{Im}\Sigma_{\text{PH}}^R$ , and  $\text{Im}\Sigma_{\text{ex}}^R$  still vanishes. As a result, the specific heat is again determined by the real part of the self-energy from backscattering. The self-energy due to backscattering for a generic  $U(Q)$  is given by Eq. (3.76), hence  $\delta C(T)$  becomes

$$\delta C(T)/T = -\frac{9\zeta(3)}{\pi^2} (u_0^2 + u_{2k_F}^2 - u_0 u_{2k_F}) C_{\text{FG}}/E_F. \quad (4.24)$$

This expression is the final result for the non-analytic correction to the specific heat to order  $u^2$ . For  $u_0 = u_{2k_F} = u$ , it reduces to the contact-potential result, Eq. (4.14).

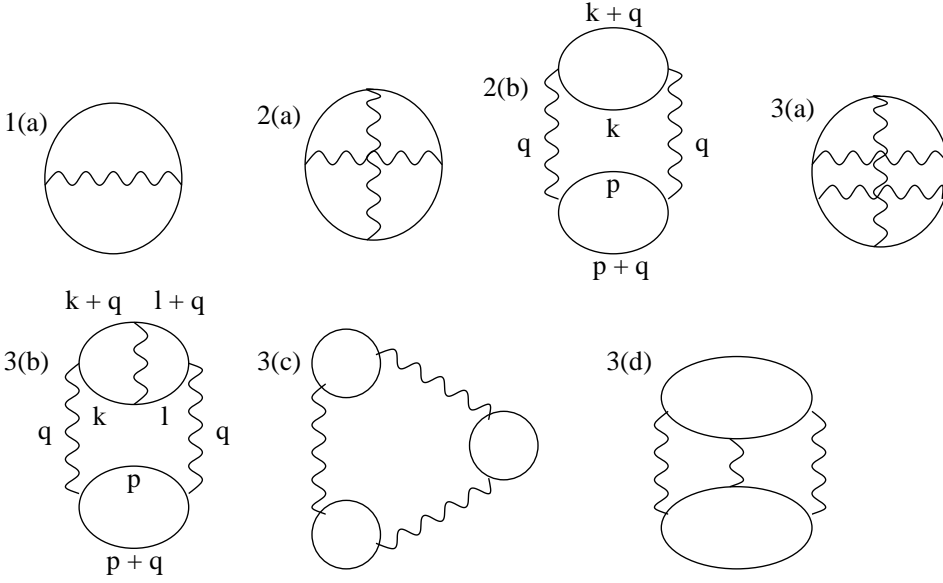


FIG. 7: Diagrams for the thermodynamic potential containing maximum number of particle-hole bubbles. For the Coulomb potential, diagrams 1(a), 2(b) and 3(c) represent ring diagram series to third order in the interaction

## B. Specific heat via the thermodynamic potential

The calculation of the specific heat via the self-energy presented in the previous Section is quite involved, as it requires a detailed knowledge of  $\Sigma(\omega, k)$ . To verify the main result of the previous Section—that there is no contribution to the specific heat from the collective mode—and to understand it from a different perspective, we employ an alternate approach. In particular, we obtain the specific heat by finding the thermodynamic potential,  $\Xi$ , directly, and then using relation Eq. (4.2). In this approach, fermions are integrated out from the very beginning, and the intricate details of their self-energy are not important. Another advantage of working with the thermodynamic potential is that the entire calculation can be performed in Matsubara frequencies.

### 1. Luttinger-Ward expansion

To generate a perturbative expansion of  $\Xi$ , we follow the Luttinger-Ward approach [42, 43], in which  $\Xi$  is expressed in terms of the exact Green's functions and the skeleton self-energies, as specified in Eq. (4.8). To begin with, we consider the contact-interaction case. The diagrams for the self-energy describing the interaction of fermions with collective modes have been discussed in Sec. III. Expanding the result for the self-energy, Eq. (3.22), back in powers of interaction  $U$  and substituting the resulting series for  $\Sigma$  and  $\Sigma_\nu$  into Eq. (4.8), we generate the series for the thermodynamic potential. The non-trivial diagrams for  $\Xi$  up to third order in  $U$  are shown in Fig. 7. Explicitly,

$$\begin{aligned} \Xi &= \Xi_0 + \int_q \left[ -U\Pi_m - \frac{1}{2}(U\Pi_m)^2 + \frac{1}{3}(U\Pi_m)^3 - \frac{1}{2}(U\Pi_m)^4 + \frac{1}{5}(U\Pi_m)^5 + \dots \right] \\ &= \int_q \left[ -2U\Pi_m + \frac{1}{2}(U\Pi_m)^2 + \frac{1}{2}\ln(1 - U\Pi_m) + \frac{3}{2}\ln(1 + U\Pi_m) \right], \end{aligned} \quad (4.25)$$

where  $\Pi_m(q)$  is the polarization bubble in Matsubara frequencies. Again, we will need only the asymptotic forms of  $\Pi_m(q)$  for  $Q$  near 0 and near  $2k_F$ . Analytically continuing the corresponding retarded expressions [Eqs. (3.3) and (3.4)] to Matsubara frequencies  $\Omega_m = 2\pi mT$ , we obtain

$$\Pi_m(\Omega_m, Q) = -\frac{m}{2\pi} \left[ 1 - \frac{|\Omega_m|}{\sqrt{\Omega_m^2 + (v_F Q)^2}} \right], \quad Q \rightarrow 0; \quad (4.26)$$

and

$$\Pi_m(\Omega_m, Q) = -\frac{m}{2\pi} \left[ 1 - \left( \frac{Q - 2k_F}{2k_F} + \sqrt{\left( \frac{Q - 2k_F}{2k_F} \right)^2 + \left( \frac{\Omega_m}{2k_F v_F} \right)^2} \right)^{1/2} \right], Q \approx 2k_F. \quad (4.27)$$

One observes immediately that the series in Eq. (4.25) converges for small  $U$  because  $\Pi_m(\Omega_m, Q)$  is regular for any  $\Omega_m$  and  $Q$  [in contrast with  $\Pi^R(\Omega, Q)$  which is singular at the boundary of the particle-hole continuum  $\Omega^2 = (v_F Q)^2$ ]. Every order in  $U$  then gives a finite contribution to the thermodynamic potential which can be calculated separately from other orders. Therefore, there is no need for re-summation of the perturbation theory for  $\Xi$  for a weak interaction. This tells us that the  $\mathcal{O}(U^2)$  term in the specific heat cannot have any non-perturbative contributions, *i.e.*, to second order in  $U$ ,  $\Xi$  is given just by

$$\Xi - \Xi_0 = \Xi_2 = -\frac{1}{2} \int_q (U \Pi_m)^2. \quad (4.28)$$

This explains the absence of collective-mode contribution to  $C(T)$ , which we have demonstrated explicitly in Sec. IV A 2.

## 2. Evaluation of the thermodynamic potential in Matsubara frequencies

Next, we show how the non-analytic  $T^2$  correction to the specific heat emerges in the Matsubara formalism. The  $T^2$ -term in  $C(T)$  comes from a non-analytic,  $T^3$ -piece in  $\Xi$ , and we will be searching for this term in Eq. (4.28). We first show that the  $Q$ -integral of  $\Pi_m^2$  taken over momenta near  $Q = 0$  and  $Q = 2k_F$  contains a non-analytic,  $\Omega_m^2 \ln |\Omega_m|$  part. Indeed, squaring the small- $Q$  form of  $\Pi_m$  [Eq. (4.26)] and substituting the result into Eq. (4.28), we find

$$\int \frac{dQ Q}{2\pi} \Pi_m^2(\Omega_m, Q) \rightarrow \frac{m^2}{(2\pi)^3} \Omega_m^2 \int_0^{\simeq 2k_F} \frac{dQ Q}{\Omega_m^2 + (v_F Q)^2} = \frac{m^2}{(2\pi)^3 v_F^2} \Omega_m^2 \ln \frac{E_F}{|\Omega_m|}. \quad (4.29)$$

Similarly, the square of the second term in the bubble near  $2k_F$  [Eq. (4.27)], yields another  $\Omega_m^2 \ln |\Omega_m|$ -term with the same prefactor, as from the region of small  $Q$ . To see this, we substitute the square of Eq. (4.27) into Eq. (4.28), re-define the integration variable as  $x = (Q - 2k_F)/(2k_F)$ , and retain only the square of the second term in  $\Pi_m^2$ :

$$\int_{Q \approx 2k_F} \frac{Q dQ}{2\pi} \Pi_m^2(\Omega_m, Q) \Rightarrow \frac{m^2}{(2\pi)^3} (2k_F)^2 \int_{-1}^1 dx \left[ x + \sqrt{x^2 + \left( \frac{\Omega_m}{2k_F v_F} \right)^2} \right]. \quad (4.30)$$

The precise limits of the integration over  $x$  are not important. Expanding in frequency, we obtain

$$\int_{Q \approx 2k_F} \frac{dQ Q}{2\pi} \Pi_m^2(\Omega_m, Q) \Rightarrow \frac{m^2}{(2\pi)^3} (2k_F)^2 \int_{-1}^1 dx \left( x + |x| + \frac{\Omega_m^2}{4k_F v_F^2 |x|} + \dots \right) \quad (4.31)$$

$$\Rightarrow \frac{m^2}{(2\pi)^3 v_F^2} \Omega_m^2 \ln \frac{E_F}{|\Omega_m|}. \quad (4.32)$$

Comparing Eq. (4.32) and Eq. (4.29), we see that the non-analytic contributions from  $Q = 0$  and  $2k_F$  are equal. Substituting the sum of the two contributions into Eq. (4.28), we obtain

$$\Xi_2 = -\frac{1}{2} U^2 \int_q \Pi_m^2 = -\frac{u^2 T}{\pi v_F^2} \sum_{\Omega_m=0}^{E_F} \Omega_m^2 \ln \frac{E_F}{\Omega_m} = -\frac{4\pi u^2 T^3}{v_F^2} S(M), \quad (4.33)$$

where

$$S(M) \equiv \sum_{m=0}^M m^2 \ln \frac{M}{m} = \frac{1}{6} M(M+1)(2M+1) \ln M - \sum_{m=1}^{M-1} (m+1)^2 \ln(m+1) \quad (4.34)$$

and  $M = [E_F/2\pi T] \gg 1$ . The choice of  $E_F$  as an upper limit in Eq. (4.33) is completely arbitrary; since we are looking for a universal contribution to the thermodynamic potential, the choice of cutoff is not important. Next, we use the Euler-Maclaurin formula :

$$\sum_{m=1}^{M-1} f(m) = \int_0^M f(x)dx - \frac{1}{2}[f(M) + f(0)] + \sum_{p=1}^N B_{2p} \frac{f^{(2p-1)}(M) - f^{(2p-1)}(0)}{(2p)!}, \quad (4.35)$$

where  $B_k$  are the Bernoulli coefficients and  $f^{(n)}$  is the  $n$ -th derivative of  $f$ . Applying this formula to Eq. (4.34), we see that the derivatives  $f^{(2k-1)}(M)$  for  $k \geq 2$  form a series in  $1/M$  for large  $M$ , whereas  $f^{(1)}(M)$  and  $f^{(2k-1)}(0)$  give  $M$ -independent contributions for  $k \geq 1$ . Combining the result of the Euler-Maclaurin expansion with the first term in Eq. (4.34) and taking the limit of  $M \rightarrow \infty$ , we arrive at

$$\sum_{m=0}^M m^2 \ln \frac{M}{m} = \frac{1}{9}M^3 - \frac{1}{12}M - \alpha + \frac{1}{360M} + \dots \quad (4.36)$$

The  $M$ -independent term,  $\alpha$ , is represented by the following series

$$\begin{aligned} \alpha &= \frac{1}{9} - \sum_{p=1}^{\infty} \frac{1}{(2p)!} A_{2p} \frac{d^{2p-1}}{dx^{2p-1}} [x^2 \ln x]_{x=1} \\ &= \frac{1}{9} - \frac{1}{12} + \frac{1}{360} - \frac{1}{7560} + \dots = 0.0304\dots \end{aligned} \quad (4.37)$$

Although we have not been able to prove this analytically, we observe that, to very high accuracy,

$$\alpha = \frac{\zeta(3)}{4\pi^2}. \quad (4.38)$$

The same constant is obtained when calculating the specific heat in real frequencies, when the Matsubara sums are converted into integrals (see Appendix E). We will thus treat relation (4.38) as an exact one.

Terms of order  $M^3$ ,  $M$ ,  $1/M$ , etc. in  $S(M)$  generate regular- $T^0$ ,  $T^2$ ,  $T^4$ , etc.-corrections to  $\Xi_2$ , whereas a constant term ( $-\alpha$ ) gives a universal, non-analytic  $T^3$ -contribution to  $\Xi_2$ . This contribution is precisely what we need. Retaining only this term in Eq. (4.33) and substituting the result into Eq. (4.2), we obtain the same correction to the specific heat as the one found by expressing the specific heat via the self-energy, Eq. (4.23).

For a finite-range interaction, a slight modification of the analysis presented in this Section leads to the result identical to that in Eq. (4.24).

For the sake of completeness, in Appendix E we evaluate the specific heat by computing the thermodynamic potential in real frequencies and show explicitly how the contribution from the zero-sound is cancelled out.

### C. specific heat in a generic Fermi liquid

Now we are in a position to discuss a more general question—what happens to the  $T^2$  term in the specific heat if the interaction is not weak. First, we discuss a model case of contact interaction of arbitrary strength and then move on to the case of a generic Fermi liquid.

#### 1. contact interaction

To second order in contact interaction  $u$ , relevant diagrams for the thermodynamic potential contain the square of the polarization bubble [cf. Fig. 7, 2(a) and 2(b)]. Since  $Q = 0$  and  $Q = 2k_F$  contributions to the thermodynamic potential are identical for this case, we evaluate the  $Q = 0$ -contribution first, and then just double the result at the end. In Sec. IV B 2, we have shown that the non-analytic,  $T^3$  contribution to the thermodynamic potential comes from the square of the dynamic part of  $\Pi_m$ . According to Eq. (4.25), higher orders in  $u$  generate higher powers of  $\Pi_m$ . Another effect of higher orders is that self-energy insertions result in replacing the bare Green's functions by exact one. As the main contribution to the  $T^3$ -term in  $\Xi$  comes from the states near the Fermi surface, one can approximate exact  $G$  by its expression near the pole

$$G(\omega_m, k) = \frac{Z}{i\omega_m - \epsilon_k^*}, \quad (4.39)$$

where  $Z$  is the renormalization factor,  $\epsilon_k^* = v_F^*(k - k_F)$ ,  $v_F^* = k_F/m^*$ , and  $m^*$  is the renormalized mass. Parameters  $Z$  and  $m^*$  are some functions of the bare interaction  $u$ , whose forms, in general, are not known. This amounts to replacing the prefactor and the Fermi velocity in Eq. (4.26)

$$\Pi_m(\Omega_m, Q) \rightarrow \Pi_m^*(\Omega, Q) = -\frac{m^* Z^2}{2\pi} \left[ 1 - \frac{|\Omega_m|}{\sqrt{\Omega_m^2 + (v_F^* Q)^2}} \right]. \quad (4.40)$$

A term of order  $n$  in series Eq. (4.25) contains  $(\Pi_m^*)^n$  and thus generates a binomial expansion in powers of  $\mathcal{D}^* = |\Omega_m|/\sqrt{\Omega_m^2 + (v_F^* Q)^2}$

$$(\Pi_m^*)^n = (-)^n (Z^2 m^*/2\pi)^n \sum_{l=0}^n (-)^l C_n^l \mathcal{D}^{*l}, \quad (4.41)$$

where  $C_n^l$  is the binomial coefficient. It is easy to make sure that only the term with  $l = 2$  in Eq. (4.41) yields  $\Omega_m^2 \ln|\Omega_m|$  upon the momentum integration, whereas all other terms yield just  $\Omega_m^2$ . As was shown in Sec. IV B 2, the frequency sum

$$T \sum_{\Omega_m=0}^{E_F} \Omega_m^2 \ln|\Omega_m| \quad (4.42)$$

gives a universal  $T^3$  contribution to the thermodynamic potential, responsible for the  $T^2$  term in the specific heat (see (4.33)). At the same time, the frequency sum

$$T \sum_{\Omega_m=0}^{E_F} \Omega_m^2 \quad (4.43)$$

contributes only analytic- $T^2, T^4$ , etc.-terms to  $\Xi$ , but no  $T^3$ -term. The problem therefore reduces to collecting the combinatorial coefficients of  $\mathcal{D}^{*2}$  terms at each order and re-summing the perturbation series.

Expanding each term in Eq. (4.25) to order  $\mathcal{D}^{*2}$  and using

$$\sum_{k=1}^{\infty} kx^{k-1} = \left( \frac{1}{1-x} \right)^2, \quad (4.44)$$

we find that the  $T^2$ -term in the specific heat is given by

$$\delta C(T)/T = -\frac{9\zeta(3)}{\pi^2} u_{\text{eff}}^2 C_{\text{FG}}^*/E_F^*. \quad (4.45)$$

Here  $C_{\text{FG}}^* = \pi m^* T/3$ ,  $E_F^* = k_F v_F^*/2$ , and

$$u_{\text{eff}}^2 = (u^*)^2 [1 + 2u^* + 6(u^*)^2 + 4(u^*)^3 + \dots] = (u^*)^2 \left[ \frac{3}{2} \left( \frac{1}{1-u^*} \right)^2 + \frac{1}{2} \left( \frac{1}{1+u^*} \right)^2 - 1 \right], \quad (4.46)$$

where

$$u^* \equiv Z^2 m^* U/2\pi. \quad (4.47)$$

This result is valid for  $0 \leq u^* < 1$ . The divergence of  $u_{\text{eff}}^2$  at  $u^* = 1$ , resulting from the spin-channel, signals an instability towards a magnetically-ordered state. A plot of  $u_{\text{eff}}^2(u^*)$  is presented in Fig. 8.

## 2. generic interaction

The result for a contact interaction, Eq. (4.45), is of a rather limited use, as, in general, the Fourier transform of the interaction does depend on the momentum transfer. To obtain a form of  $\delta C(T)$ , valid for a generic Fermi liquid, we first go back to the second-order diagrams for the thermodynamic potential, and identify the structure of the vertices contributing to the non-analytic part of  $C(T)$ .

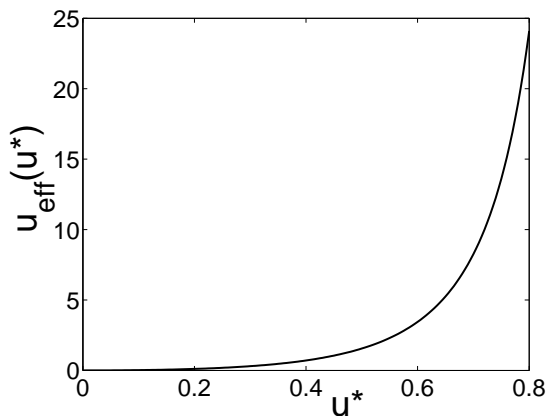


FIG. 8: Effective coupling for a  $T^2$ -term in the specific heat  $u_{\text{eff}}^2$  [ Eq. (4.46)] as a function of the renormalized interaction  $u^*$ , Eq. (4.47).

We consider first a small- $Q$  contribution to the diagram 2(b) in Fig. 7. It is proportional to  $U^2(0) T \sum_{\Omega} \int d^2 Q \Pi^2(\Omega_m, Q)$ , where the integration is restricted to small  $Q$ . Each of the two polarization bubbles is obtained by the integration over internal fermion momenta,  $\mathbf{k}$  in the upper bubble and  $\mathbf{p}$  in the lower one. At first glance,  $\mathbf{k}$  and  $\mathbf{p}$  are completely uncorrelated, as the integrations over  $\mathbf{k}$  and  $\mathbf{p}$  are independent of each other. This would imply that the total momenta for the two vertices in diagram 2(b) are arbitrary. In general, this is indeed true. However, a non-analytic,  $T^3$ -term in the thermodynamic potential arises only from a product of non-analytic,  $|\Omega_m|/Q$  parts of the two polarization bubbles, integrated over  $Q$ . In Appendix F, it is shown that the  $|\Omega_m|/Q$ -term in  $\Pi_m(\Omega_m, Q)$  comes from an integral  $\int d^2 k G(\omega_m + \Omega_m, \mathbf{k} + \mathbf{Q}) G(\omega_m, k)$  from only over those regions of  $k$  where  $\mathbf{k}$  is nearly orthogonal to  $\mathbf{Q}$  (and the same for  $\mathbf{p}$  in the other bubble). Since both  $\mathbf{k}$  and  $\mathbf{p}$  are almost orthogonal to  $\mathbf{Q}$ , they are either nearly parallel or nearly antiparallel to each other. In Appendix F, it is also shown that the contribution from the nearly parallel  $\mathbf{k}$  and  $\mathbf{p}$  vanishes, *i.e.*, the non-analytic, “ $Q = 0$ ” contribution to  $\Xi$  involves only a vertex with a small momentum transfer  $Q$  and small total momentum  $\mathbf{k} + \mathbf{p}$  (“backscattering” vertex). The same consideration holds for the  $U^2(2k_F)$ -term from diagram 2(b) in Fig. 7 and for the  $U(0)U(2k_F)$ -term from diagram 2(a) in Fig. 7. In both cases, the  $T^3$ -term in  $\Xi$  comes only from those momentum range, where  $\mathbf{k}$  and  $\mathbf{p}$  are nearly antiparallel. We thus see that the  $T^2$ -term in  $C(T)$  involves only vertices of the type  $(\mathbf{k}, -\mathbf{k}; \mathbf{k}, -\mathbf{k})$  and  $(\mathbf{k}, -\mathbf{k}; -\mathbf{k}, \mathbf{k})$ .

Consider now what happens when we add higher-order terms in the interaction. They lead to two types of corrections: self-energy insertions into the fermion lines in the two bubbles and corrections to the vertices. The self-energy corrections are of the Fermi-liquid type: they account for the appearance of the quasi-particle  $Z$ -factors, and for the replacement of the bare fermion mass by the effective one. Vertex corrections lead to a variety of diagrams. A typical  $n$ -th order diagram contains  $n$  bubbles. [We remind that these bubbles are either explicit, as in diagrams 2(b) and 3(c), or are obtained after integrating over the fermion variables, as in the rest of the diagrams. Some diagrams, *e.g.*, 3(b), contains bubbles both explicitly and implicitly.] To obtain a  $T^2$  contribution to  $C(T)$ , one needs to take the dynamic,  $|\Omega_m|/Q$ -parts of the two out of  $n$  bubbles, and set  $\Omega = 0, Q \rightarrow 0$  in the remaining  $n - 2$  ones, as any extra factor of  $\Omega/Q$ , as well as any extra factors of  $Q$  eliminates the logarithmic divergence of the momentum integral. The dynamic terms can come either from the two bubbles, already present in the skeleton second-order diagrams, or from the bubbles associated with the vertex corrections. It is intuitively plausible that, once the two dynamic bubbles are chosen at the  $n$ -th order, while the rest of diagram is evaluated at  $\Omega_m = 0$ , thus constituting the  $n$ -th order correction to the *static* vertex. In other words, it is plausible that the non-analytic,  $T^3$ -term in the thermodynamic potential can be expressed as the two second-order *skeleton* diagrams, in which the wavy lines are replaced by exact static vertices,  $\Gamma^k(\mathbf{k}, -\mathbf{k}; \mathbf{k}, -\mathbf{k})$  and  $\Gamma^k(\mathbf{k}, -\mathbf{k}; -\mathbf{k}, \mathbf{k})$ , and bare fermion lines are replaced by solid ones.

This conjecture, however, needs to be verified, as diagrams for the thermodynamic potential contain combinatoric factors. *A priori*, it is not clear whether these factors, combined with those associated with the selection of the two dynamic bubbles, would give just the right combinatoric factors to form the perturbative series for the static vertices. In order to verify this conjecture, we explicitly evaluated the  $T^3$ -term in the thermodynamic potential to the third order in  $U(Q)$ , and compared the result with that obtained by inserting renormalized static vertices into two-bubble skeleton diagrams. This derivation is presented in Appendix F. We find the two expressions, obtained directly and via skeleton diagrams, are identical. We did not attempt to prove that this equivalence holds to all orders in  $U(Q)$ , but the agreement between the two third-order results is a promising sign. In what follows, we assume that this



agreement holds to all orders in  $U(Q)$ , i.e., the non-analytic part of the thermodynamic potential is a product of two (renormalized) dynamic bubbles and two exact static vertices,  $\Gamma^k(\mathbf{k}, -\mathbf{k}; \mathbf{k}, -\mathbf{k})$  and  $\Gamma^k(\mathbf{k}, -\mathbf{k}; -\mathbf{k}, \mathbf{k})$ . To first order in  $U$ , these vertices reduce just to  $U(0)$  and  $U(2k_F)$ , respectively.

Vertices  $\Gamma^k(\mathbf{k}, -\mathbf{k}; \mathbf{k}, -\mathbf{k})$  and  $\Gamma^k(\mathbf{k}, -\mathbf{k}; -\mathbf{k}, \mathbf{k})$  are exact in a sense that they include *all* static corrections, coming from the states both away from *and* near the Fermi surface. The latter produce powers of the static bubble,  $\Pi_m(\Omega_m = 0, Q \rightarrow 0) = -Z^2 m^*/2\pi$ , which, we remind, comes from the states in a narrow range near the Fermi surface [2]. In other words, the vertices include all corrections, except those coming from the dynamic part of the polarization bubble. In conventional notations [1, 2], vertices  $\Gamma(\mathbf{k}, -\mathbf{k}; \mathbf{k}, -\mathbf{k})$  and  $\Gamma(\mathbf{k}, -\mathbf{k}; -\mathbf{k}, \mathbf{k})$  are related to  $\Gamma^k(\theta)$ , defined by Eq. (1.16). As the incoming momenta are nearly anti-parallel to each other, angle  $\theta$  in Eq. (1.16) can be put equal to  $\pi$ .

Vertex  $\Gamma^k(\pi)$ , as a tensor in the spin space, can be represented as

$$\Gamma_{\alpha\beta,\gamma\delta}^k(\pi) = \Gamma^k(\mathbf{k}, -\mathbf{k}; \mathbf{k}, -\mathbf{k})\delta_{\alpha\gamma}\delta_{\beta\delta} - \Gamma^k(\mathbf{k}, -\mathbf{k}; -\mathbf{k}, \mathbf{k})\delta_{\alpha\delta}\delta_{\beta\gamma}. \quad (4.48)$$

Quasi-particle  $Z$ -factors, resulting from the self-energy insertions into the fermion lines of the bubbles, can be incorporated into a relation between  $\Gamma^k$  and the quasi-particle scattering amplitude [2]

$$f_{\alpha\beta,\gamma\delta}(\pi) = Z^2 \Gamma_{\alpha\beta,\gamma\delta}^k(\pi). \quad (4.49)$$

Next, representing the scattering amplitude in terms of its charge- and spin components

$$\begin{aligned} f_{\alpha\gamma,\beta\delta}(\mathbf{k}, -\mathbf{k}) &= f_{\alpha\gamma,\beta\delta}(\pi) = \frac{\pi}{m^*} [f_c(\pi)\delta_{\alpha\gamma}\delta_{\beta\delta} + f_s(\pi)\sigma_{\alpha\gamma}\sigma_{\beta\delta}] \\ &= \frac{\pi}{m^*} [\{f_c(\pi) - f_s(\pi)\}\delta_{\alpha\gamma}\delta_{\beta\delta} + 2f_s(\pi)\delta_{\alpha\delta}\delta_{\beta\gamma}], \end{aligned} \quad (4.50)$$

and comparing Eq. (4.50) with Eq. (4.48), we obtain

$$Z^2 \Gamma^k(k, -k; k, -k) = \frac{\pi}{m^*} [f_c(\pi) - f_s(\pi)], \quad Z^2 \Gamma^k(k, -k; -k, k) = -2 \frac{\pi}{m^*} f_s(\pi). \quad (4.51)$$

Substituting  $Z^2 \Gamma^k(\mathbf{k}, -\mathbf{k}, \mathbf{k}, -\mathbf{k})$  instead of  $U(0)$  and  $Z^2 \Gamma^k(\mathbf{k}, -\mathbf{k}; -\mathbf{k}, \mathbf{k})$  instead of  $U(2k_F)$  into Eq. (4.24), we obtain the final form of the non-analytic part of the specific heat in a generic Fermi liquid

$$\delta C(T)/T = -\frac{3\zeta(3)}{2\pi (v_F^*)^2} [f_c^2(\pi) + 3f_s^2(\pi)] T. \quad (4.52)$$

On the other hand,  $\delta C(T)$  does not have a simple closed form in terms of the Landau interaction function,  $F(\theta)$ . Indeed, the Landau function is related to vertex  $\Gamma^\omega$ , defined in Eq. (1.17), rather than to  $\Gamma^k$ :

$$F_{\alpha\beta,\gamma\delta}(\theta) = Z^2 \Gamma_{\alpha\beta,\gamma\delta}^\omega(\theta) = \frac{\pi}{m^*} [\{\gamma_c(\pi) - \gamma_s(\pi)\}\delta_{\alpha\gamma}\delta_{\beta\delta} + 2\gamma_s(\pi)\delta_{\alpha\delta}\delta_{\beta\gamma}]. \quad (4.53)$$

A perturbative expansion for  $\Gamma^\omega(\pi)$  includes static vertex corrections from the states away from the Fermi surface but not in its vicinity, *i.e.*, it neglects the vertex corrections associated with  $\Pi(\Omega = 0, Q \rightarrow 0)$ . Whereas there is a simple relation between the partial components of functions  $\Gamma^k(\theta)$  and  $\Gamma^\omega(\theta)$  [2], in order to relate these two functions at a given angle, *e.g.*,  $\theta = \pi$ , one has to invoke an infinite number of partial components. In this respect, the universal sub-leading term in the specific heat is different from the leading, Fermi-liquid term,  $C(T)/T = \text{const}$ , which is expressed in terms of  $\langle F_c(\theta) \cos \theta \rangle$ , where  $F_c$  is the charge component of the Landau function.

To emphasize an absence of a simple relation between  $\Gamma^k(\theta)$  and  $\Gamma^\omega(\theta)$ , we present the relation between the charge- and spin components of scattering amplitude,  $f_a(\pi)$ , and those of the vertex,  $\gamma_a(\pi)$  ( $a = c, s$ ), to third order in  $U(Q)$ . Using results from Appendix F, we obtain

$$\begin{aligned} f_c(\pi) &= \gamma_c(\pi) - (\gamma_c(\pi) - \gamma_s(\pi))(\gamma_c(\pi) - \gamma_s(\pi) + 2\langle \gamma_s(\theta) \rangle) - \langle \gamma_s(\theta) \gamma_s(\pi - \theta) \rangle; \\ f_s(\pi) &= \gamma_s(\pi) - \langle \gamma_s(\theta) \gamma_s(\pi - \theta) \rangle, \end{aligned} \quad (4.54)$$

where  $\langle \dots \rangle$  stands for averaging over  $\theta$ . To the same accuracy, the terms of order  $(\Gamma^\omega)^2$  can be expressed via the bare interaction potential  $U(Q = 2k_F \sin \theta/2)$  using the first-order relations:  $\Gamma_c^\omega(\theta) = U(0) - U(\theta)/2$  and  $\Gamma_s^\omega(\theta) = -(1/2)U(\theta)$ . The relations between  $\Gamma^\omega$  and  $U(Q)$  to second order are presented in Appendix F.

The rather complicated relations between  $\Gamma_a^k(\pi)$  and  $\Gamma_a^\omega(\pi)$  are simplified if bare interaction  $U(Q)$  is strongly peaked at  $Q = 0$ , so that  $\Gamma_c^\omega(\pi)$  is much larger than  $\Gamma_s^\omega(\theta)$  for a generic  $\theta$ , including  $\theta = \pi$ . In this limit, perturbative series for the relation between  $\Gamma_c^k$  and  $\Gamma_c^\omega$  can be summed up exactly, and  $\Gamma_c^k(\pi)$  can be expressed in terms of  $\Gamma_c^\omega(\pi)$  as

$$f_c(\pi) = \frac{\gamma_c(\pi)}{1 + \gamma_c(\pi)} \quad (4.55)$$

In addition, if the condition  $\gamma_s(\theta)$  is met then, the contribution to the specific heat from  $\gamma_c(\pi)$  dominates, and the singular term in the specific heat becomes

$$\delta C(T)/T = -\frac{3m\zeta(3)}{4\pi} \left( \frac{\gamma_c(\pi)}{1 + \gamma_c(\pi)} \right)^2 \frac{T}{E_F}. \quad (4.56)$$

### 3. Non-analytic term in the specific heat for the Coulomb interaction

The limiting case of  $\gamma_c(\pi) \rightarrow \infty$  in Eq. (4.56) corresponds to the Coulomb interaction in the weak coupling limit, when the dimension-less gas parameter,  $r_s \equiv \sqrt{2}me^2/k_F$ , is small. [We remind that Eq. (4.56) is valid only in the limit  $\gamma_s(\theta) \ll 1$ .] [Recall that  $\Gamma_c^\omega(\theta)$  is expressed via  $U(0)$  and  $U(\theta)$ , whereas  $\Gamma_s^\omega(\theta)$  is expressed only via  $U(\theta)$  and, for generic  $\theta$ , is proportional to  $r_s$ .] We see that in this limit  $\Gamma_c^\omega(\pi)$  drops out from Eq. (4.56), and the singular term in the specific heat becomes

$$\delta C(T)/T = -\frac{3m\zeta(3)}{4\pi} \frac{T}{E_F}. \quad (4.57)$$

For the Coulomb interaction, the  $T^2$ - term in the specific heat is universal, *i.e.*, it is independent of  $r_s$  at small  $r_s$ . This result is in full agreement with Ref. [31].

For the sake of completeness, we explicitly calculate the specific heat for the Coulomb potential by summing-up the RPA (ring) sequence of diagrams for the thermodynamic potential (diagrams 1(a), 2(b), 3(c) ... in Fig. 7). A sum of these diagrams results in a familiar expression for  $\Xi$

$$\Xi = -\frac{T}{2} \sum_{i\Omega_m} \int \frac{d^2Q}{(2\pi)^2} \ln \frac{1}{1 - 2V(Q)\Pi_m(\Omega_m, Q)}, \quad (4.58)$$

where  $V(Q) = 2\pi e^2/Q$  and a factor of two in front of  $\Pi_m$  comes from the spin summation. Replacing the Matsubara sum by a contour integral and using Eq. (4.2), we obtain the following expression for the correction to the specific heat:

$$\delta C(T)/T = \frac{\partial}{\partial T} \frac{1}{8\pi^2 T^2} \int_0^\infty d\Omega \frac{\Omega}{\sinh^2 \Omega/2T} \int_0^\infty dQ Q \arg \frac{1}{1 - 2V(Q)\Pi^R(\Omega, Q)}. \quad (4.59)$$

The pole of the effective interaction at  $\Omega^2 = \Omega_p^2(Q) \equiv v_F^2 \kappa Q/2$  corresponds to a 2D plasmon mode, where  $\kappa \equiv 2me^2$  is the screening wave-vector. Near the plasmon pole,

$$\frac{1}{1 - 2V(Q)\Pi^R(\Omega, Q)} \approx \frac{\Omega_p^2(Q)}{(\Omega + i0^+)^2 - \Omega_p^2(Q)} \quad (4.60)$$

the argument of the effective interaction changes by  $-\pi$  when  $Q$  intersects the plasmon curve. The plasmon's contribution to  $\delta C(T)$  comes from the region  $2\Omega^2/v_F^2\kappa < Q < \Omega/v_F$ . As typical  $\Omega \simeq T$ , one can neglect the contribution from the lower limit of  $Q$  for  $T \ll \kappa v_F$ . We then obtain a universal and interaction-independent plasmon contribution to  $\delta C(T)$

$$C_{\text{PL}}(T)/T = -\frac{9\zeta(3)}{2\pi^2} \frac{C_{\text{FG}}}{E_F}. \quad (4.61)$$

For the contribution from the particle-hole region, we find

$$C_{\text{PH}}(T)/T = -\frac{\partial}{\partial T} \frac{1}{8\pi^2 T^2} \int_0^\infty d\Omega \frac{\Omega}{\sinh^2 \Omega/2T} \int_{\Omega/v_F}^\infty dQ Q \tan^{-1} W(Q, \Omega), \quad (4.62)$$

where

$$W(Q, \Omega) \equiv \frac{\kappa\Omega}{\sqrt{v_F^2 Q^2 - \Omega^2} (Q + \kappa)}. \quad (4.63)$$

The integral over  $Q$  in Eq. (4.62) diverges logarithmically at the upper limit, where  $\tan^{-1} W(Q, \Omega) \approx W(Q, \Omega)$ . The divergence is cut at  $Q \simeq k_F$  as Eq. (4.63) is only valid for small  $Q$ . Subtracting off and adding  $W(Q, \Omega)$  in Eq. (4.62), we split  $C_{\text{PH}}(T)$  into two parts as

$$C_{\text{PH}}(T) = C_{\text{PH}}^{(1)}(T) + C_{\text{PH}}^{(2)}(T); \quad (4.64a)$$

$$C_{\text{PH}}^{(1)}(T)/T = -\frac{\partial}{\partial T} \frac{1}{8\pi^2 T^2} \int_0^\infty d\Omega \frac{\Omega}{\sinh^2 \Omega/2T} \int_{\Omega/v_F}^\infty dQ Q [\tan^{-1} W(Q, \Omega) - W(Q, \Omega)]; \quad (4.64b)$$

$$C_{\text{PH}}^{(2)}(T)/T = -\frac{\partial}{\partial T} \frac{1}{8\pi^2 T^2} \int_0^\infty d\Omega \frac{\Omega}{\sinh^2 \Omega/2T} \int_{\Omega/v_F}^{k_F} dQ Q W(Q, \Omega). \quad (4.64c)$$

The integral over  $Q$  for  $C_{\text{PH}}^{(1)}(T)$  is convergent at the upper limit, and the integral can be extended to infinity—thus this contribution is universal. One can readily make sure that typical  $Q \simeq \Omega/v_F \simeq T/v_F \ll \kappa$ , so that  $\kappa$  drops out from function  $W(Q, \Omega)$  in Eq. (4.63). Evaluating the integral, we obtain

$$C_{\text{PH}}^{(1)}(T)/T = \frac{9\zeta(3)}{4\pi^2} \frac{C_{\text{FG}}}{E_F}, \quad (4.65)$$

which differs by a factor of  $(-1/2)$  from the plasmon contribution Eq. (4.61). The sum of the two contributions is

$$\delta C(T)/T = C_{\text{PL}}(T)/T + C_{\text{PH}}^{(1)}(T)/T = -\frac{9m\zeta(3)}{4\pi} \frac{T}{E_F}, \quad (4.66)$$

which coincides with Eq. (4.57).

Finally, the second term in Eq. (4.64a),  $C_{\text{PH}}^{(2)}(T)$ , gives a regular, linear-in- $T$ , correction to  $C(T)$ . To logarithmic accuracy,

$$\int_{\Omega/v_F}^{k_F} dQ Q W(Q, \Omega) \approx (\kappa\Omega/v_F) \int_{\kappa}^{k_F} dQ/Q = (\kappa\Omega/v_F) \ln k_F/\kappa, \quad (4.67)$$

and

$$C_{\text{PH}}^{(2)}(T) = -C_{\text{FG}}(T) \frac{\sqrt{2}}{\pi} r_s |\ln r_s|. \quad (4.68)$$

We remind that our treatment is applicable for  $r_s \ll 1$ . Notice that the  $r_s |\ln r_s|$  correction to  $C(T)/T$  can be interpreted as the result of the mass renormalization

$$\delta m/m = -\frac{\sqrt{2}}{\pi} r_s \ln r_s^{-1}. \quad (4.69)$$

This last expression coincides with that obtained in Ref. [14] by evaluating the low-energy asymptotic form of the self-energy.

## V. CONCLUSIONS

This paper presents a detailed perturbation theory for interacting fermions in 2D and analyzes non-analytic corrections to the Fermi-liquid behavior beyond the second-order in interaction. We derived a full expression for the fermion self-energy near the mass shell, valid to an infinite order in a weak short-range interaction. Recent study [13] found, that to second order in  $U$ , the imaginary part of the self-energy diverges as  $\ln |\Delta|$  upon approaching the mass shell, where  $\Delta = \omega - \epsilon_k = 0$ . Following this lead, we demonstrated that beyond second order, divergences become of the power-law form in  $|\Delta|$ , and get stronger with increasing order of the perturbation theory. We identified the divergent contribution as originating from the interaction between fermions and zero-sound collective excitations. In the perturbation theory, the collective mode coincides with the upper edge of the particle-hole continuum. This degeneracy causes divergences at any finite order of the perturbation theory. We demonstrated that a re-summation of the power-law divergent terms to all orders in the interaction eliminates the power-law divergences in the self-energy, as the zero-sound mode splits off the continuum. The still remaining logarithmic divergences near the mass shell are eliminated by a finite curvature of the fermion spectrum. A fully renormalized self-energy is then completely free from

divergences. We found that for a contact interaction, the real part of the self-energy vanishes on the Fermi surface, while the imaginary part of  $\Sigma$  behaves as  $\omega^2 \ln |\omega|$ . Near the mass shell, both  $\text{Re}\Sigma^R$  and  $\text{Im}\Sigma^R$  evolve rapidly as scaling functions of variables  $\Delta/(u^2\omega)$  and  $\Delta E_F/\omega^2$ . The first scaling variable emerges after the re-summation of power-law divergent diagrams, whereas the second one describes the effect of a finite curvature of the Fermi surface. We demonstrated that the interaction of fermions with the zero-sound mode gives rise to a kink in the spectral function near  $\Delta = u^2\omega/2$ . This prediction is amenable to a direct check in photoemission measurements or in momentum-conserved tunneling between two layers of the 2D electron gases.

In the second part of the paper, we discussed the non-analytic part of the specific heat:  $\delta C(T) \propto T^2$ . We found that the collective-mode contribution to the fermion self-energy does not affect the specific heat, i.e., a non-analytic term in  $C(T)$  is determined only by the perturbative part of the self-energy. This result was also verified by calculating the thermodynamic potential directly, in both real- and Matsubara frequency formalisms. We also considered the  $T^2$ -term in the specific heat for a generic Fermi liquid. We showed that it can be expressed in a simple way via the spin and charge components of the quasi-particle scattering amplitude at angle  $\theta = \pi$  between the incoming momenta. On the other hand,  $\delta C(T)$  cannot be expressed compactly in terms of the Landau interaction function. Finally, we found for the Coulomb interaction, not amenable to a direct perturbative treatment due to infrared singularities, a non-analytic  $T^2$ -term in  $C(T)$  is universal and independent of the gas parameter,  $r_s$ , for small  $r_s$ .

### A. acknowledgments

We acknowledge stimulating discussions with I. Aleiner, B. Altshuler, A. Andreev, F. Essler, W. Metzner, A. Millis, and A. Nersisyan. The research has been supported by NSF DMR 0240238 (A. V. Ch.), NSF DMR-0308377 (D. L. M.), and NSF DMR-0237296 (L. I. G.). The work of D. L. M. and L. I. G. during their stay at the Argonne National Laboratory was supported by the US DOE Office of Science under contract No. W-31-109-ENG-38.

## APPENDIX A: BACKSCATTERING CONTRIBUTION TO THE SELF-ENERGY

In this Appendix, we present the calculation of a non-analytic part of the self-energy, resulting from backscattering processes at  $T = 0$ . This part of the self-energy contains two contributions: from processes with small momentum transfers  $\vec{k}_1 \approx \vec{k}'_1$ ,  $\vec{k}_2 \approx \vec{k}'_2$  [see Fig. 1(b)] and from processes with momentum transfers near  $2k_F$ :  $\vec{k}_1 \approx -\vec{k}'_1$ ,  $\vec{k}_2 \approx -\vec{k}'_2$  [see Fig. 1(c)] ( $g_2$ - and  $2k_F$ -processes, correspondingly). The contribution to the self-energy from the  $g_2$ -process was obtained in [13], and here we just cite the result. In Matsubara frequencies,

$$\Sigma_{g_2}(\omega_m, k) = -i \frac{u^2}{8\pi E_F} \left[ \omega_m^2 \ln \frac{E_F}{\omega_m - i\epsilon_k} + \frac{1}{4} (\omega_m + i\epsilon_k)^2 \ln \frac{\omega_m - i\epsilon_k}{\omega_m + i\epsilon_k} \right]. \quad (\text{A1})$$

We neglected regular terms of order  $\omega_m^2$  in (A1). Although the second term in Eq. (A1) is also formally of order  $\omega^2$  for a generic ratio of  $\omega_m$  and  $\epsilon_k$ , we have to keep it in order to compensate for a superficial divergence in the first term at  $\omega_m = \pm i\epsilon_k$  in Eq. (A1). Converting to real frequencies and taking the imaginary part, we obtain

$$\text{Im}\Sigma_{g_2}^R(k, \omega) = \frac{u^2}{8\pi E_F} \left[ \omega^2 \ln \frac{E_F}{|\omega|} + \omega^2 \ln \left| \frac{\omega}{\omega + \epsilon_k} \right| - \frac{1}{4} (\omega - \epsilon_k)^2 \ln \left| \frac{\omega - \epsilon_k}{\omega + \epsilon_k} \right| \right]. \quad (\text{A2})$$

We note in passing that while the logarithmic factors in Eq. (A1) comes from the integration over boson momenta  $Q$  that exceeds  $\omega_m/v_F$ , the boson frequency ( $\Omega_m$ ) is smaller than the fermion one ( $\omega_m$ ); e.g., for positive  $\omega_m$ , the non-analytic contribution comes from  $-\omega_m < \Omega_m < 0$ . This implies that a non-analytic part of the self-energy cannot be obtained within a renormalization-group scheme, in which internal energies in the self-energy diagram are assumed to be larger than the external ones. Notice also that the self-energy in Eq. (A2) is regular at  $\omega = \pm\epsilon_k$ , since the superficial divergences in the second and third terms cancel each other. Both of these terms are of order  $\omega^2$  for a generic ratio of  $\omega$  and  $\epsilon_k$ , and hence, to logarithmic accuracy, one can neglect them compared to the first term. Eq. (A2) then simplifies to

$$\text{Im}\Sigma_{g_2}^R(\omega, k) = \frac{u^2}{8\pi E_F} \omega^2 \ln \frac{E_F}{|\omega|}. \quad (\text{A3})$$

Next, we calculate the contribution of the  $2k_F$ -scattering to the self-energy. Substituting Eq. (4.27) for the polarization bubble near  $Q = 2k_F$  into the second-order expression for self-energy

$$\Sigma(k, \omega_m) = -U^2 \int \int \frac{d^2 Q d\Omega}{(2\pi)^3} G(\omega_m + \Omega_m, \mathbf{k} + \mathbf{Q}) \Pi_m(\Omega_m, Q), \quad (\text{A4})$$

and expanding the quasi-particle spectrum  $\epsilon_{\mathbf{k}+\mathbf{Q}}$  near  $Q = 2k_F$  as

$$\epsilon_{\mathbf{k}+\mathbf{Q}} = -\epsilon_k + v_F k_F \theta^2 + (2k_F^2/m) q, \quad (\text{A5})$$

where  $q = (Q - 2k_F)/2k_F$  and  $\pi - \theta$  is the angle between  $\mathbf{k}$  and  $\mathbf{Q}$  ( $|\theta| \ll \pi$ ), we obtain, after re-scaling the variables,

$$\Sigma_{2k_F}(\omega_m, k) = -\frac{mU^2 k_F}{2\pi^4} \int_{-\infty}^{\infty} dq \int_{-\infty}^{\infty} d\bar{\Omega}_m \left[ q + \sqrt{q^2 + \bar{\Omega}_m^2} \right]^{1/2} \int_0^{\infty} \frac{d\theta}{\theta^2/2 + q - \bar{\epsilon}_k - i(\bar{\omega}_m + \bar{\Omega}_m)}, \quad (\text{A6})$$

where  $\bar{\omega}_m = \omega_m/4E_F$ ,  $\bar{\Omega}_m = \omega_m/4E_F$ , and  $\bar{\epsilon}_k = \epsilon_k/4E_F$ . Using

$$\int_0^{\infty} \frac{dz}{z^2 + a} = \frac{\pi}{2} \frac{\text{sgnRe}(a)}{\sqrt{a}}, \quad (\text{A7})$$

we can re-write Eq. (A6) as

$$\Sigma_{2k_F}(\omega_m, k) = -\frac{\sqrt{2}mU^2 k_F}{4\pi^3} \int_{-\infty}^{\infty} dq \int_{-\infty}^{\infty} d\bar{\Omega}_m \left[ q + \sqrt{q^2 + \bar{\Omega}_m^2} \right]^{1/2} \frac{\text{sgnRe}(\sqrt{q - \bar{\epsilon}_k - i(\bar{\omega}_m + \bar{\Omega}_m)})}{\sqrt{q - \bar{\epsilon}_k - i(\bar{\omega}_m + \bar{\Omega}_m)}}. \quad (\text{A8})$$

As we are interested in a  $\omega^2 \ln \omega$  contribution, we need to check the behavior of the integrand for large  $|q|$  (logarithms come from the integration over the range where internal variables are larger than the external ones). For  $q \rightarrow +\infty$ , the integrand approaches a finite limit ( $\sqrt{2}$ ) as  $\sqrt{2}(1 + \bar{\Omega}_m^2/8q^2)$ ; neither the leading nor sub-leading terms in this asymptotic form produce a logarithm upon integrating over  $q$ . However, for negative and large  $q$ ,  $(q + \sqrt{q^2 + \bar{\Omega}_m^2})^{1/2} \approx |\bar{\Omega}_m|/(\sqrt{2}|q|)$ , and  $\sqrt{q - \bar{\epsilon}_k - i(\bar{\omega}_m + \bar{\Omega}_m)} \approx -i\sqrt{|q|} \text{sgn}(\bar{\Omega}_m + \bar{\omega}_m)$ , so that the integrand behaves as  $|q|^{-1}$ ; hence the logarithmic singularity does come from this region of  $q$ . To logarithmic accuracy, we obtain

$$\Sigma_{2k_F}(\omega_m, k) = -i \frac{mU^2 k_F}{4\pi^3} \int_{-\infty}^{\infty} d\bar{\Omega}_m |\bar{\Omega}_m| \text{sgn}(\bar{\Omega}_m + \bar{\omega}_m) \int_{-E_F/v_F}^{-|\bar{\omega}_m|/v_F} \frac{dq}{q}. \quad (\text{A9})$$

Evaluating the integrals, we find

$$\Sigma_{2k_F}(\omega_m, k) = -i \frac{u^2}{8\pi} \frac{\omega_m^2}{E_F} \ln \frac{E_F}{|\omega_m|}. \quad (\text{A10})$$

Continuing to real frequencies and taking the imaginary part yields

$$\text{Im} \Sigma_{2k_F}^R(\omega, k) = \frac{u^2}{8\pi E_F} \omega^2 \ln \frac{E_F}{|\omega|}. \quad (\text{A11})$$

Comparing this result with Eq. (A3), we see that the non-analytic parts of  $\text{Im} \Sigma^R$  resulting from the  $g_2-$  and  $2k_F-$  processes are identical within logarithmic accuracy. The result for the sum of the two terms is quoted in Eq. (3.5). Observe that, according to Eq. (A11), a non-analytic,  $\omega^2 \ln |\omega|$  part of  $\Sigma_{2k_F}(\omega_m, k)$  comes from negative  $q$ , *i.e.*, from  $Q < 2k_F$ , where the static polarization bubble is just a constant; thus a singular correction is entirely dynamical. A singular,  $(Q - 2k_F)^{1/2}$ , behavior of the static bubble  $\Pi(\Omega = 0, Q)$  for  $Q > 2k_F$  does not give rise to an imaginary part of the self-energy—this result follows due to the fact that a static density fluctuation cannot decay the quasi-particles. However, the fact that even for a dynamic bubble, only the region of  $Q < 2k_F$  is responsible for a non-analytic part of  $\Sigma(k, \omega)$  is rather peculiar and has not been emphasized explicitly in earlier work [13]. Note in this regard that both regions of  $Q < 2k_F$  and  $Q > 2k_F$  contribute to a non-analytic behavior of the spin susceptibility [13, 16].

Now, we evaluate the integrals in Eq. (A8) beyond logarithmic accuracy. The result is

$$\text{Im} \Sigma_{2k_F}^R(k, \omega) = \frac{u^2}{8\pi E_F} \left[ \omega^2 \ln \frac{E_F}{|\omega|} + \omega^2 \ln \left| \frac{\epsilon_k}{\omega} \right| - (\omega + \epsilon_k)^2 \ln \left| \frac{\epsilon_k}{\omega + \epsilon_k} \right| \right]. \quad (\text{A12})$$

Again, the last two terms are of order  $\omega^2$  for a generic ratio of  $\omega$  and  $\epsilon_k$  but we keep them in order to demonstrate that  $\text{Im} \Sigma_{2k_F}^R(\omega, k)$  remains finite at  $\omega = \pm \epsilon_k$ .

## APPENDIX B: NON-SYMMETRIZED VERTEX

In this Appendix, we derive an expression for forward-scattering part of the non-symmetrized vertex,  $\bar{\Gamma}$ , summing up diagrams with the maximum number of polarization bubbles to all orders in contact interaction,  $U$ . We then anti-symmetrize the vertex, and substitute the result into the Dyson equation [ Eq. (3.20)] to obtain the corresponding part of the self-energy. The diagrams for a non-symmetrized vertex up to the third order are presented in Fig. 3. In the Matsubara technique, we associate a factor of  $-U$  with each of the interaction lines, and a factor  $-2$  with each of the polarization bubble. There is also an extra factor of  $-1$  for exchange processes in which the two outgoing legs are permuted (the last diagrams of second and third order in Fig. 3). We present here a general recipe for calculating the  $\nu^{th}$  ( $\nu > 1$ ) order vertex diagram. As is seen from the Fig. 3, the vertex consists of two parts. The first part comes from the direct interaction and contains a spin factor  $\delta_{\alpha\gamma}\delta_{\beta\varepsilon}$ . The second part is due to the exchange interaction, and comes with a spin factor  $\delta_{\alpha\varepsilon}\delta_{\beta\gamma}$ . At each order, there is only one exchange diagram whose contribution is  $-(-U)^\nu \Pi^{\nu-1} \delta_{\alpha\varepsilon}\delta_{\beta\gamma}$ . (At second and third orders, these are the first and third diagrams in the third column of Fig. 3, respectively.) The rest of diagrams are due to the direct interaction and contain various number of bubbles. At order  $\nu$ , the number of these bubbles ( $R$ ) varies from 0 to  $\nu - 1$ . For a diagram with  $R$  bubbles,  $R + 1$  interaction lines are used up in making a chain of bubbles and connecting it to two external solid lines. The remaining  $N = \nu - R - 1$  interaction lines can be arranged anywhere either at the two ends of the chain of bubbles or inside the  $R$  bubbles. There are  $S = R + 2$  sites where  $N$  interaction lines can be placed. The number of diagrams with  $R$  bubbles is equal to the number of ways to arrange  $N$  lines among  $S$  sites:

$$\frac{(S + N - 1)!}{(S - 1)!N!} = \frac{\nu!}{(R + 1)!(\nu - R - 1)!}. \quad (\text{B1})$$

Consequently, the contribution to  $\bar{\Gamma}$  from diagrams with  $R$  bubbles is

$$\frac{\nu!}{(R + 1)!(\nu - R - 1)!} (-U)^\nu (-2)^R \Pi^{\nu-1} \delta_{\alpha\gamma}\delta_{\beta\varepsilon}. \quad (\text{B2})$$

The total contribution from all bubble diagrams at the order  $\nu$  is then

$$\sum_{R=0}^{\nu-1} \frac{\nu!(-2)^R}{(R + 1)!(\nu - R - 1)!} (-U)^\nu \Pi^{\nu-1} \delta_{\alpha\gamma}\delta_{\beta\varepsilon} = -\frac{(1 - (-1)^\nu)}{2} U^\nu \Pi^{\nu-1} \delta_{\alpha\gamma}\delta_{\beta\varepsilon} \quad (\text{B3})$$

where we have used an identity

$$\sum_{R=0}^{\nu} \frac{\nu!(-2)^R}{R!(\nu - R)!} = (1 - 2)^\nu = (-1)^\nu. \quad (\text{B4})$$

Adding up direct and exchange terms, we obtain the following form for non-symmetrized vertex at order  $\nu > 1$ :

$$\bar{\Gamma}_{\alpha\beta,\gamma\varepsilon}^\nu = -\frac{1}{2}(1 - (-1)^\nu)U^\nu \Pi^{\nu-1} \delta_{\alpha\gamma}\delta_{\beta\varepsilon} - (-U)^\nu \Pi^{\nu-1} \delta_{\alpha\varepsilon}\delta_{\beta\gamma}. \quad (\text{B5})$$

The vertex function can now be readily summed up to all orders, with the result

$$\bar{\Gamma}_{\alpha\beta,\gamma\varepsilon}(p_1, p_2; p_1 - q, p_2 + q) = \bar{\Gamma}_{\alpha\beta,\gamma\varepsilon}(q) = -U \delta_{\alpha\gamma}\delta_{\beta\varepsilon} + \sum_{\nu=1}^{\infty} \bar{\Gamma}_{\alpha\beta,\gamma\varepsilon}^\nu = -\delta_{\alpha\gamma}\delta_{\beta\varepsilon} \frac{U}{1 - (UII)^2} - \delta_{\alpha\varepsilon}\delta_{\beta\gamma} \frac{U^2 \Pi(q)}{1 + UII(q)}. \quad (\text{B6})$$

Using an SU(2) identity

$$\delta_{\alpha\varepsilon}\delta_{\beta\gamma} = (1/2) (\sigma_{\alpha\gamma}^a \sigma_{\beta\varepsilon}^a + \delta_{\alpha\gamma}\delta_{\beta\varepsilon}), \quad (\text{B7})$$

and introducing dimensionless spin and charge vertices  $\mathcal{G}_\rho$  and spin  $\mathcal{G}_\sigma$ , defined in Eq. (3.16), we obtain Eq. (3.15). Anti-symmetrizing the vertex as prescribed by Eq. (3.17) and substituting the result into the Dyson equation (3.20),

we obtain for the self-energy

$$\begin{aligned}
\Sigma_{\alpha\beta}(p) &= \delta_{\alpha\beta} \int_q UG(p-q) - \int_{p'} U\bar{\Gamma}_{\gamma\alpha;\gamma\beta} G(p')\Pi(p-p') + \int_{p''} U\bar{\Gamma}_{\gamma\alpha;\beta\gamma} G(p'')\Pi(p-p'') \\
&= \delta_{\alpha\beta} \int_q UG(p-q) + 2\delta_{\alpha\beta} \int_{p'} \left\{ \frac{U^2}{1-(U\Pi)^2} + \frac{U^3}{1+U\Pi} \right\} G(p')\Pi(p-p') \\
&\quad - \delta_{\alpha\beta} \left\{ \int_{p''} \frac{U^2}{1-(U\Pi)^2} + \frac{U^3}{1+U\Pi} \right\} G(p'')\Pi(p-p'') \\
&= \delta_{\alpha\beta} \int_q UG(p-q) + \delta_{\alpha\beta} \int_q \frac{U^2\Pi(q)}{1-(U\Pi)^2} G(p-q) + \delta_{\alpha\beta} \int_q \frac{U^3\Pi(q)^2}{1+U\Pi} G(p-q). \tag{B8}
\end{aligned}$$

Re-arranging the result, we obtain the self-energy in the form of Eq. (3.22).

### APPENDIX C: RELATION BETWEEN EQS.(4.5) AND (4.11).

In this Appendix, we discuss the relation between the two results for the specific heat: the one derived in Ref. [1] [Eq.(4.5)] and the one following from the Luttinger-Ward functional for the thermodynamic potential [42] [Eq.(4.11)]. We show that the two expressions yield identical results for the  $T^2$ -term in the specific heat, provided that one uses in temperature-dependent self-energy in Eq.(4.5) (the recipe in Ref. [1] is to use the self-energy at  $T=0$ ).

For the sake of simplicity, we focus on the contact interaction and consider only a perturbative part of the thermodynamic potential, neglecting the interaction with the zero-sound mode.

We begin with the Luttinger-Ward approach. To second order in  $u$ , the Luttinger-Ward formula for the entropy is

$$S = S_0 + \frac{\partial}{\partial T} \left[ \frac{N_0}{2} T \sum_m \int d\epsilon_k \Sigma(\omega_m, k, T) G_0(\omega_m, k) \right]. \tag{C1}$$

Here  $S_0$  is the entropy of an ideal gas,  $N_0 = m/2\pi$  is the density of states per spin projection,  $G_0 = (i\omega_m - \epsilon_k)^{-1}$  is the bare Green's function, and  $\Sigma(\omega_m, k, T)$  is the self-energy, which depends on  $T$  both implicitly, via  $\omega_m = \pi T(2m+1)$ , and also explicitly. The second-order self-energy in Matsubara frequencies is, to logarithmic accuracy, [13]

$$\Sigma(\omega_m, k, T) = -\frac{i}{2E_F} u^2 T \sum_{\Omega_m} |\Omega_m| \text{sign}(\omega_m + \Omega_m) \ln \frac{E_F}{\epsilon_k - i(2\Omega_m + \omega_m)} - \frac{i}{4E_F} u^2 T \sum_{\Omega_m} |\Omega_m| \text{sign}(\omega_m + \Omega_m) \ln \frac{E_F}{\epsilon_k - i\omega_m}. \tag{C2}$$

The first term in Eq.(C2) comes from backscattering and includes the sum of contributions from the  $g_2$ - and  $2k_F$ -processes. The second term in Eq.(C2) comes from forward scattering.

Had there been no dependence on  $\epsilon_k$  under the logarithm in (C2), the integration over  $\epsilon_k$  in (C1) would have been straightforward, as it would have involved only  $G_0(\omega_m, k)$ . Using the familiar relations

$$\mathcal{P} \int d\epsilon_k \text{Re} G_0^R(\omega, \epsilon_k) = 0, \quad \int d\epsilon_k \text{Im} G_0^R(\omega, \epsilon_k) = -\pi; \tag{C3}$$

and converting the Matsubara sums into the contour integrals, one could readily verify that the expression for the entropy would have involved only  $\text{Re}\Sigma^R(\omega, k, T)$  on the mass shell and that both terms in (C2) would have contributed to the entropy.

Because of the  $k$ -dependence under the logarithms in (C2), the actual situation is different. Indeed, substituting the second term in (C2) into (C1) we find that the integral over  $\epsilon_k$  reduces to

$$\int_{-E_F}^{E_F} \frac{d\epsilon_k}{\epsilon_k - i\omega_m} \ln \frac{E_F}{\epsilon_k - i\omega_m} = \frac{1}{2} \ln^2 \frac{E_F - i\omega}{-E_F - i\omega} \tag{C4}$$

The result in (C4) vanishes in the limit of  $|\omega_m| \ll E_F$ . Thus, to logarithmic accuracy, forward scattering does not contribute to the entropy. It is instructive, however, to see how the zero for the integral in (C4) comes about. In fact, there are two contributions to this integral, each of order  $\ln E_F/|\omega_m|$ . The first comes from the region of small  $\epsilon_k$ :  $\epsilon_k \simeq \omega_m$ . For this contribution, the dependence on  $\epsilon_k$  under the logarithm can be neglected, *i.e.*, the logarithmic factor can be approximated by  $\ln E_F/|\omega_m|$ . The integration over  $\epsilon_k$  then yields

$$\ln \frac{E_F}{|\omega_m|} \int \frac{d\epsilon_k}{\epsilon_k - i\omega_m} = i\pi \text{sgn}\omega_m \ln \frac{E_F}{|\omega_m|}. \tag{C5}$$

The second contribution comes from the region of large  $\epsilon_k : \epsilon_k \gg \omega_m$ . Here, we obtain, combining the contributions from positive and negative  $\epsilon_k$

$$\begin{aligned} \int_{-E_F}^{E_F} \frac{d\epsilon_k}{\epsilon_k - i\omega_m} \ln \frac{E_F}{\epsilon_k - i\omega_m} &\approx \int_{|\omega_m|}^{E_F} \frac{d\epsilon_k}{\epsilon_k} \ln \frac{-\epsilon_k - i\omega_m}{\epsilon_k - i\omega_m} \\ &= -i\pi \text{sgn}\omega_m \ln \frac{E_F}{|\omega_m|}. \end{aligned} \quad (\text{C6})$$

Combining (C5) and (C6), we find that for the forward scattering contribution to  $\Sigma$ , the net integral over  $\epsilon_k$  vanishes. For the backscattering contribution, the integral over  $\epsilon_k$  is

$$\int \frac{d\epsilon_k}{\epsilon_k - i\omega_m} \ln \frac{E_F}{\epsilon_k - i\omega_m - 2i\Omega_m}. \quad (\text{C7})$$

There are again two contributions to this integral to order  $\ln E_F/|\omega_m|$ . The contribution from  $\epsilon_k \simeq \omega_m$  is the same as (C5), while the one from  $\epsilon_k \gg \omega_m$  is

$$-i\pi \text{sgn}\Omega_m \ln \frac{E_F}{|\omega_m|}. \quad (\text{C8})$$

It follows from (C2) that, at low temperatures, the dominant contribution to the self-energy comes from such  $\Omega_m$  that are of different sign compared to  $\omega_m$ . As a result, for the backscattering part of the self-energy, the small- $\epsilon_k$ - and large- $\epsilon_k$ -contributions to the integral over  $\epsilon_k$  add up instead of canceling out.

The outcome of this analysis is that, to logarithmic accuracy, one can still formally neglect the dependence on  $\epsilon_k$  in the logarithm in (C2); however, one should simultaneously neglect the forward-scattering contribution to the self-energy, and multiply backscattering contribution by a factor of two. Converting the Matsubara sum in Eq. (C1) into a contour integral, one can express the entropy via the real part of the self-energy on the mass shell, as

$$S = S_0 - N_0 \int_{-\infty}^{\infty} d\omega \left[ \frac{\omega}{T} \frac{\partial n_0}{\partial \omega} \text{Re}\Sigma^R(\omega, T) - \left( n_0 - \frac{1}{2} \right) \frac{\partial}{\partial T} \text{Re}\Sigma^R(\omega, T) \right] \quad (\text{C9})$$

We emphasize again that this expression is two times larger than the one that one would obtain by just neglecting the dependence on  $\epsilon_k$  in the forward scattering self-energy.

Next, we find the relation between the two terms in (C9). If the self-energy were independent of  $T$ , the second term would not contribute, and the entropy would be given just by the first term. We show, however, that the two terms in (C9) are in fact equal, *i.e.*, the entropy can be formally re-expressed via only the first term in (C9), but with another extra factor of two.

To demonstrate this, we need an expression for  $\text{Re}\Sigma^R(\omega, T)$ . The easiest way to obtain it is to convert Matsubara self-energy into  $\text{Im}\Sigma^R(\omega, T)$  and then obtain  $\text{Re}\Sigma^R(\omega, T)$  by a Kramers-Kronig transformation. Approximating the logarithm in the first term in (C2) as  $\ln E_F/|\Omega_m|$ , we obtain

$$\text{Im}\Sigma^R(\omega, T) = \frac{u^2}{4\pi E_F} \int_{-\infty}^{\infty} d\Omega \ln \frac{E_F}{|\Omega|} \left[ \coth \frac{\Omega}{2T} - \tanh \frac{\omega + \Omega}{2T} \right]. \quad (\text{C10})$$

Substituting the Kramers-Kronig transform of (C10) into (C9), and integrating in the second term in (C9) by parts, we find after some algebra that the two terms in (C9) contribute equally to the entropy.

As a result, the net expression for the entropy in the Luttinger-Ward formalism is given by

$$S = S_0 - 2N_0 \int_{-\infty}^{\infty} d\omega \frac{\omega}{T} \frac{\partial n_0}{\partial \omega} e\Sigma^R(\omega, T). \quad (\text{C11})$$

It differs by a factor of four from what one would have obtained neglecting both  $\epsilon_k$  under the logarithm in (C2) and the  $T$ -dependence of  $\text{Re}\Sigma^R(\omega, T)$ .

Eq. (C11) is very similar to the one from Ref. [1] which, to the lowest order in the interaction, reduces to

$$S = S_0 + \frac{2}{\pi} N_0 \int_{-\infty}^{\infty} d\omega \int d\epsilon_k \frac{\omega}{T} \frac{\partial n_0}{\partial \omega} \text{Im} [\Sigma(\omega, k) G_0(\omega, \epsilon_k)]. \quad (\text{C12})$$

We first assume, and then verify, that once  $\Sigma(\omega, \epsilon_k)$  is evaluated *in real frequencies* and substituted into (C12), the momentum dependence of the self-energy can be neglected. Using (C3), we then obtain that (C11) and (C12) coincide if one substitutes the  $T$ -dependent self-energy in (C12).



Finally, we show that the momentum-dependent part of  $\Sigma(\omega, k)$  does not contribute to the entropy. The proof is somewhat tricky. The backscattering term in the second-order self-energy [first term in (A2)] does indeed contain the dependence on  $\epsilon_k$  under the logarithm, just like in the Matsubara self-energy. Because of this dependence, there is a non-zero contribution to the entropy from  $\text{Im}\Sigma_B^R \text{Re}G_0^R$  term in (C12). Should one keep it, this would modify the answer for  $S$  by a factor of two, compared to (C11).

However, in contrast to the Matsubara self-energy, which is strictly perturbative, the self-energy in real frequencies does develop mass-shell singularities in the forward-scattering part. We remind that the reason for these singularities is the presence of the zero-sound mode that, within the perturbation theory, coincides with the upper boundary of the particle-hole continuum. These mass-shell singularities give rise a non-perturbative part of the self-energy,  $\Sigma_{\text{ZS}}$  and also modify the part of the self-energy coming from the interaction with the particle-hole continuum,  $\Sigma_{\text{ex}} + \Sigma_{\text{PH}}$  [see Eq.(3.24)].

We show that the two contributions to the entropy – one from  $\text{Im}\Sigma_B^R \text{Re}G_0^R$  and the other from  $\text{Im}\Sigma_F^R \text{Re}G_0^R$  – cancel each other. To this end, we demonstrate that

$$B(\omega) \equiv \frac{m}{2\pi} \mathcal{P} \int d\epsilon_k \frac{\text{Im}\Sigma^R(\omega, \epsilon_k)}{\omega - \epsilon_k}. \quad (\text{C13})$$

where  $\Sigma^R$  is a sum of backscattering and forward-scattering contributions, does not contain terms non-analytic in  $\omega$ .

We begin with the backscattering part. As it was discussed in Sec. II, there are two types of backscattering processes:  $g_2$  and  $2k_F$ . The self-energy from the  $g_2$ -process is given by Eq. (A2). Terms that are independent of  $\epsilon_k$  obviously do not contribute to  $B(\omega)$ . Substituting the rest of Eq. (A2) into (C13), we obtain

$$B_{g_2} = -\frac{m}{32} \frac{u^2}{E_F} \omega |\omega|. \quad (\text{C14})$$

In (C14), we neglected terms of order  $\omega$ , which contribute just to the renormalization of the effective mass at  $T = 0$ . It can be also verified that the subleading term to (C14) is analytic and scales as  $\omega^3/E_F$ .

The  $2k_F$ -contribution to the self-energy is given by (A12). Substituting this contribution into (C13) and evaluating the integral over  $\epsilon_k$ , we find that  $B_{2k_F}(\omega)$  contains regular terms of order  $\omega$ ,  $\omega^3$ , etc., but no  $\omega|\omega|$  term. Therefore, for our purposes,

$$B_{2k_F}(\omega) = 0. \quad (\text{C15})$$

Consider now the forward-scattering ( $g_4$ ) part. The imaginary part of  $\Sigma_{\text{ZS}}$  is analytic near the mass shell and does not contribute to  $B$ . The imaginary parts of  $\Sigma_{\text{PH}}$  and  $\Sigma_{\text{ex}}$ , however, depend on  $\Delta = \omega - \epsilon_k$  logarithmically away from the immediate vicinity of the mass shell, where the logarithmic dependence is regularized [see (3.26), (3.31) and (3.49)]. Substituting the regularized expression, Eq. (3.49) into (C13) we find that the  $B_{g_4}$  reduces to

$$B_{g_4} = \frac{m}{16\pi^2} \frac{u^2}{E_F} |\omega| \omega \int_{-\infty}^{\infty} \frac{dx}{x - \delta} \ln|x| = \frac{m}{8\pi^2} \frac{u^2}{E_F} \delta |\omega| \omega \int_0^{\infty} \frac{dx \ln x}{x^2 - \delta^2}, \quad (\text{C16})$$

where  $\delta \propto u$  is *positive*. Performing the integration, we obtain

$$B_{g_4} = \frac{m}{32} \frac{u^2}{E_F} \omega |\omega|, \quad (\text{C17})$$

We see that it is opposite in sign to the contribution from the  $g_2$ - process, Eq. (C14). Adding up the three contributions, Eqs. (C14), (C15) and (C17), we obtain that the total  $B(\omega) = 0$ . This proves that the momentum dependence of  $\Sigma$  in (C12) can indeed be neglected.

#### APPENDIX D: SPECIFIC HEAT IN ELIASHBERG-TYPE THEORIES

In this Appendix, we consider the specific heat for the case when the fermion self-energy depends only on the frequency but not on momentum. Such a situation occurs, *e.g.*, in Eliashberg-type theories, which describes the interaction of fermions with slow boson modes [41]. We show that in order to obtain a correct form of the linear-in- $T$ , Fermi-liquid contribution to the specific heat, one can use the approximate relation Eq. (4.1) (from Ref. [1]), which expresses the thermodynamic potential solely in terms of an exact fermion Green's function. However, a correct form of the sub-leading, non-analytic part of the specific heat can only be obtained using the full Luttinger-Ward expression, while Eq. (4.1) gives an erroneous result, even if one uses the self-energy at finite  $T$ ,  $\Sigma(\omega_m, T)$ .

A general form of the thermodynamic potential,  $\Xi$ , for a system of interacting fermions is given by Luttinger-Ward formula, Eq. (4.8). It expresses  $\Xi$  in terms of the full Green's function and infinite series of skeleton self-energies. In many cases, though, the interaction between fermions is strongly enhanced in a particular interaction channel. In such a case, multiple interactions between fermions in the same channel can be adequately described as an exchange of corresponding low-energy bosonic collective modes. If, in addition, these modes are slow compared to fermions, the self-energy of fermions will be independent of the momentum,  $\Sigma(\omega_m, k) = \Sigma(\omega_m)$ , and corrections to fermion-boson vertex can be neglected due to the Migdal theorem. For these cases, the Luttinger-Ward formula reduces to a closed-form expression in terms of full propagators of fermions and low-energy bosons

$$\begin{aligned} \Xi = & -2T \sum_{\omega_m} \int \frac{d^D k}{(2\pi)^D} \left[ \frac{1}{2} \ln [\epsilon_{\mathbf{k}}^2 + \{\omega_m + \Sigma(\omega_m)\}^2] - i\Sigma(\omega_m)G(k, \omega_m) \right] \\ & + \frac{1}{2}T \sum_{\Omega_m} \int \frac{d^D Q}{(2\pi)^D} [\ln[D^{-1}(Q, \Omega_m)] + 2\Pi(\Omega_m, Q)D(\Omega_m, Q)] \\ & + T^2 g^2 \sum_{\omega_m, \omega'_m} \int \frac{d^D k d^D k'}{(2\pi)^{2D}} G(k, \omega_m)D(\mathbf{k} - \mathbf{k}', \omega_m - \omega'_m)G(k', \omega'_m). \end{aligned} \quad (\text{D1})$$

Here  $G(k, \omega_m) = [i\{\omega_m + \Sigma(\omega_m)\} - \epsilon_{\mathbf{k}}]^{-1}$  is the full fermion Green's function,  $D(Q, \Omega_m) = (D_0^{-1}(Q, \Omega) - 2\Pi(\Omega_m, Q))^{-1}$  is the full boson propagator (a factor of 2 is due to the spin summation),  $D_0(Q, \Omega)$  is the bare boson propagator,  $\Sigma(\Omega_m)$  and  $\Pi(\Omega_m, Q)$  are the fermion and boson self-energies, respectively, and  $g$  is the effective fermion-boson coupling. [In this Appendix, the Matsubara self-energy is defined with an  $i$  up front.] Eq. (D1) was first obtained in the context of the electron-phonon interaction [6, 44] (in which case  $D_0$  is the phonon propagator), and was applied later to the electron-electron interaction mediated by Landau-damped collective modes [17, 45, 46, 47, 48, 49]. In the latter case, the frequency dependence of  $D(Q, \Omega_m)$  comes predominantly from the boson self-energy, and the bare boson propagator  $D_0(Q, \Omega_m)$  can be approximated by its static form  $D_0(Q) \equiv D_0(Q, 0)$  [17, 45, 47, 48]. Notice that Eq. (D1) is applicable to the interaction with both charge- and spin modes, except for the spin case it has to be modified slightly due to the spin structure of the interaction [49].

The fermion and boson self-energies,  $\Sigma(\omega_m)$  and  $\Pi(\Omega_m)$ , are obtained from the condition that  $\Xi$  is stationary with respect to variations in  $\Sigma(\omega_m)$  and  $\Pi(\Omega_m)$ . Conditions

$$\delta\Xi/\delta\Sigma(k) = \delta\Xi/\delta\Pi(k) = 0$$

yield [44]

$$\begin{aligned} \Sigma(\omega_m) = & iTg^2 \sum_{\omega'_m} \int \frac{d^D k'}{(2\pi)^D} G(k', \omega'_m)D(\mathbf{k} - \mathbf{k}', \omega_m - \omega'_m); \\ \Pi(\Omega_m, Q) = & -Tg^2 \sum_{\omega_m} \int \frac{d^D k}{(2\pi)^D} G(k, \omega_m)G(\mathbf{k} - \mathbf{Q}, \omega_m - \Omega_m). \end{aligned} \quad (\text{D2})$$

Using Eq. (D2), the last term in Eq. (D1) can be re-written as

$$-T \sum_{\Omega_m} \int \frac{d^D Q}{(2\pi)^D} \Pi(\Omega_m)D(Q, \Omega_m) \quad (\text{D3})$$

or, equivalently,

$$2iT \sum_{\omega_m} \int \frac{d^D k}{(2\pi)^D} \Sigma(\omega_m)G(k, \omega_m). \quad (\text{D4})$$

Accordingly, Eq. (D1) reduces to

$$\begin{aligned} \Xi = & -2T \sum_{\omega_m} \int \frac{d^D k}{(2\pi)^D} \left[ \frac{1}{2} \ln [\epsilon_{\mathbf{k}}^2 + \{\omega_m + \Sigma(\omega_m)\}^2] - i\Sigma(\omega_m)G(k, \omega_m) \right] \\ & + \frac{1}{2}T \sum_{\Omega_m} \int \frac{d^D Q}{(2\pi)^D} \ln [D^{-1}(Q, \Omega_m)], \end{aligned} \quad (\text{D5})$$

or, equivalently, to

$$\begin{aligned} \Xi &= -T \sum_{\omega_m} \int \frac{d^D k}{(2\pi)^D} \ln \left[ \epsilon_{\mathbf{k}}^2 + \{(\omega_m + \Sigma(\omega_m))\}^2 \right] \\ &\quad + \frac{1}{2} T \sum_{\Omega_m} \int \frac{d^D Q}{(2\pi)^D} \left[ \ln[D^{-1}(Q, \Omega_m)] + 2\Pi(\Omega_m)D(Q, \Omega_m) \right]. \end{aligned} \quad (\text{D6})$$

Each of the last two expressions can be simplified further. In Eq. (D5), we switch from the integration over momentum to that over  $\epsilon_k$  using  $\int d^D k / (2\pi)^D = N_0 \int d\epsilon_k$ , where  $N_0$  is the density of states. Integrating over  $\epsilon_k$ , we find that the first line in Eq. (D5) reduces to

$$\begin{aligned} &-2T \sum_{\omega_m} \int \frac{d^D k}{(2\pi)^D} \left[ \frac{1}{2} \ln \left[ \epsilon_{\mathbf{k}}^2 + \{(\omega_m + \Sigma(\omega_m))\}^2 \right] - i\Sigma(\omega_m)G(k, \omega_m) \right] \\ &= -TN_0 \sum_{\omega_m} (|\omega_m + \Sigma(\omega_m)| - |\Sigma(\omega_m)|). \end{aligned} \quad (\text{D7})$$

As the sign of  $\Sigma(\omega_m)$  coincides with that of  $\omega_m$ , the self-energy drops out, and Eq. (D7) reduces to the result for non-interacting fermions,  $\Xi_{\text{FG}}$ . Substituting Eq. (D7) back into Eq. (D5), we obtain

$$\Xi = \Xi_{\text{FG}} + \frac{1}{2} T \sum_{\Omega_m} \int \frac{d^D Q}{(2\pi)^D} \ln[D^{-1}(Q, \Omega_m)], \quad (\text{D8})$$

where

$$\Xi_{\text{FG}} = -TN_0 \sum_{\omega_m} |\omega_m| \quad (\text{D9})$$

is the thermodynamic potential of a free Fermi gas. Eq. (D8) is often called a Luttinger-Ward expression for the thermodynamic potential in Eliashberg-type theories. For a spin interaction, the factor 1/2 in the second term in Eq. (D8) is replaced by 3/2 [49]. We note in passing that the frequency sum in  $\Xi_{\text{FG}}$  formally diverges, but its temperature-dependent part, which is what we need, can be extracted by using the following spectral representation

$$|\omega_m| = -\frac{1}{\pi} \int \frac{dx x}{x - i\omega_m}. \quad (\text{D10})$$

The above relation in conjunction with the following identity

$$T \sum_{\omega_m} \frac{1}{x - i\omega_m} = \frac{1}{2} - n_F(\omega_m), \quad (\text{D11})$$

can be used to extract the  $T$ -dependent part of  $\Xi_{\text{FG}}$ , we thus obtain the familiar Fermi-gas result,  $C_{\text{FG}} = (2\pi^2 N_0/3)T$ .

For the thermodynamic potential in the form of Eq. (D6), we can use the fact that for Landau-damped collective modes  $\Pi(\Omega_m) \propto |\Omega_m|$  and expand in  $\Pi$ , as higher powers of  $\Omega$  in the summand in Eq. (D6) generally lead to higher powers of  $T$  in  $\Xi$ . Expanding the logarithm, we see that the term linear in  $\Pi$  drops out, and the thermodynamic potential is given by

$$\Xi = -T \sum_{\omega_m} \int \frac{d^D k}{(2\pi)^D} \ln \left[ \epsilon_{\mathbf{k}}^2 + \{\omega_m + \Sigma(\omega_m)\}^2 \right] = -2T \sum_{\omega_m} \int \frac{d^D k}{(2\pi)^D} \ln G^{-1}(k, \omega). \quad (\text{D12})$$

This is the same expression as Eq. (4.8), obtained by a different approach as compared to that in Ref. [1]. In a Fermi liquid,  $\Sigma(\omega_m) = \lambda\omega_m$  at the lowest frequencies. Substituting this form into Eq. (D12), we immediately obtain

$$C_{\text{FL}} = C_{\text{FG}}(1 + \lambda), \quad (\text{D13})$$

Thus, both approaches—the one based on the Luttinger-Ward functional and the one used in Ref. [1]—give the same result for the FL-part of  $C(T)$ .

The issue now is whether the approximate form of  $\Xi$  [Eq. (D12)], when modified to include a finite-temperature self-energy can correctly describe the non-analytic corrections to the Fermi liquid. We argue that it does not. Indeed, expanding the logarithm to second order in  $\Pi_m$  in Eq. (D6), we obtain

$$\Xi = -T \sum_{\omega_m} \int \frac{d^D k}{(2\pi)^D} \ln [\epsilon_{\mathbf{k}}^2 + \{\omega_m + \Sigma(\omega_m)\}^2] + T \sum_{\omega_m} \int \frac{d^D Q}{(2\pi)^D} \Pi^2(Q, \Omega_m) D_0^2(Q). \quad (\text{D14})$$

To avoid further complications with a long-range interaction, we assume that  $D_0(0)$  is finite. Then, as we showed in Sec. IV B, the integral over  $Q$  gives  $\Omega_m^2 \ln |\Omega_m|$  which, upon summation over  $\Omega_m$ , results in a non-analytic term in  $\Xi$  ( $T^3$  in 2D and  $T^4 \ln T$  in 3D—see Appendix G). For these situations, the boson contribution to Eq. (D6) cannot be neglected when evaluating the non-analytic term in the specific heat.

We note in passing that expanding the logarithm in Eq. (D8) to order  $\Pi^2 D_0^2$  results in

$$\Xi = \Xi_{FG} - \frac{1}{4} T \sum_{\omega} \int \frac{d^D q}{(2\pi)^D} \Pi^2(q, \Omega) D_0^2(q). \quad (\text{D15})$$

Comparing Eqs. (D14) and (D15), we see that the first term in Eq. (D14) must be twice the integral of  $\Pi^2 D_0^2$ . This is consistent with the observation we made in Sec. IV A, where we found a factor of four difference between  $-2T \ln G^{-1}$  [the first term in Eq. (D14)] and Eq. (D15). However, a factor of two difference was attributed to neglecting the temperature dependence of  $\Sigma(\omega_m)$  while converting from Matsubara to real frequencies.

For completeness, we also demonstrate how one can obtain the Fermi-liquid result, Eq. (D13) from Eq. (D8), which expresses  $\Xi$  in terms of the boson propagator. As we have already mentioned, in order to get a Fermi-liquid,  $T^2$ -term in  $\Xi$ , one has to expand to first order in  $\Pi(\Omega_m, Q) \propto |\Omega_m|$ . To reproduce Eq. (D13), one therefore needs to relate the Landau damping term to  $\lambda$ . This relation can be found for arbitrary  $D_0(Q)$ . To shorten the presentation, we just consider a model form of  $D_0(Q)$ —a Lorentzian peaked at  $Q = 0$

$$D_0(Q) = \frac{D_0}{Q^2 + \xi^{-2}}. \quad (\text{D16})$$

For this form of  $D_0(Q)$ , the fermion self-energy at the lowest frequencies is readily obtained from Eq. (D2):

$$\Sigma(\omega_m) = \lambda \omega_m, \quad \lambda = \frac{g^2}{4\pi v_F \xi^{-1}}. \quad (\text{D17})$$

The polarization bubble at low frequencies and small momenta is also obtained from Eq. (D2):

$$\Pi(\Omega_m, Q) = \frac{\gamma}{D_0} \frac{|\Omega_m|}{Q}, \quad (\text{D18})$$

where  $\gamma = mg^2/(\pi v_F)$  (we set interatomic distance  $a = 1$ ). Substituting Eq. (D18) into Eq. (D8), integrating over boson momentum and collecting terms of order  $T^2$  in  $\Xi$ , we obtain

$$\Xi = -mT \sum_{\omega_m} |\omega_m| + \frac{1}{8} \gamma \xi T \sum_{\Omega_m} |\Omega_m|. \quad (\text{D19})$$

Summation over boson frequencies is performed by using spectral representation, in the same way as the sum over fermion frequencies in Eq. (D9). For temperature-dependent parts of the two sums in Eq. (D19) we find

$$T \sum |\omega_m| \rightarrow \frac{\pi}{6} T^2; \quad T \sum |\Omega_m| \rightarrow -\frac{\pi}{3} T^2. \quad (\text{D20})$$

Substituting this into Eq. (D19), we obtain

$$\Xi = -\frac{m\pi}{6} T^2 \left[ 1 + \frac{g^2}{4\pi v_F \xi^{-1}} \right]. \quad (\text{D21})$$

Comparing Eq. (D21) and Eq. (D17), we see that

$$\Xi = -\frac{m\pi}{6} T^2 [1 + \lambda], \quad (\text{D22})$$

*i.e.*, Eq. (D13) is reproduced.

Finally, we discuss the specific heat near a Quantum Critical Point (QCP) which, formally, corresponds to the limit of  $\xi = \infty$  in Eq. (D16). Here, we find

$$\Xi = \Xi_{\text{FG}} + \frac{1}{4\sqrt{3}}\gamma^{2/3}T \sum |\Omega_m|^{2/3}. \quad (\text{D23})$$

Evaluating the sum using

$$T \sum |\Omega_m|^{2/3} \rightarrow -\frac{T}{u} \sum \int \frac{dx x^4 \text{sgn} x}{x^3 + i\Omega_m} \quad (\text{D24})$$

where  $u = \int_0^\infty dz/(z^3 + 1) = 2\pi/(3\sqrt{3})$ , we obtain

$$\Xi = \Xi_{\text{FG}} - \frac{0.4803}{\pi}\gamma^{2/3}T^{5/3}. \quad (\text{D25})$$

Using Eq. (4.2), we obtain

$$C(T) = C_{\text{FG}} + \frac{0.5337}{\pi}\gamma^{2/3}T^{2/3}. \quad (\text{D26})$$

Eq. (D25) also allows one to verify the conjecture in Ref. [1] that Eq. (D12) can be used to evaluate the specific heat beyond the Fermi-liquid term. Evaluating the self-energy at QCP, we find [17, 48]

$$\Sigma(\omega_m) = \omega_m^{2/3}\omega_0^{1/3}, \quad \omega_0^{1/3} = \frac{1}{2\pi\sqrt{3}} \frac{g^2}{v_F\gamma^{1/3}}. \quad (\text{D27})$$

Substituting this result into Eq. (D12), and evaluating the momentum integral and the frequency sum, we obtain

$$\Xi = -T \sum_{\omega_m} \int \frac{d^D k}{(2\pi)^D} \log [\epsilon_{\mathbf{k}}^2 + \{\omega_m + \Sigma(\omega_m)\}^2] = \Xi_{\text{FG}} - \frac{0.3546}{\pi}\gamma^{2/3}T^{5/3}, \quad (\text{D28})$$

which differs from Eq. (D25) by a numerical prefactor. We see that using the zero-temperature self-energy in Eq. (D12), we do not reproduce Eq. (D25). This is another indication that Eq. (D12) is not valid for the calculations of  $C(T)$  beyond the Fermi-liquid term.

To avoid confusion, we emphasize that Eq. (D6) is valid only for Eliashberg-type theories. For the problem that we considered in the main text, the self-energy is  $k$ -dependent, and this eventually makes Eq. (4.8) valid to second order in  $U$ , provided that one uses a finite- $T$  self-energy instead of a zero- $T$  one. In view of the above consideration, however, we do not expect Eq. (4.8) to remain valid at higher orders in  $U$ . In any event, it is always safe to use Eq. (D5) in the calculations of the specific heat.

## APPENDIX E: EVALUATION OF THE THERMODYNAMIC POTENTIAL IN REAL FREQUENCIES

In this Appendix, we find the specific heat by calculating the thermodynamic potential which is expressed in real frequencies. The evaluation of the second-order contribution to  $\Xi$  is straightforward: we just replace the Matsubara sum in Eq. (4.33) by a contour integral. Using Eq. (4.2), we obtain

$$\delta C(T)/T = -\frac{\partial^2 \Xi_2}{\partial T^2} = U^2 \frac{\partial}{\partial T} \int_0^\infty \frac{d\Omega}{4\pi} \frac{\Omega}{T^2 \sinh^2 \Omega/2T} \int \frac{d^2 Q}{(2\pi)^2} \Pi_2^R(\Omega, Q), \quad (\text{E1})$$

where  $\Pi_2^R(\Omega, Q) = \text{Im} \Pi^2(\Omega + i0^+, Q)$  [see Eq. (3.10)]. When differentiating  $\Xi$  with respect to  $T$ , we assumed that the non-analytic part of the particle-hole bubble does not depend on temperature—keeping this source of the temperature dependence would result only in analytic,  $T^2$ -terms in  $C(T)/T$ . Using Eq. (3.11) for the singular part of  $\Pi_2^R(\Omega, Q)$  near  $Q = 0$ , performing elementary integrations, and multiplying the result by 2 to account for the contribution from  $2k_F$ , we indeed reproduce Eq. (4.23).

Next, we demonstrate how non-perturbative contributions to  $C(T)$  cancel out in the real-frequency formalism. To this end, we use series Eq. (4.25) for the thermodynamic potential

$$\Xi = \Xi_0 + \int_q \left[ -2U\Pi_m + \frac{1}{2}(U\Pi_m)^2 - \frac{1}{2} \ln \mathcal{G}_\rho - \frac{3}{2} \ln(-\mathcal{G}_\sigma) \right], \quad (\text{E2})$$

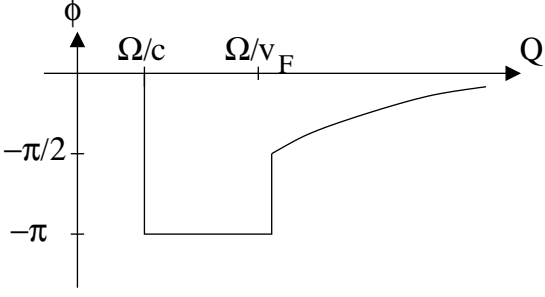


FIG. 9: Argument of charge vertex,  $\phi = \arg \mathcal{G}_\rho$ , where  $\mathcal{G}_\rho$  is defined in Eq. (3.16), as a function of the boson momentum  $Q$  at fixed frequency  $\Omega$ .  $Q = \Omega/c$  corresponds to the position of zero-sound pole, whereas  $Q = \Omega/v_F$  corresponds to the position of particle-hole continuum boundary.

where the effective vertices of charge and spin channels,  $\mathcal{G}_\rho$  and  $\mathcal{G}_\sigma$ , are defined in Eq. (3.16). We recall that the charge term  $-(1/2) \ln \mathcal{G}_\rho$  contains the contribution from the zero-sound mode. It is convenient to single out first- and second-order contributions in  $U$ , *i.e.*, to re-arrange Eq. (E2) as

$$\Xi = \Xi_0 + \Xi_1 + \Xi_2 + \Xi', \quad (\text{E3})$$

where

$$\Xi_1 = - \int_q U \Pi, \quad \Xi_2 = - \frac{1}{2} \int_q (U \Pi_m)^2, \quad (\text{E4})$$

and

$$\Xi' = \Xi_1 - 2\Xi_2 + \int_q \left[ -\frac{1}{2} \ln \mathcal{G}_\rho - \frac{3}{2} \ln(-\mathcal{G}_\sigma) \right] \quad (\text{E5})$$

contains a combined contribution of all higher orders. Our goal is to show that there is no non-analytic contribution to the specific heat from  $\Xi'$ . Converting Matsubara sums into contour integrals, we obtain for the non-perturbative part of the specific heat corresponding to  $\Xi'$

$$\begin{aligned} C'(T)/T &= - \frac{\partial^2 \Xi'}{\partial T^2} = \frac{\partial}{\partial T} \int_0^\infty \frac{d\Omega}{2\pi} \frac{\Omega}{T^2 \sinh^2 \Omega/2T} \int \frac{d^2 Q}{(2\pi)^2} \\ &\times \left[ \frac{1}{2} \arg \mathcal{G}_\rho + \frac{3}{2} \arg(-\mathcal{G}_\sigma) - U^2 \Pi_2^R \right] \end{aligned} \quad (\text{E6})$$

When differentiating Eq. (E6), we assumed again that the only  $T$ -dependence comes from the Bose distribution function. The  $T$ -dependence of vertices becomes important either near a finite-temperature critical point [8] or in 1D; neither of the cases are considered in this paper.

The momentum dependence of  $\arg \mathcal{G}_\rho$  at fixed  $\Omega > 0$  is shown in Fig. 9 (solid line). For  $Q < \Omega/c$ , where  $c$  is the zero-sound velocity,  $\text{Re} \mathcal{G}_\rho > 0$  and  $\text{Im} \mathcal{G}_\rho = 0$ , hence  $\arg \mathcal{G}_\rho = 0$ . At the zero-sound pole,  $Q = \Omega/c$ ,  $\arg \mathcal{G}_\rho$  jumps from zero to  $-\pi$ . It remains equal to  $-\pi$  until  $Q$  reaches the boundary of the particle-hole continuum,  $Q = \Omega/v_F$ . At this point,  $\arg \mathcal{G}_\rho$  jumps from  $-\pi$  to  $-\pi/2$  and decreases monotonically upon further increase in  $Q$ . On the other hand,  $\arg \mathcal{G}_\sigma$  is nonzero only inside the particle-hole continuum ( $Q > \Omega/v_F$ ). Finally, as  $\Pi_2^R \propto \delta(\Omega^2 - v_F^2 Q^2)$ , this term is only relevant at the boundary of the particle-hole region. This behavior of  $\arg \mathcal{G}_\rho$ ,  $\arg \mathcal{G}_\sigma$ , and  $\Pi_2^R$  suggests that it is convenient to split the momentum integral into the one over  $Q < \Omega/v_F$  and another one over  $Q > \Omega/v_F$ , and consider three terms in Eq. (E6) separately. In the region  $Q < \Omega/v_F$ , only the collective mode contributes to the momentum integral in Eq. (E6), and this contribution is given by

$$\int_{Q < \Omega/v_F} \frac{d^2 Q}{(2\pi)^2} \frac{1}{2} \arg \mathcal{G}_\rho = \frac{1}{2\pi} \int_{\Omega/c}^{\Omega/v_F} dQ Q \left( -\frac{\pi}{2} \right) = - \left( \frac{1}{v_F^2} - \frac{1}{c^2} \right) \frac{\Omega^2}{8} \approx - \frac{u^2 \Omega^2}{8 v_F^2}. \quad (\text{E7})$$

At the last step, we have expanded the full result to order  $u^2$ . The contribution from  $\arg \mathcal{G}_\rho$  in the particle-hole region  $Q > \Omega/v_F$  is

$$\begin{aligned} & \int_{Q > \Omega/v_F} \frac{d^2 Q}{(2\pi)^2} \frac{1}{2} \left[ -\tan^{-1} \left( \frac{u}{1+u} \frac{\Omega}{\sqrt{v_F^2 Q^2 - \Omega^2}} \right) + \frac{u}{1+u} \frac{\Omega}{\sqrt{v_F^2 Q^2 - \Omega^2}} \right] \\ &= \left( \frac{u}{1+u} \right)^2 \frac{\Omega^2}{16v_F^2} \approx u^2 \frac{\Omega^2}{16v_F^2}. \end{aligned} \quad (\text{E8})$$

To ensure the convergence of the  $Q$ -integral at large momenta, we subtracted off a term proportional to  $\text{Im}\Pi^R$ , which gives no  $T^2$ -contribution to  $C(T)$ , and used that  $\int_0^\infty dx (\tan^{-1} x^{-1/2} - x^{-1/2}) = -\pi/2$ . The contribution from  $\arg \mathcal{G}_\sigma$  comes only from the particle-hole region and is equal to

$$\begin{aligned} & \int_{Q > \Omega/v_F} \frac{d^2 Q}{(2\pi)^2} \frac{3}{2} \left[ \tan^{-1} \left( \frac{u}{1-u} \frac{\Omega}{\sqrt{v_F^2 Q^2 - \Omega^2}} \right) - \frac{u}{1-u} \frac{\Omega}{\sqrt{v_F^2 Q^2 - \Omega^2}} \right] \\ &= - \left( \frac{u}{1-u} \right)^2 \frac{3\Omega^2}{16v_F^2} \approx -u^2 \frac{3\Omega^2}{16v_F^2}. \end{aligned} \quad (\text{E9})$$

Again, a term proportional to  $\text{Im}\Pi^R$  has been subtracted off to ensure convergence. Finally, the  $U^2\Pi_2^R$ -term in Eq. (E6), coming from the boundary of the particle-hole region, yields

$$\frac{1}{4} u^2 \frac{\Omega^2}{v_F^2}. \quad (\text{E10})$$

Adding up Eqs. (E7-E10), we find that

$$C'(T) = 0, \quad (\text{E11})$$

as it was anticipated. Once again, this means that non-perturbative corrections do not change the result at order  $u^2$ —it is still given by Eq. (4.14).

## APPENDIX F: EVALUATION OF THE DIAGRAMS FOR THE THERMODYNAMIC POTENTIAL

### 1. second-order in the interaction

We have shown in the main text that, to second order in  $U(Q)$ , the thermodynamic potential,  $\Xi$ , contains a non-analytic,  $T^3$ -term whose magnitude depends only on  $U(0)$  and  $U(2k_F)$ . To this order in the interaction,  $\Xi$  consists of two particle-hole bubbles, and the argument for the non-analyticity in  $\Xi$  was that it originated from both  $Q = 0$  and  $Q = 2k_F$  non-analyticities of the bubbles. This argument, however, does not specify the relation between fermion momenta in the two bubbles, and therefore it does not distinguish between the cases when the total incoming momentum in the two vertices of diagrams 2(b) and 3(a) in Fig. 7 is near zero or near  $2k_F$ .

Now, we look into diagrams 2(b) and 3(a) in Fig. 7 in more detail, and show that the non-analytic term in  $\Xi$  involves only vertices with “1D” momentum structure  $(\mathbf{k}, -\mathbf{k}; \mathbf{k}, -\mathbf{k})$  ( $Q = 0$  contribution) and  $(\mathbf{k}, -\mathbf{k}; -\mathbf{k}, \mathbf{k})$  ( $Q = 2k_F$  contribution). For definiteness, we consider diagram 2(b) and focus on the  $Q = 0$  contribution. The  $2k_F$ -contribution to diagram 2(b) and diagram 2(a) can be treated in a similar manner.

The argument why the momenta in the two bubbles are related to each other is based on the observation that in order to have  $\Xi = T \sum_{\Omega_m} \Xi_\Omega \propto T^3$ , the summand  $\Xi_\Omega \propto \int d^2 Q \Pi^2(\Omega_m, Q)$  must be non-analytic in  $\Omega$ . The momentum integral does, indeed, diverge logarithmically at  $v_F Q \gg \Omega_m$ , as  $\Pi^2(\Omega_m, Q)$  contains a term  $\Omega_m^2/Q^2$ , which is just the product of the  $\Omega_m/Q$  terms in each of the bubbles. Then  $\Xi_\Omega \propto \Omega_m^2 \ln |\Omega_m|$ , and the summation over Matsubara frequencies yields  $\Xi \propto T^3$ .

We now demonstrate that the  $|\Omega_m|/Q$  term in  $\Pi(\Omega_m, Q)$  comes from integration over internal momenta  $\mathbf{k}$  in a narrow range around  $\mathbf{k} \cdot \mathbf{Q} = 0$ . To see this, we recall that the bubble has the following form -

$$\Pi(\Omega_m, Q) = (1/2\pi^2) T \sum_{\omega_m} \int d^2 k G_0(\omega_m, \mathbf{k}) G_0(\omega + \Omega, \mathbf{k} + \mathbf{Q}). \quad (\text{F1})$$

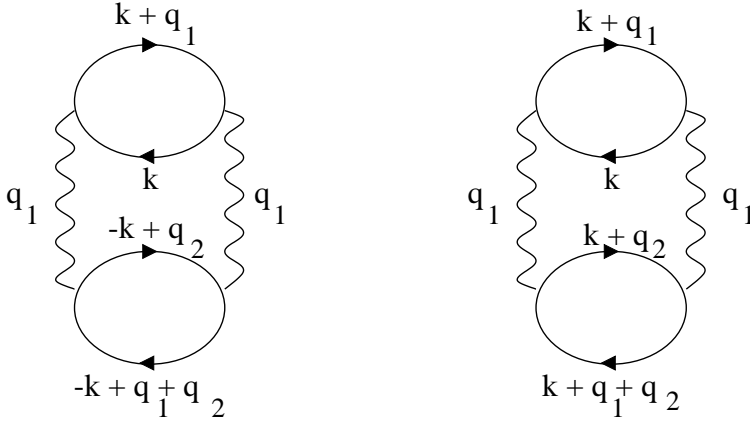


FIG. 10: A second-order ring diagram for the thermodynamic potential. Momenta  $\mathbf{q}_1$  and  $\mathbf{q}_2$  are small:  $\mathbf{q}_1, \mathbf{q}_2 \ll |\mathbf{k}| \approx k_F$ . Labelling on the left and right diagrams corresponds to backscattering and forward scattering, correspondingly.

Expanding  $\epsilon_{\mathbf{k}+\mathbf{Q}}$  near the Fermi surface as  $\epsilon_k + v_F Q \cos \theta$  and replacing the integration over  $d^2k$  by that over  $d\epsilon_k d\theta$ , we obtain

$$\Pi(\Omega_m, Q) \propto T \sum_{\omega_m} \int d\epsilon_k \int d\theta \frac{1}{(i\omega_m - \epsilon_k)(i\omega_m + i\Omega_m - \epsilon_k - v_F Q \cos \theta)}. \quad (\text{F2})$$

For the dynamic part of  $\Pi(\Omega_m, Q)$ , the order in which the integration over  $\epsilon_k$  and frequency summation are performed does not matter. Integrating over  $\epsilon_k$  first, and then summing over frequency, we obtain

$$\Pi(\Omega, Q) \propto \int d\theta \frac{\Omega_m}{i\Omega_m - v_F Q \cos \theta}. \quad (\text{F3})$$

Integration over  $\theta$  gives

$$\Pi(\Omega_m, Q) \propto \frac{|\Omega_m|}{\sqrt{\Omega_m^2 + v_F^2 Q^2}}. \quad (\text{F4})$$

It is important that typical  $|\cos \theta|$  in the angular integral are of order  $|\Omega_m|/v_F Q$ . For large  $Q$ , Eq. (F4) reduces to  $\Pi(\Omega_m, Q) \propto |\Omega_m|/Q$ , whereas typical angles are near  $\pm\pi/2$ :  $|\theta \pm \pi/2| \simeq |\Omega_m|/v_F Q$ , *i.e.*,  $\mathbf{k}$  and  $\mathbf{Q}$  are nearly orthogonal.

Since typical momenta in both bubbles in diagram 2(b) of Fig. 7 are nearly orthogonal to the same vector,  $\mathbf{Q}$ , they are either almost parallel or antiparallel. In the first case, the momentum structure of both vertices in diagram 2(b) is  $(\mathbf{k}, \mathbf{k}; \mathbf{k}, \mathbf{k})$ , in the second, it is  $(\mathbf{k}, -\mathbf{k}; \mathbf{k}, -\mathbf{k})$ . We now demonstrate that only the backscattering vertex,  $(\mathbf{k}, -\mathbf{k}; \mathbf{k}, -\mathbf{k})$ , contributes to the non-analyticity in  $\Xi$ . To see this, we evaluate diagram 2(b) in a different way, namely, via integrating the product of four Green's functions over a common fermion momentum (momentum  $\mathbf{k}$  in Fig. 10) rather than pairing them into bubbles. As shown in Fig. 10, the momenta of the four Green's functions involved are labelled as either  $G_{\mathbf{k}} G_{\mathbf{k}+\mathbf{q}_1} G_{-\mathbf{k}+\mathbf{q}_2} G_{-\mathbf{k}+\mathbf{q}_1+\mathbf{q}_2}$  (backscattering) or  $G_{\mathbf{k}} G_{\mathbf{k}+\mathbf{q}_1} G_{\mathbf{k}+\mathbf{q}_2} G_{\mathbf{k}+\mathbf{q}_1+\mathbf{q}_2}$  (forward scattering). The arguments presented above for a single bubble suggest that the non-analyticity in  $\Xi$  comes from the region of small  $q_1$  and  $q_2$ . We show that the integral over small  $q_1$  and  $q_2$  indeed gives the correct result, but only in the first case, when two fermion momenta are near  $\mathbf{k}$  and another two are near  $-\mathbf{k}$ , while in the second case, when all four momenta are near  $\mathbf{k}$ , the integral over small  $q_1$  and  $q_2$  vanishes.

We begin with the first case. We first assume, and then verify, that one can expand the quasi-particle spectra to second order in  $q_1$  and  $q_2$ . For a circular Fermi surface, we have

$$\epsilon_{\mathbf{k}+\mathbf{q}_1} = \epsilon_k + v_F q_1 \cos \theta_1 + \frac{q_1^2}{2m}; \epsilon_{-\mathbf{k}+\mathbf{q}_2} = \epsilon_k - v_F q_2 \cos \theta_2 + \frac{q_2^2}{2m}; \epsilon_{-\mathbf{k}+\mathbf{q}_1+\mathbf{q}_2} = \epsilon_k - v_F (q_1 \cos \theta_1 + q_2 \cos \theta_2) + \frac{(\mathbf{q}_1 + \mathbf{q}_2)^2}{2m}. \quad (\text{F5})$$

We also assume, following the reasoning for a single bubble, that both  $\mathbf{q}_1$  and  $\mathbf{q}_2$  are nearly orthogonal to  $\mathbf{k}$ . This implies that  $\mathbf{q}_1$  and  $\mathbf{q}_2$  are either nearly parallel or nearly antiparallel. Collecting the overall factor for diagram 2(b),



expanding in  $\theta_1$  and  $\theta_2$  near  $\pm\pi/2$  and introducing new variables  $x = v_F q_1 \cos\theta_1$ ,  $y = v_F q_2 \cos\theta_2$ , we obtain the contribution to diagram 2(b) from small  $q_1$  and  $q_2$

$$\begin{aligned} \Xi_{Q=0}^B &= -\frac{2mU^2(0)}{(2\pi)^5 v_F^2} T^3 \sum_{\omega_m, \Omega_m, \omega'_m} \int_{-\infty}^{\infty} d\epsilon_k \int_{-\infty}^{\infty} dx \int_{-\infty}^{\infty} dy \int_0^{\infty} dq_1 \int_0^{\infty} dq_2 \\ &\quad \times \frac{1}{(i\omega_m - \epsilon_k)(i\omega + i\Omega_m - \epsilon_k - x - q_1^2/2m)} \frac{1}{i\omega'_m - \epsilon_k + y - q_2^2/2m} \\ &\quad \times \left[ \frac{1}{i\omega'_m + i\Omega_m - \epsilon_k + x + y - (q_1 + q_2)^2/(2m)} + \frac{1}{i\omega'_m + i\Omega_m - \epsilon_k + x + y - (q_1 - q_2)^2/(2m)} \right]. \end{aligned} \quad (\text{F6})$$

Integrating over  $y$  first, and then over  $x$ , we obtain

$$\begin{aligned} \Xi_{Q=0}^B &= \frac{mU^2(0)}{(16\pi^3 v_F^2)} T^3 \sum_{\omega_m, \Omega_m, \omega'_m} \int_{-\infty}^{\infty} d\epsilon_k \int_0^{\infty} dq_1 \int_{-\infty}^{\infty} dq_2 [\text{sgn}(\omega_m + \Omega_m) + \text{sgn}\Omega_m] [\text{sgn}\omega'_m - \text{sgn}(\omega'_m + \Omega_m)] \\ &\quad \times \frac{1}{i\omega_m - \epsilon_k} \frac{1}{i\omega_m + 2i\Omega_m - \epsilon_k - q_1(q_1 + q_2)/m}. \end{aligned} \quad (\text{F7})$$

Integrating next over  $\epsilon_k$ , then over  $q_2$ , and finally over  $q_1$  using

$$\int_{-\infty}^{\infty} dq_2 \frac{1}{q_1(q_1 + q_2)/(m) - 2i\Omega_m} = i \frac{\pi m}{q_1} \text{sgn}\Omega [\text{sgn}\omega_m - \text{sgn}(\omega_m + 2\Omega_m)], \quad (\text{F8})$$

we obtain, to logarithmic accuracy

$$\Xi_{Q=0}^B = -\frac{m^2 U^2(0)}{(16\pi v_F^2)} T \sum_{\Omega_m} \ln \frac{E_F}{|\Omega_m|} S_{\Omega}, \quad (\text{F9})$$

where

$$S_{\Omega} = T \sum_{\omega_m} [\text{sgn}\omega_m - \text{sgn}(\omega_m + 2\Omega_m)] [\text{sgn}(\omega_m + \Omega_m) + \text{sgn}\Omega_m] T \sum_{\omega'_m} [\text{sgn}\omega'_m - \text{sgn}(\omega'_m + \Omega_m)]. \quad (\text{F10})$$

Performing the frequency summation, we finally obtain

$$\Xi_{Q=0}^B = -\frac{u_0^2}{(2\pi v_F^2)} T \sum_{\Omega_m} \Omega_m^2 \ln \frac{E_F}{|\Omega_m|}, \quad (\text{F11})$$

where  $u_0 = mU(0)/(2\pi)$ . In Sec. IV B, we have shown that

$$T \sum_{\Omega} \Omega^2 \ln \frac{E_F}{|\Omega|} = -2T^3 \zeta(3) + \dots, \quad (\text{F12})$$

where the dots stand for regular  $T^2, T^4$ , etc terms [see Eq. (4.36) and Eq. (4.37)]. Thus,

$$\Xi_{Q=0}^B = \zeta(3) u_0^2 \frac{T^3}{\pi v_F^2}. \quad (\text{F13})$$

The evaluation of the  $2k_F$ -contribution from diagram 2(b) and of the entire contribution of diagram 2(a) (the latter involves only a process in which one of the vertices carries momentum near zero and the other one near  $2k_F$ ) proceeds in the same way. The net result from the two diagrams is

$$\Xi^B = \zeta(3) (u_0^2 + u_{2k_F}^2 - u_0 u_{2k_F}) \frac{T^3}{\pi v_F^2}. \quad (\text{F14})$$

In all three contributions, the total momentum in each vertex is near zero, *i.e.*, both the vertices with momentum transfers near zero and near  $2k_F$ , have the structure of  $(\mathbf{k}, -\mathbf{k}; \mathbf{k}, -\mathbf{k})$  and  $(\mathbf{k}, -\mathbf{k}; -\mathbf{k}, \mathbf{k})$ , respectively. Calculating the specific heat corresponding to  $\Xi$  in Eq. (F14), we find that the result for  $C(T)$  coincides with that in Eq. (4.24).

The remaining task is to show that the contribution from forward scattering, *i.e.*, from processes of the type  $(\mathbf{k}, \mathbf{k}; \mathbf{k}, \mathbf{k})$ , vanishes. To see this, we repeat the same calculation, assuming now that the momenta in all four Green's functions in Fig. 7 2(b) are nearly parallel to each other. Instead of Eq. (F6), we then obtain

$$\Xi_{Q=0}^F = -\frac{2mU^2(0)}{(2\pi)^5 v_F^2} T^3 \sum_{\omega_m, \Omega_m, \omega'_m} \int_{-\infty}^{\infty} d\epsilon_k \int_{-\infty}^{\infty} dx \int_{-\infty}^{\infty} dy \int_0^{\infty} dq_1 \int_0^{\infty} dq_2 \frac{1}{(i\omega - \epsilon_k)(i(\omega + \Omega) - \epsilon_k - x - q_1^2/(2m))} \\ \times \frac{1}{i\omega'_m - \epsilon_k - y - q_2^2/2m} \left[ \frac{1}{i\omega'_m + i\Omega_m - \epsilon_k - x - y - (q_1 + q_2)^2/2m} + \frac{1}{i\omega'_m + i\Omega_m - \epsilon_k - x - y - (q_1 - q_2)^2/2m} \right].$$

Integrating first over  $y$ , and then over  $x$ , we obtain

$$\Xi_{Q=0}^F \propto \int_{-\infty}^{\infty} d\epsilon_k \frac{1}{i\omega_m - \epsilon_k} \left( \frac{1}{i\omega_m - \epsilon_k + q_1 q_2/m} + \frac{1}{i\omega_m - \epsilon_k - q_1 q_2/m} \right). \quad (\text{F15})$$

This integral vanishes as the poles of the integrand are located in the same half-plane of  $\epsilon_k$ . This completes our proof of the statement that, to second order in the interaction, the singular part of  $\Xi$  comes only from backscattering, *i.e.*, from the diagrams containing vertices with zero total momentum.

## 2. third order in the interaction

Next, we consider the diagrams for  $\Xi$  to third order in  $U$ . As we have shown in Sec. IV B, the non-analyticity in  $\Xi$  results from the logarithmic singularity in the momentum integral, followed by the Matsubara sum

$$T \sum_{\Omega_m} \int_{|\Omega_m|} dQ Q \frac{\Omega_m^2}{Q^2} \propto T \sum_{\Omega_m} \Omega_m^2 \ln |\Omega_m| \propto T^3.$$

At the second order, the singular term in the momentum integral,  $\Omega_m^2/Q^2$  is obtained by multiplying the dynamic parts of two polarization bubbles. Higher-order diagrams contain higher powers of the polarization bubbles; however, we still need to select terms that behave only as  $\Omega_m^2/Q^2$ : both less or more divergent terms do not result in a logarithmic non-analyticity of the momentum integral, and hence in a  $T^3$  non-analyticity in  $\Xi$ . At the third order, such terms are obtained by selecting the dynamic parts of two out of three polarization bubbles, while putting  $\Omega_m = 0$  in the third bubble. A subtle point here is that the static part of the bubble involves the integration over *all* internal fermion momenta,  $\mathbf{l}$ , *i.e.*, in contrast to the dynamic part, there is no correlation between the directions of boson momentum,  $\mathbf{Q}$ , and  $\mathbf{l}$ . Hence, vertices that appear in the third order diagrams are generally not “one-dimensional” in a sense that the four fermion momenta are not directed along the same line. Furthermore, despite the fact that the static polarization for free fermions in 2D  $\Pi(\Omega = 0, Q)$  is a constant ( $= -m/2\pi$ ) for all  $Q \leq 2k_F$ , only  $\Pi(\Omega = 0, Q \rightarrow 0)$  comes from the states in the immediate vicinity of the Fermi surface. For generic  $Q$ , the static polarization bubble involves fermion states away from the Fermi surface [50]. As a result, the convolution of  $U(Q)$  and two fermion propagators, which form a polarization bubble with non-zero external momentum, cannot be expressed as the angular average of bare interaction between the particles on the Fermi surface. As an example, consider the “ $Q = 0$ ” contribution from diagram 3(b) in Fig. 7. This contribution involves only bubbles with small external momenta, *i.e.*, all internal fermion momenta— $\mathbf{p}$ ,  $\mathbf{k}$ , and  $\mathbf{l}$ —are located near the Fermi surface. Two of these momenta, *e.g.*,  $\mathbf{p}$  and  $\mathbf{k}$ , must be nearly antiparallel; otherwise there is no non-analyticity in  $\Xi$ . However, the direction of the third momentum— $\mathbf{l}$ —with respect to  $\mathbf{k}$  is arbitrary. As a result, depending on the choice of two antiparallel momenta, the “ $Q = 0$ ” contribution from diagram 3(b) contains a term proportional to  $u_0^2 u_\pi$ , where

$$u_\theta = (m/2\pi)U(2k_F \sin \theta/2), \quad (\text{F16})$$

as well as another one proportional to  $u_0^2 \langle u_\theta \rangle$ , where

$$\langle u_\theta \rangle = \frac{1}{\pi} \int_0^\pi u(\theta) d\theta. \quad (\text{F17})$$

In this last term, the integration goes over the entire Fermi surface. [It is understood that  $u_\pi = u_{2k_F}$ .]

The same reasoning applies to the  $2k_F$ -contribution from this diagram. In addition, the  $2k_F$ -contribution involves the convolutions of the interaction potential with the Green's functions forming bubble. As we just said, the corresponding momentum integral is not confined to the Fermi surface. Evaluating the integrals, we find that the  $2k_F$ -part

of diagram 3(b) contains a term proportional to  $u_\pi^2 u_0$  and another one proportional to  $u_\pi^2 \langle \langle u_\theta \rangle \rangle$ , where

$$\langle \langle u_\theta \rangle \rangle = \frac{1}{\pi} \int_0^\pi d\theta u_\theta \cos \frac{\theta}{2} \ln \frac{\sqrt{1 + \sin \theta/2} + \sqrt{1 - \sin \theta/2}}{\sqrt{1 + \sin \theta/2} - \sqrt{1 - \sin \theta/2}}. \quad (\text{F18})$$

(These two terms occur for different choices of two anti-parallel momenta.) If  $u$  does not depend on  $\theta$ , then  $\langle \langle u_\theta \rangle \rangle = u$ . The first term –proportional to  $u_\pi^2 u_0$ – involves the static bubble,  $\Pi(0, 2k_F)$ , which, once again, is determined by the states far away from the Fermi surface. This term is similar to the “ $Q = 0$ ” contribution from the states near the Fermi surface, simply because for free fermions in  $D = 2$ ,  $\Pi(2k_F) = \Pi(0)$ . To distinguish between the Fermi-surface and non-Fermi surface contributions, we multiply  $\Pi(2k_F)$  by  $\langle \langle 1 \rangle \rangle$  (according to Eq. (F18),  $\langle \langle 1 \rangle \rangle = 1$ ) to emphasize that the integration is not confined to the Fermi surface.

Applying this reasoning to all third order diagram, and combining all choices of choosing two dynamic and one static bubble, we find

$$\Xi_{3a} = -(u_0 \langle u_\theta u_{\pi-\theta} \rangle + 2u_0 u_\pi \langle u_\theta \rangle) K + (u_\pi \langle \langle u_\theta^2 \rangle \rangle + 2u_0 u_\pi \langle \langle u_\theta \rangle \rangle) K \quad (\text{F19a})$$

$$\Xi_{3b} = (4u_0^2 \langle u_\theta \rangle + 2u_0^2 u_\pi) K + [4u_\pi^2 \langle \langle u_\theta \rangle \rangle + 2u_\pi^2 u_0 \langle \langle 1 \rangle \rangle] K \quad (\text{F19b})$$

$$\Xi_{3c} = -4 [u_0^3 + u_\pi^3 \langle \langle 1 \rangle \rangle] K \quad (\text{F19c})$$

$$\Xi_{3d} = 2u_\pi \langle u_\theta u_{\pi-\theta} \rangle K + 2u_0 \langle \langle u_\theta^2 \rangle \rangle K, \quad (\text{F19d})$$

where  $K \equiv \zeta(3)T^3/\pi v_F^2$ . Adding up Eqs. (F19a-F19d), we obtain a total third-order contribution to  $\Xi$

$$\begin{aligned} \Xi_3 = & [-4u_0^3 + 2u_0^2 u_\pi + (4u_0^2 - 2u_0 u_\pi) \langle u_\theta \rangle - (u_0 - 2u_\pi) \langle u_\theta u_{\pi-\theta} \rangle] K \\ & + [(-4u_\pi^3 + 2u_0 u_\pi^2) \langle \langle 1 \rangle \rangle + (4u_\pi^2 - 2u_0 u_\pi) \langle \langle u_\theta \rangle \rangle - (u_\pi - 2u_0) \langle \langle u_\theta^2 \rangle \rangle] K. \end{aligned} \quad (\text{F20})$$

Combining the last expression with the second-order result, Eq. (F14), and using relation Eq. (4.2) between  $\Xi$  and  $C(T)$ , we obtain for  $C(T)/T$  to third order in  $u$

$$\delta C(T)/T = -\frac{3m\zeta(3)}{4\pi} \frac{T}{E_F} \left[ (2\tilde{u}_0 - \tilde{u}_\pi + 2\langle \langle u_\theta^2 \rangle \rangle - \langle u_\theta u_{\pi-\theta} \rangle)^2 + 3(\tilde{u}_\pi + \langle u_\theta u_{\pi-\theta} \rangle)^2 \right], \quad (\text{F21})$$

where

$$\tilde{u}_0 = u_0 (1 - 2u_0 + 2\langle u_\theta \rangle), \quad \tilde{u}_\pi = u_\pi (1 - 2u_\pi \langle \langle 1 \rangle \rangle + 2\langle \langle u_\theta \rangle \rangle). \quad (\text{F22})$$

Next, we verify whether Eq. (F22) can be obtained by substituting the renormalized static vertices into the second-order result for the specific heat, Eq. (F14). To first order in  $u$ , we simply have:  $\Gamma^k(\mathbf{k}, -\mathbf{k}; \mathbf{k}, -\mathbf{k}) = u_0$  and  $\Gamma^k(\mathbf{k}, -\mathbf{k}; -\mathbf{k}, \mathbf{k}) = u_{2k_F}$ . To evaluate the third-order contribution to  $C(T)$ , we need to renormalize the vertices up to second order—the third order terms will then result as cross-products of first and second-order terms. Evaluating the vertex corrections, presented diagrammatically in Fig. 3, in the same way as we evaluated the diagrams for  $\Xi$ , we obtain

$$\Gamma^k(\mathbf{k}, -\mathbf{k}; \mathbf{k}, -\mathbf{k}) = \frac{2\pi}{m} [\tilde{u}_0 + \langle \langle u_\theta^2 \rangle \rangle]; \quad (\text{F23a})$$

$$\Gamma^k(\mathbf{k}, -\mathbf{k}; -\mathbf{k}, \mathbf{k}) = \frac{2\pi}{m} [\tilde{u}_\pi + \langle u_\theta u_{\pi-\theta} \rangle]. \quad (\text{F23b})$$

Replacing  $u_0$  and  $u_{2k_F}$  in Eq. (F14) by renormalized vertices, Eq. (F23a) and Eq. (F23b), correspondingly, we find after simple manipulations that it does indeed reproduce Eq. (F21). This proves, to order  $u^3$ , that the non-analytic term in the specific heat is expressed in terms of renormalized static vertices  $\Gamma^k(\mathbf{k}, -\mathbf{k}; \mathbf{k}, -\mathbf{k})$  and  $\Gamma^k(\mathbf{k}, -\mathbf{k}; \mathbf{k}, -\mathbf{k})$ , *i.e.*, in terms of  $\Gamma^k(\pi)$ .

Using now the relations between  $\Gamma(\mathbf{k}, -\mathbf{k}; \mathbf{k}, -\mathbf{k})$  and  $\Gamma(\mathbf{k}, -\mathbf{k}; \mathbf{k}, -\mathbf{k})$  and the spin and charge components of  $\Gamma^k(\pi)$

$$\Gamma(k, -k; k, -k) = \Gamma_c^k(\pi) - \Gamma_s^k(\pi), \quad \Gamma(k, -k; -k, k) = -2\Gamma_s^k(\pi), \quad (\text{F24})$$

and restoring quasi-particle  $Z$  factors and  $m^*/m$ , which come from self-energy insertions not considered above, we obtain Eq. (4.52).

It is also instructive to re-express  $\Gamma^k(\pi)$  not in terms of the bare interaction potential, but in terms of another vertex— $\Gamma^\omega(\theta)$ , which, we remind, is the static vertex renormalized by the states away from the Fermi surface. To this end, we

separate the Fermi-surface and non-Fermi-surface contributions to Eq. (F23a, F23b), *i.e.*, re-write Eq. (F23a, F23b) to order  $u^3$  as

$$\Gamma^k(\mathbf{k}, -\mathbf{k}; \mathbf{k}, -\mathbf{k}) = \frac{2\pi}{m} [u_0 + \langle\langle u_\theta^2 \rangle\rangle] [1 - 2u_0 + 2\langle u_\theta \rangle]; \quad (\text{F25a})$$

$$\Gamma^k(\mathbf{k}, -\mathbf{k}; -\mathbf{k}, \mathbf{k}) = \frac{2\pi}{m} u_\pi [1 - 2u_\pi \langle\langle 1 \rangle\rangle + 2\langle\langle u_\theta \rangle\rangle] \left(1 + \frac{\langle u_\theta u_{\pi-\theta} \rangle}{u_\pi}\right). \quad (\text{F25b})$$

(For simplicity, we neglected the  $Z$ -factor and effective mass renormalizations here and in what follows.) The first brackets in both formulas come from the states away from the Fermi surface, *i.e.*, they give  $\Gamma^\omega(\pi)$ . The second brackets come from states near the Fermi surface and account for the difference between  $\Gamma^k$  and  $\Gamma^\omega$ . Introducing spin and charge components of  $\Gamma^\omega$  in the same way as in Eq. (F24), *i.e.*, as

$$\begin{aligned} \Gamma^k(k, -k, k, -k) &= \frac{\pi}{m} [f_c(\pi) - f_s(\pi)], & \Gamma^k(k, -k; -k, k) &= -2\frac{\pi}{m} f_s(\pi) \\ \Gamma^\omega(k, -k, k, -k) &= \frac{\pi}{m} [\gamma_c(\pi) - \gamma_s(\pi)], & \Gamma^\omega(k, -k; -k, k) &= -2\frac{\pi}{m} \gamma_s(\pi), \end{aligned} \quad (\text{F26})$$

we obtain

$$\begin{aligned} \gamma_c^\omega(\pi) &= u_0 - \frac{1}{2}u_\pi (1 - 2u_\pi \langle\langle 1 \rangle\rangle + 2\langle\langle u_\theta \rangle\rangle) + \langle\langle u_\theta^2 \rangle\rangle \\ \gamma_s^\omega(\pi) &= -\frac{1}{2}u_\pi (1 - 2u_\pi \langle\langle 1 \rangle\rangle + 2\langle\langle u_\theta \rangle\rangle). \end{aligned} \quad (\text{F27})$$

Substituting Eq. (F27) into Eq. (F25b) and (F24), we obtain the relation between  $f_a$  and  $\gamma^a$  presented in the main text [ Eq. (4.54)].

Finally, when the interaction is strongly peaked at  $Q = 0$ , so that  $u_0$  is much larger than  $u_\theta$  for a generic  $\theta$ , including  $\theta = \pi$ , only corrections to  $u_0$  matter. These corrections come from the ring diagrams and can be summed up exactly. The full combinatoric factor for the  $u_0^n$  term from the ring diagram of order  $n$  is  $(-1)^n 2^{n-2} (n-1)$ . Evaluating the sum over  $n$ , we reproduce Eq. (4.56).

---

[\*] Permanent address.

- [1] A. A. Abrikosov, L. P. Gorkov, and I. E. Dzyaloshinski, *Methods of quantum field theory in statistical physics*, (Dover Publications, New York, 1963).
- [2] E. M. Lifshitz and L. P. Pitaevski, *Statistical Physics*, (Pergamon Press, 1980).
- [3] see e.g., T. Timusk and B. Statt, Rep. Prog. Phys. **62**, 61 (1999).
- [4] see, e.g., P. Coleman, C. Pepin, Q. Si, R. Ramazashvili, Journal of Physics: Condensed Matter **13**, 723-738, (2001); Q. Si et al, Nature, **413**, 804 (2001).
- [5] A. Abanov, A. Chubukov and J. Schmalian, Advances in Physics **52**, 119 (2003).
- [6] G. M. Eliashberg, Sov. Phys. JETP **16**, 780 (1963).
- [7] S. Doniach and S. Engelsberg, Phys. Rev. Lett. **17**, 750 (1966).
- [8] W. F. Brinkman and S. Engelsberg, Phys. Rev. **169**, 417 (1968).
- [9] D. J. Amit, J. W. Kane, and H. Wagner, Phys. Rev. **175**, 313 (1968); *ibid.* **175**, 326 (1968).
- [10] This terms are often associated in the literature with the interaction with phonons [6] or spin fluctuations (“paramagnons”) [7],[8]). However, they arise already at the second order in the fermion-fermion interaction, with no boson modes involved—cf. Ref. [9].
- [11] D. Belitz, T. R. Kirkpatrick, and T. Vojta, Phys. Rev. B **55**, 9452 (1997)
- [12] D. Coffey and K. S. Bedell, Phys. Rev. Lett. **71**, 1043 (1993).
- [13] a) A. V. Chubukov and D. L. Maslov, Phys. Rev. B **68**, 155113 (2003); b) *ibid.* **69**, 121102 (2004)
- [14] V. M. Galitski and S. Das Sarma, cond-mat/0311559
- [15] M. A. Baranov, M. Yu. Kagan, and M. S. Mar’enko, JETP Lett. **58**, 709 (1993).
- [16] G. Y. Chitov and A. J. Millis, Phys. Rev. Lett. **86**, 5337 (2001); Phys. Rev. B **64**, 0544414 (2001).
- [17] A. V. Chubukov, C. Pépin, and J. Rech, Phys. Rev. Lett. **92**, 147003 (2004).
- [18] D. S. Greywall, Phys. Rev. B **27**, 2747 (1983); G. R. Stewart, Rev. Mod. Phys. **86**, 755 (1984); A. Casey, H. Patel, J. Nyeki, B. P. Cowan, and J. Saunders, Phys. Rev. Lett. **90**, 115301 (2003).
- [19] D. Belitz, T. R. Kirkpatrick, and T. Vojta, Phys. Rev. Lett. **82**, 4707 (1999); D. Belitz and T. Vojta, *ibid.* **89**, 247202 (2002).
- [20] J. A. Hertz, Phys. Rev. B **14**, 1165 (1976); A. Millis, Phys. Rev. B **48**, 7183 (1993); T. Moriya, *Spin Fluctuations in Itinerant Electron Magnets* (Springer-Verlag, Berlin, 1985).

- [21] A. M. Rudin, I. L. Aleiner, and L. I. Glazman, Phys. Rev. B **55**, 9322 (1997).
- [22] G. Zala, B. N. Narozhny, I. L. Aleiner, Phys. Rev. B **64**, 214204 (2001).
- [23] C. Castellani, C. Di Castro, and W. Metzner, Phys. Rev. Lett. **72**, 316 (1994).
- [24] H. Fukuyama and M. Ogata, J. Phys. Soc. Jpn. **63**, 3923 (1995).
- [25] C. Halboth and W. Metzner, Phys. Rev. B **57**, 8873 (1998).
- [26] Yu. A. Bychkov, L. P. Gor'kov, and I. E. Dzyaloshinskii, Zh. Eksp. Teor. Fiz. **50**, 738 (1966) [Sov. Phys. JETP **23**, 489 (1966)]; I. E. Dzyaloshinskii and A. I. Larkin, Zh. Eksp. Teor. Fiz. **65**, 411 (1973) [Sov. Phys. JETP **38**, 202 (1974)].
- [27] P. W. Anderson, Phys. Rev. Lett. **65**, 2306 (1990).
- [28] A. V. Chaplik, Zh. Eksp. Teor. Fiz. **60**, 1845 (1971) [Sov. Phys. JETP **33**, 997 (1971)]; C. Hodges, H. Smith and J. W. Wilkins, Phys. Rev. B **4**, 302 (1971); P. Bloom, Phys. Rev. B **12**, 125 (1975).
- [29] J. C. Campuzano, M. Randeria, M. R. Norman and H. Ding, in "The Gap Symmetry and Fluctuations in High Tc Superconductors", edited by J. Bok *et al.*, (Plenum, 1998).
- [30] J. P. Eisenstein, T. J. Gramila, L. N. Pfeiffer, and K. W. West Phys. Rev. B **44**, 6511-6514 (1991); J. P. Eisenstein, L. N. Pfeiffer, and K. W. West Phys. Rev. Lett. **69**, 3804-3807 (1992); S. Q. Murphy, J. P. Eisenstein, L. N. Pfeiffer, and K. W. West Phys. Rev. B **52**, 14825-14828 (1995).
- [31] G. Catelani and I. L. Aleiner, cond-mat/04053333.
- [32] J. Sólyom, Adv. Phys. **28**, 201 (1979).
- [33] I. E. Dzyaloshinskii and A. I. Larkin, Zh. Eksp. Teor. Fiz. **61**, 791 (1972) [Sov. Phys. JETP **34**, 202 (1972)].
- [34] G. I. Japaridze and A. A. Nersesyan, Phys. Lett. **94** A, 224 (1983).
- [35] R. Saha and D. L. Maslov (unpublished).
- [36] T. Ando, A. B. Fowler, and F. Stern, Rev. Mod. Phys. **54**, 437 (1982).
- [37] G. Guilianini and J. J. Quinn, Phys. Rev. B **26**, 4421 (1982).
- [38] We have chosen to present the result for the Coulomb potential as a function of  $\epsilon_k$  rather than of  $\Delta$ , in contrast to what we did for the short-range case. The reason is that, in terms of  $\Delta$ , the kink in Eq.(3.92) is at  $\Delta = \omega$ , *i.e.*, not close to the mass shell, so that  $\Delta$  is not a convenient variable any more.
- [39] E. G. Mishchenko and A. V. Andreev, Phys. Rev. B **65**, 235310 (2002).
- [40] D. V. Khveshchenko and M. Yu. Reizer, Phys. Rev. B **57**, 4245 (1998).
- [41] G. M. Eliashberg, Sov. Phys. JETP **11**, 696 (1960).
- [42] J. M. Luttinger and J. C. Ward, Phys. Rev. **118**, 1417 (1960).
- [43] A. Wasserman and M. Springford, Adv. Phys. **45**, 471 (1996).
- [44] J. Bardeen and M. Stephen, Phys. Rev. B **136**, A1485 (1964); Y. Wada, Phys. Rev. **135**, A1481 (1964); D. J. Scalapino in "Superconductivity" R. D. Parks, ed., Marcel Dekker, New York, 1969, vol. 1, p.449. For a recent review, see F. Marsiglio and J.P. Carbotte in "The physics of Superconductors", K.H. Bennemann and J.B. Ketterson eds, Springer, 2003, vol. 1, p. 233 and R. Haslinger and A. Chubukov, Phys. Rev. **68**, 214508 (2003).
- [45] B. Altshuler, L. B. Ioffe and A. J. Millis, Phys. Rev. B **52**, 5563 (1995).
- [46] C. Castellani, C. DiCastro, and M. Grilli, Z. Phys. B **103**, 137 (1997). S. Caprara, M. Sulpizi, A. Bianconi, C. Di Castro and M. Grilli, Phys. Rev. B **59**, 14980 (1999); A. Perali, C. Castellani, C. Di Castro, M. Grilli, E. Piegari and A. A. Varlamov, Phys. Rev. B **62**, R9295 (2000); S. Andergassen, S. Caprara, C. Di Castro and M. Grilli, Phys. Rev. Lett. **87**, 056401-1 (2001).
- [47] A. Abanov, A. V. Chubukov and J. Schmalian, Adv. Phys. **52**, 119 (2003); A. V. Chubukov, D. Pines and J. Schmalian, in "The physics of Superconductors", K. H. Bennemann and J. B. Ketterson eds, Springer, 2003, vol. 1, p. 495.
- [48] R. Roussev and A. J. Millis, Phys. Rev. B **63**, 140504 (2001), Z. Wang, W. Mao and K. Bedell, Phys. Rev. Lett. **87**, 257001 (2001), A. Chubukov, A. Finkelstein, R. Haslinger and D. Morr, Phys. Rev. Lett. **90**, 077002 (2003).
- [49] R. Haslinger and A. Chubukov, Phys. Rev. **67**, 140504 (2003).
- [50] A. V. Chubukov, Phys. Rev. **48**, 1097 (1993).